



HAL
open science

Machine learning based wearable multi-channel electromyography : application to bionics and biometrics

Sherif Mohamed Said

► **To cite this version:**

Sherif Mohamed Said. Machine learning based wearable multi-channel electromyography : application to bionics and biometrics. Bioengineering. Université Paris-Est, 2020. English. NNT : 2020PESC0086 . tel-03543121

HAL Id: tel-03543121

<https://theses.hal.science/tel-03543121>

Submitted on 25 Jan 2022

HAL is a multi-disciplinary open access archive for the deposit and dissemination of scientific research documents, whether they are published or not. The documents may come from teaching and research institutions in France or abroad, or from public or private research centers.

L'archive ouverte pluridisciplinaire **HAL**, est destinée au dépôt et à la diffusion de documents scientifiques de niveau recherche, publiés ou non, émanant des établissements d'enseignement et de recherche français ou étrangers, des laboratoires publics ou privés.



THÈSE de DOCTORAT

Présentée par

Sherif Mohamed Roshdy SAID

Pour l'obtention du
GRADE DE DOCTEUR

De

L'Université Paris-Est Créteil

Ecole Doctorale MATHÉMATIQUES ET STIC (ED 532)

Spécialité de doctorat : Signal, Image, Automatique

**Machine Learning-based Wearable Multi-channel
Electromyography: Application to Bionics and Biometrics**

**Apprentissage Machine d'un Modèle d'électromyographie de
Surface: Application en Bionique et en Biométrie**

Le 15 Décembre 2020, devant le jury composé de

Prof. Mouloud ADEL	Aix-Marseille Université	Rapporteur
Prof. Régine Le Bouquin JEANNES	Université de Rennes 1	Rapporteur
Prof. Patrick SIARRY	Université Paris-Est Créteil	Examineur
Ass. Prof. Samer ALKORK	American Univ. of the Middle East (Koweit)	Examineur/ Co-encadrant
Prof. Amine NAIT-ALI	Université Paris-Est Créteil	Directeur

Abstract

Over the last few decades, wearable technologies have several bioengineering applications. In this thesis, a Multi-channel surface electromyography (sEMG) wearable armband has been used: (1) to control a 3D bionic arm, and we have designed (2) for an access control system in biometrics. The first application is related to bionics, whereas the second application is related to the security field.

Regarding our first contribution, 920 EMG signals have been collected from 23 volunteer subjects where the purpose was to train an EMG based gesture recognition model. The bionic control approach has been validated and optimized for a right arm amputee. In terms of processing, numerous Machine-Learning classifiers have been applied. It has been found that the Support Vector Machine classifier exhibit 90.5% success rate.

On the other hand, in the second contribution, we explored new experiments where the application consists of using EMG signals for both verification and identification purposes. More specifically, each subject is asked to perform a sequence of specific hand gestures. Each hand gesture allows the generation of one character of a global signature (i.e., password). Therefore, when considering verification mode, features are extracted from the EMG signals in both frequency and time domains. Three classifiers have been used, namely: K-nearest Neighbors (KNN), Linear Discernment Analysis (LDA), and Ensemble of Classifiers. Results show that the KNN classifier allows performance of 97.4%. While in the user's identification system, three previous classifiers have been considered as well. Experiments show that best performance (accuracy is 86.01%) have been obtained using KNN.

In this thesis, the Deep-learning approach has been considered by achieving what is known as "Data augmentation". Therefore, Convolutional Neural Network (CNN) is used to train the model from EMG scalograms. When considering verification mode, performances of 98.31% has been reached. On the other hand, in the identification case, two CNN structures have been evaluated, namely squeeze-net structure and Alex-net structure. Results show that squeeze-net allows a promising performance of 81.84%.

Keywords

Wearable technologies, Bionic arm, Gestures recognition, Biometrics, Identification, Verification, sEMG signal, Features Extraction, CNN

Résumé

Les technologies portables ont été largement utilisées au cours des dernières décennies dans les applications de bio-ingénierie. Dans le cadre de nos travaux de thèse, un bracelet portable permettant l'acquisition sans fils de signaux d'électromyogramme de surface (sEMG) a été utilisé dans une étude de recherche, afin de : (1) contrôler une prothèse bionique que nous avons nous-même conçue, (2) contrôler, entre autres, les accès aux ressources par vérification biométrique. La première contribution est liée au domaine de la santé, alors que la deuxième contribution relève de l'aspect sécuritaire.

Dans le contexte de l'application bionique, nos expérimentations nous ont menés à collecter chez 23 sujets sains, des signaux sEMG (920 au total) servant à entraîner un modèle de reconnaissance de gestes que l'on a validé sur un sujet présentant un handicap (bras amputé). En termes de traitement de données, de nombreux classifieurs d'apprentissage automatique ont été évalués. Ainsi, le classifieur de machine à vecteur de support (SVM) s'est avéré prometteur au regard du taux de classification atteint (90,5%).

Par ailleurs, dans la deuxième contribution, nous avons étudié la possibilité d'utiliser les signaux sEMG multicanaux (collectés par bracelet EMG sans fils) comme modalité biométrique pour la vérification et l'identification des individus. Dans ce contexte, nous avons construit une base de données de signaux sEMG multicanaux (8960 au total) en impliquant 56 sujets volontaires. Chaque sujet effectue une combinaison spécifique de gestes de la main générant ainsi des signaux EMG dont le code permet de former un mot de passe. Lorsque l'on considère la vérification des utilisateurs, des signatures sont extraites, à la fois du domaine fréquentiel et du domaine temporel. Ainsi, dans nos travaux, trois classifieurs ont été considérés, à savoir : K-plus proches voisins (KNN), analyse de discernement linéaire (LDA) et méthodes ensemblistes. Les résultats montrent que le KNN présente une précision de 97,4%.

Quant à l'identification biométrique, trois classifieurs sont également utilisés pour classer les données : KNN, LDA et méthodes ensemblistes. Le meilleur résultat en termes de performance moyenne atteint 86,01% pour KNN.

Dans la dernière partie de cette thèse, nous avons considéré des approches d'apprentissage profond en procédant à l'augmentation des données. Ainsi, les Réseaux de Neurones Convolutifs (CNN) sont entraînés à partir de scalogrammes d'EMG, conduisant ainsi, en mode vérification à une performance de 98,3%. Enfin, en mode identification, deux architectures CNN ont été appliquées (*squeeze-net* et *structure Alex-net*). Les résultats nous ont permis d'atteindre 81,84% avec (*squeeze-net*).

Mots clés

Technologies portables, Bras Bionique, Reconnaissance des gestes, Identification, Vérification, Biométrie, Signal sEMG, CNN, Classification.

Publications

Journal publications

- Said, S., Boulkaibet, I., Sheikh, M., Karar, A. S., Alkork, S., & Nait-ali, A. (2020). Machine-Learning-Based Muscle Control of a 3D-Printed Bionic Arm. *Sensors*, 20(11), 3144.
- Said, S.; Karar, A.S.; Beyrouthy, T.; Alkork, S.; Nait-ali, A. (2020). Biometrics Verification Modality Using Multi-Channel sEMG Wearable Bracelet. *Applied Sciences*, 10, 6960.

International Conferences

- Said, S., Sheikh, M., Al-Rashidi, F., Lakys, Y., Beyrouthy, T., & Nait-ali, A. (2019, April). A Customizable Wearable Robust 3D Printed Bionic Arm: Muscle Controlled. In *2019 3rd International Conference on Bio-engineering for Smart Technologies (BioSMART)* (pp. 1-6). IEEE.

Book Chapters

- Said, S., Al Kork, S., & Nait-Ali, A. (2019). Wearable Technologies in Biomedical and Biometric Applications. In **Biometrics under Biomedical Considerations** (pp. 211-227). Springer, Singapore.
- Brahim, I., Dhibou, I., Makni, L., Said, S., & Nait-ali, A. (2020). Wearable Multi-channel EMG Biometrics: Concepts. In **Hidden Biometrics** (pp. 91-100). Springer, Singapore.

Awards

- Best Entrepreneurial-ship Project in **RoboRave 2019 Competition**, USA.

ACKNOWLEDGEMENT

My Supervisor: I would like to express my sincere gratitude to my supervisor **Prof. Amine NAIT-ALI**, who has guided and taught me a lot throughout the journey of studying for the Ph.D., which allowed me to learn and acquire the spirit of scientific research and much more.

Lab Director: I would like to thank **Prof. Yacine AMIRAT**, the director of LISSI Lab, for all the support he offered to me during the Doctorate study period.

Defense Committee: I would like to thank all jury members for offering valuable time to review my thesis and examine my defense. Many thanks to them for their helpful comments, questions, and insightful remarks.

My Parents: I would like to designate the entire fruitful outcome of this work to my father, who has been waiting for so long to see the result of his son's work, to my mother, who hasn't stopped praying for this work to be done.

My Family: I would like to thank my wife, who has stood by me through all my travels, my absences, and my fits of pique. She supported the family during much of my graduate studies. Along with her, I want to acknowledge my daughter, **Jomana**, and my son **Mohamed** ; they are the source of love and joyful time always spent with them.

My thankfulness and appreciation to my extended family, particularly brother and sister, for their support, encouragement, patience and praying for me during the time of my study.

My Colleagues: Nevertheless, I cannot forget the support of my colleagues especially **Dr. Samer AIKORK, Dr. Abdullah KARAR, and Mr. Murtaza SHEIKH**, who always supported me as brothers. They worked with me a lot, supported me, and encouraged me to work hard. Thanks to anyone who has ever supported me even with a word during this journey, which contains many values and lessons to learn.

Contents

1	Chapter 1 Generalities about Wearable Technology systems	23
1.1	Introduction	24
1.2	Wearable systems on the market.....	25
1.2.1	BITalino Kit.....	25
1.2.2	MySignals Kit.....	26
1.2.3	Myo Armband.....	27
1.3	EMG Signal.....	28
1.4	Wearable Technologies in Bionic arm.....	29
1.5	Wearable Technologies in Biometrics	30
1.6	Conclusion.....	33
2	Chapter 2 State of the Art on sEMG Control Systems.....	34
2.1	Introduction	35
2.2	State of the Art on EMG Gesture Recognition System and Bionic Arm.....	35
2.2.1	Review of EMG Gesture Recognition System	35
2.2.2	Review of 3D printed Bionic Arm.....	41
2.3	State of the Art of EMG biometrics system	44
2.4	Conclusion.....	47
3	Chapter 3 Design and Implementation of a 3-D Printed Bionic Arm Controlled by Machine Learning Based Algorithm.....	49
3.1	Introduction	51
3.2	Bionic Arm.....	52
3.2.1	Methodology.....	52
3.2.2	Acquisition of sEMG signal.....	53
3.2.3	Bionic Arm Mechanical Design.....	54
3.2.4	Electronics and Control.....	59

3.3	Feature Extraction and Classification	61
3.3.1	Data Collection Protocol.....	61
3.3.2	Data Processing.....	62
3.3.3	Features Extraction	63
3.3.4	Classification.....	64
3.4	Results	66
3.5	Real-time Implementation.....	68
3.6	Conclusion.....	70
4	Chapter 4 EMG based Biometrics Modality for Users Verification.....	71
4.1	Introduction	72
4.2	Database Collection Protocol.....	73
4.3	Features Extraction for sEMG Users Verification	76
4.4	Machine Learning Models	79
4.5	Results	81
4.6	Conclusion.....	86
5	Chapter 5 sEMG Machine-learning based Biometrics Modality for Users Identification	88
5.1	Introduction	89
5.2	Features Extraction.....	91
5.3	Machine Learning Models	93
5.4	Results	94
5.5	Conclusion.....	97
6	Chapter 6 Deep Learning for sEMG Biometrics System.....	98
6.1	Introduction	100
6.2	Deep Learning for Biometrics Users Verification System.....	103
6.2.1	Input Generation	103
6.2.2	Continuous Wavelet Transform (CWT)	104

6.2.3	Data Augmentation	106
6.2.4	Convolutional Neural Network Structure and Training.....	106
6.2.5	Testing and Results	109
6.3	Deep Learning for Biometrics Users Identification System	112
6.3.1	Input Generation	113
6.3.2	Wavelet-Based Denoising.....	114
6.3.3	Data Augmentation	115
6.3.4	CNN Architecture and Training.....	115
6.3.5	Testing and Results	116
6.4	Conclusion.....	117
7	Chapter 7 Conclusion & Perspectives.....	118
8	Bibliography	123

List of Figures

Figure 1-1 Myo armband structure	28
Figure 1-2 sEMG signal generated by Myo Armband.....	28
Figure 1-3 Wearable Armband for biometrics verification	32
Figure 2-1 Basic Steps of Hand Gesture Recognition (Yasen, M., and Jusoh, S., 2019).....	37
Figure 2-2 Models of 3D printed upper limb (Jelle ten Kate, Gerwin Smit & Paul Breedveld, 2017) (a) Andrianesis' Hand: an externally powered forearm prosthesis,(b) Body-powered hand prosthesis, (c) Scand: a passive adjustable forearm prosthesis,(d) IVIANA 2.0: a passive forearm prosthesis, (e) Adams Arm: EMG controlled Bionic Arm.....	43
Figure 3-1 Amputation case with the user wearing a Myo armband	52
Figure 3-2 Schematic chart of the process for bionic arm control.....	53
Figure 3-3 Eight (sEMG) sensors raw data for wave-out hand action.....	54
Figure 3-4 Bionic arm 3D model on computer-aided design (CAD) software.....	55
Figure 3-5 Case 1: Stress results at 3.350 Kg load	57
Figure 3-6 Case 1: Displacement results at 3.350 Kg load	57
Figure 3-7 Case 1: Strain Result at 3.350 kg load	58
Figure 3-8 Case 2: Stress result at 2.350 combined load	58
Figure 3-9 Case 2: Displacement results at 2.350 kg combined load	58
Figure 3-10 Case 2: Strain result at 2.350 kg combined load	58
Figure 3-11 Bionic Arm load test	59
Figure 3-12 Amputee wearing the bionic arm	59
Figure 3-13 Chestnut board controller	61
Figure 3-14 Flowchart of controlling the bionic arm.....	61
Figure 3-15 Filtered and rectified EMG signal (a) Raw sEMG signal, (b) Mean value removed sEMG signal, (c) Filtered and rectified sEMG signal, (d) sEMG envelope signal ..	63
Figure 3-16 (a)Writing with the pen (two fingers closed action); (b) holding of a notebook (one finger closed action); (c) using the PC mouse (one finger closed action); (d) holding a ball (fist action).	69
Figure 3-17 Success rate of hand actions.....	70
Figure 4-1 EMG Authentication System Schematic Chart.....	74
Figure 4-2 Acquisition of sEMG data of a user to create the database (Enrolment)	75

Figure 4-3 PSD of EMG signal.....	78
Figure 4-4 Segmentation of EMG signal	78
Figure 4-5 Average Testing Accuracy of Verification System.....	83
Figure 4-6 FAR and FRR of the Three Classifiers	83
Figure 5-1 Biometrics Identification System Schematic Chart	91
Figure 5-2 Absolute and log absolute value of EMG signal.....	93
Figure 6-1 Schematic diagram of ConvNet architecture (Chen, L., Fu, J., Wu, Y., Li, H., & Zheng, B., 2020)	102
Figure 6-2 Schematic Chart of Users verification System using Deep Learning	103
Figure 6-3 Generated Scalograms of 6 different sEMG signals for different users, (a)User 1,(b)User 2, (c)User 3, (d)User 4, (e)User 5, (f)User 6.....	105
Figure 6-4 Organization of Fire Modules in the Convolutional Layer	108
Figure 6-5 Schematic Chart of Users Identification System using Deep Learning	113
Figure 6-6 Denoised Signal using Different Threshold Values	115
Figure 6-7 Scalograms of Denoised Signal using Different Threshold Values	116

List of tables

Table 1-1 Examples of crimes using physical features	33
Table 3-1 Stress Analysis Results	58
Table 3-2 Detailed cost analysis of the bionic arm	60
Table 3-3 Training and testing results for the three classifiers	67
Table 3-4 Confusion Matrix for the Support Vector Machine (SVM Classifier) Training (93.75%).....	67
Table 3-5 Confusion matrix for the SVM classifier: Testing (accuracy: 92.62%).	67
Table 3-6 Research Work Results using Myo armband.....	68
Table 4-1 Selected Parameters for the Classifiers in Users Verification System	82
Table 4-2 Results of Biometrics Users verification System	84
Table 4-3 Comparison between different research work of sEMG biometrics users verification system	86
Table 5-1 Selected Parameters of the Classifiers in Identification System.....	94
Table 5-2 Classifier Accuracy for users identification system	95
Table 5-3 Results of EMG Identification System	95
Table 6-1 Parameters of CWT	105
Table 6-2 Parameters for training fine-tuned Squeeze-Net.....	109
Table 6-3 CNN Performance results for Users Verification	109
Table 6-4 Parameters selected for Wavelet Denoising	113
Table 6-5 Parameters for Training Fine-Tuned SqueezeNet	116
Table 6-6 Performance Result for User Identification System	116

Symbols and Abbreviations

Abbreviation	Word
<i>3-D</i>	3 Dimensional
<i>ANN</i>	Artificial Neural Networks
<i>AR</i>	Augmented Reality
<i>AR</i>	Auto Regressive
<i>CAD</i>	Computer Aided Design
<i>CNC</i>	Computer Numerically Controlled
<i>CNN</i>	Convolutional Neural Network
<i>DT</i>	Decision Trees
<i>DOF</i>	Degree of Freedom
<i>DTW</i>	Dynamic Time Wrapping
<i>ECG</i>	Electrocardiogram
<i>EDA</i>	Electrodermal Activity
<i>EEG</i>	Electroencephalogram

<i>EMG</i>	Electromyography
<i>FAR</i>	False Acceptance Rate
<i>FRR</i>	False Rejection Rate
<i>FEA</i>	Finite Element Analysis
<i>FEA</i>	Finite Element Analysis
<i>GMM</i>	Gaussian Mixture Model
<i>GUI</i>	Graphical User Interface
<i>HGR</i>	Hand Gesture Recognition
<i>HW</i>	Hardware
<i>HMM</i>	Hidden Markov Model
<i>HCI</i>	Human-Computer Interaction
<i>IMU</i>	Inertial Measurement Unit
<i>IP</i>	Internet Protocol
<i>imEMG</i>	intramuscular EMG
<i>KNN</i>	K-nearest neighbour

<i>LBFGS</i>	Limited-memory Broyden–Fletcher–Goldfarb–Shanno
<i>LDA</i>	Linear Discriminant Analysis
<i>LDA</i>	Linear Discriminant Analysis
<i>MAV</i>	Mean Absolute Value
<i>MCU</i>	Microcontroller Unit
<i>MEMS</i>	Micro Electro-Mechanical Systems
<i>MLP</i>	Multi-Layer Perceptron's
<i>MLP</i>	Multi-layer Perceptrons
<i>NB</i>	Naive Bayes
<i>OS</i>	Operating System
<i>PLA</i>	Polylactic Acid
<i>PLA</i>	Polylactic Acid
<i>PSD</i>	Power Spectral Density
<i>PCA</i>	Principal Component Analysis
<i>RNN</i>	Recurrent Neural Network

<i>SNR</i>	Signal-to-Noise Ratio
<i>SDK</i>	Software Development Kit
<i>SD</i>	Standard Deviation
<i>SVM</i>	Support Vector Machine
<i>sEMG</i>	Surface Electromyography
<i>TPU</i>	Thermoplastic polyurethane
<i>VAR</i>	Variance
<i>WL</i>	Waveform Length
<i>WAMP</i>	Willison Amplitude
<i>ZC</i>	Zero-Crossing

Nomenclature

Symbol	Quantity
a_k	Auto Regression model parameters
$\Psi_{s,r}(t)^*$	Complex Conjugate
$e(t)$	Error
S_x	Estimation of the PSD
N	Length Segment
M	Length of the block
F_{max}	Maximum frequency
F_{med}	Median Frequency
F_{min}	Minimum Frequency
d_{st}	Minkowski distance
U	Normalization factor
L	Number of blocks
D	Shifting between the blocks

σ	Skewness
x_i	The value of the signal amplitude
τ	Translation
$p(x)$	Probability Density Function
$c(s, \tau)$	Wavelet Coefficient

Introduction

Wearable technologies are new technology raised in the last decades. With the advancement in this technology, its applications are immersed in several fields includes sports, health monitoring, biomedical and biometrics applications. In this thesis, the research focuses on using a wearable multi-channel armband in bionic arm control and biometrics applications. Myo armband is a wearable armband that includes eight dry sEMG electrodes. The sEMG signal measures the electrical potential of the muscles.

It has been reported that the amputee cases are rising, and there are around 50 million arm amputees in the world, around 40 million arm amputees in the developing nations. The arm amputees are suffering in doing their primary daily life activities. The prices of a functional bionic arm range around 25000\$. The research in bionics aims to detail designing a customizable sEMG-controlled wearable 3D printed bionic arm for an arm amputee. For this purpose, a 3D printed bionic arm is wholly designed, simulated, and implemented considering the bionic arm's cost and weight. Machine learning classifiers are optimized to achieve an accurate gesture recognition system to control the bionic arm.

On the other hand, it is known that electrical bio-signals can be used as biometric traits due to their hidden nature and ability to facilitate liveness detection. As a second application of this thesis, the viability of utilizing the sEMG signal as a hidden-biometric modality for user verification and identification is investigated. Several classifiers are applied in a trial to establish an accurate anti-spoofing biometrics system based on combinations of hand actions.

Specifically, in the field of electromyography-based biometrics systems, deep learning algorithms are seldom employed as they require an unreasonable amount of effort from a single person to generate tens of thousands of examples. In this work, data augmentation is used to extend the classical machine learning approach's database by augmenting multiple users' signals, thus reducing the recording burden. Convolutional Neural Network (CNN) is used to train the users in the EMG biometrics system. Squeeze net neural network structure is selected due to its faster training time as it requires fewer parameters while maintaining the accuracy level. Continuous wavelet transforms (CWT) are applied to the database to estimate the EMG signals' scalograms.

Objectives of the Thesis

The thesis focuses on the application of wearable 8-channel sEMG armband in Bionic arm control and biometrics applications.

The objective of the research conducted in the bionic arm:

- Detail a design of an affordable price 3D printed bionic arm for upper limb amputees.
- Design of adjustable socket to be attached with an amputee's arm with a maximum comfortable feeling.
- Construct a gesture recognition system based on sEMG signals.
- Create a database of sEMG signals represent gestures for the generic control scheme of the bionic arm.
- Extract the features of sEMG signals to detect four hand gestures (Fist, Open, Wave-in, and Wave-out)
- Optimize the Machine Learning algorithm's accuracy and select the best model to be used with the sEMG database.
- Perform testing on the bionic arm design and the algorithm used in the control of the bionic arm.

The design of the bionic arm should fulfill these points to ensure its success

- **Affordable:** The systems should be accessible for amputees since the selling price is one of the main factors to be considered during the design phase. The bionic arms available in the market are expensive compared to the 3D printed arm.
- **Portable:** The designed arm should be comfortable to wear for amputee cases.
- **Lightweight:** The lightweight design has been achieved by optimizing the system and using 3D printing technology in the arm's manufacturing process.
- **Generic:** To develop a bionic arm used by different amputees, database collected from different users, and machine learning algorithms applied.

Biometric authentication includes verification, and identification of users from sEMG signals has been studied. The thesis focuses on biometric systems' behavioral approach by defining a new hidden biometric system based on sEMG signals.

The objective of the research conducted in the biometric system:

- Verify the users from their hand actions as a new biometric system.
- Use the hidden biometric approach based on users' muscle actions to define an anti-spoofing biometric system.
- Construct a database from 8-channels sEMG signals. The database consists of hand gestures defining a password for each user.
- Extract the sEMG signals' main features to verify users from their hand action after declaring their identity.
- Optimize the accuracy of sEMG signals machine learning model and compare the accuracy of different machine learning models.
- Identify the users from sEMG signals without declaring their identity by extracting the main features from the sEMG signals.
- Optimize the accuracy of the machine learning models in the identification system.
- Apply deep learning algorithm after augmenting the sEMG data to find a technique of applying machine learning without extracting the features from sEMG signals, the proposed system to be used in biometrics verification and identification.
- Analyze the performance of the biometric system by calculating the false acceptance rate and false rejection rate to find the equal error rate of each proposed system.
- Accurate: The system must be accurate in the result. For biometrics verification, the result is access granted or denied, while in identification, the result is the user's identity. Therefore, the most precise algorithms to be chosen, and the success rate have been demonstrated after testing and calculating the False Acceptance Rate (FAR) and False Rejection Rate (FRR).

Thesis Contribution

The main contributions of this thesis are mentioned as follows:

- **Affordable price, lightweight, and 3-D printed bionic arm controlled by gestures:** Detailed design of an affordable price and lightweight bionic arm that comes with a bionic hand for right arm amputee cases. The bionic arm is equipped with four linear actuators that make it able to close the fingers to perform several grasping requirements. The 3D printed bionic arm was designed, simulated, and implemented for an affordable price and lightweight. The control of the bionic arm is performed by sEMG signals that are generated by the arm muscles.

- **Biometrics verification and identification system based on hand actions:**

Due to its live detection nature and anti-spoofing behavior, a biometrics system based on hand actions is optimized for the user's verification and identification. The database is created from 56 able-bodied users. Features are extracted in the frequency domain and time domain to optimize the results. Several classifiers based on K-nearest Neighbours (KNN), Linear Discernment Analysis (LDA), and Ensemble of Classifiers are constructed, trained, and statistically compared. False acceptance rate (FAR) and False Rejection Rate (FRR) are calculated for each classifier to evaluate the biometrics verification system's performance. In the user's identification system, features are extracted in the time domain from the signals to identify between the users from their biometrics identity without declaring their identity. The same three classifiers are used to classify the data; KNN, LDA, and Ensemble of Classifiers are constructed, trained, and statistically compared. The results obtained from the KNN classifier proved the concept of using the sEMG for user's verification and identification.

- **Deep Learning Algorithm for Biometrics system:** Recently, deep learning algorithms have become increasingly prominent for their unparalleled ability to learn from large amounts of data automatically. In this thesis, data augmentation is used to create a giant database out of a smaller database used in the classical machine learning approach by augmenting multiple users' signals, thus reducing the recording burden while enhancing the recognition rate. Convolutional Neural Network (CNN) is used to train the users in the EMG biometrics system. Squeeze net neural network is selected due to its faster training time as it requires fewer parameters while maintaining the accuracy level. Continuous wavelet transforms (CWT) are applied to the database to estimate the EMG signals' scalograms. In the identification system, five wavelet denoting levels have been applied to the raw data to augment the data.

Thesis Structure

The thesis starts with generalities about the nature of the sEMG signal and the wearable technology systems available on the market in chapter 1. Literature survey about results of the research done in wearable technologies, gesture recognition system based on sEMG signals, and biometric system based on behavioral of users in Chapter 2. Chapter 3 focuses on the detailed description of the bionic arm, including the detailed design of the arm, the amputee case involved in the study, the data collection of sEMG signals defining gestures, and the

application of machine learning models. Chapter 4 explains the verification process of users from the sEMG signal represents a hidden biometric system. The features extraction parameters will be mentioned in detail. Machine learning models and discussion of the results obtained are presented. Chapter 5 will discuss the Identification approach, including the features extraction process and the identification system results utilizing the same dataset used for the verification approach. Chapter 6 details the application of deep learning in the biometrics system in verification and identification approaches after augmenting the users' sEMG signals. Data augmentation is a technique that helps to increase the database of sEMG signals to avoid data acquisition from more users and more samples from each user. The sEMG signals are converted into images by applying continuous wavelet transform. These images are augmented to provide more data to be fed into the deep neural network. The biometrics systems result in using deep learning will be presented. Chapter 7 presents the conclusion and perspectives of the thesis.

1 Chapter 1 Generalities about Wearable Technology systems

Chapter Content

1.1	Introduction	24
1.2	Wearable systems on the market	25
1.2.1	BITalino Kit	25
1.2.2	MySignals Kit	26
1.2.3	Myo Armband.....	27
1.3	EMG Signal.....	28
1.4	Wearable Technologies in Bionic arm	29
1.5	Wearable Technologies in Biometrics	30
1.6	Conclusion.....	33

Summary: *The chapter briefly introduces the wearable technologies applications in biomedical, biometrics research, and biomechatronic applications. The wearable devices nowadays are equipped with multiple biosensors. Research in prosthetic devices has generated great attraction in the last decade as the number of amputees is increasing. The advances in wearable devices help in the development of bionic devices. Utilizing the fact that the wearable devices are made to be always with the owner, this makes wearable systems can effectively perform the biometrics rule of authenticating a user. The chapter offers a brief introduction about different wearable systems available in the market that offer the user the ability to acquire different bio-signals. The chapter focused on the definition of EMG signal used in this work by acquiring it using Myo armband, which is explained in this chapter.*

First, an introduction to wearable technologies is presented in section 1.1 and followed by studying the available systems on the market that offer a wearable system in section 1.2. The EMG signal selected to be studied in detail in this thesis is explained in section 1.3. The wearable technologies in the bionic arm and biometrics are described in sections 1.4 and 1.5. The chapter ended by listing the thesis's objective, thesis contribution, and thesis structure in sections 1.6, 1.7, and 1.8.

1.1 Introduction

Wearable technologies applications in the biomedical, biometrics research, biomechatronic, and different fields are gaining significant interest over the last years (V. Enzo, P. Scilingo and Gaetano, 2017). Comfortable to wear, optimum size, and lightweight monitoring systems with smart-power consumption for collecting physiological and behavioral data in ecological scenarios (e.g., at home, during daily activities like driving or sleep, during specific tasks, while driving) with comfort for different users. As a result, the quality of life can be improved by the patients monitoring care, especially for patients with chronic disease, possibly preventing the habit of going to hospitals and paying unnecessary costs.

Within this context, wearable systems have reached a level to be ready for clinical applications (P. Bonato, 2003). Many companies are investing funds for the research and development department to focus on a wearable system for clinical application. They are encouraging researchers in that field to focus more and more on improving people's life. This technology grows in a stable trend, showing a promising result that wearable systems will soon be part of everyone's daily life.

The enthusiasm for wearable frameworks starts from the need to observe people over broad timeframes. This case emerges when doctors need to screen people whose incessant condition incorporates the danger of sudden intense occasions. Wearable technology opens the door to different applications.

Research in prosthetic and medical devices has generated significant attraction in the last decade because of the increasing demand for robust bionic arm, fulfilling the patient's need to perform various tasks. Generally, gesture recognition techniques enabled the manufacturer to improve both the accuracy and functionality of bionic hands, allow the patient control over delicate operations in dangerous situations, or help patients with movement disorders and disabilities, as well as in the rehabilitation training process. The application of wearable sensors allows a more compact design and a more straightforward implementation of upper limbs.

Wearables that are equipped with embedded bio-sensors are very well suited for biometric verification and offer advantages compared to traditional biometric systems. A significant advantage is that the wearable systems are made to be always with the owner; at the same time, conventional biometric systems are installed generally at a fixed location. Wearable biometric systems can effectively perform continuous verification of the user. Another advantage is that

the owners shouldn't share their biometric traits, generally considered compassionate information, with a third party for storage since all data can be stored inside the wearable device.

1.2 Wearable systems on the market

There are many systems available on the market that offer the user the ability to acquire bio-signals. Several requirements and criteria differentiate between these systems. The cost of the system is one of the most important criteria. The connectivity with the processor either wireless or with wires. The accuracy of the bio-sensors in the system. The battery consumption rate gives the system the ability to stay powered for a long time. The Software Development Kit (SDK) is available with the design, allowing the researchers to quickly develop their systems and access the raw signals for further development.

1.2.1 BITalino Kit

BITalino development bio-medical kit is one of the most potent kits available on the market. It gives the user the ability to work on physiological data. This kit comes with an sEMG sensor that monitors the muscle activation using three wet bipolar surface electrodes (plus a ground lead), Measuring the electrical activity in muscles and nerves. Surface electromyography (sEMG) is a technique that is used in many clinical and biomedical applications in areas like HCI, neurology, rehabilitation, orthopedics, ergonomics, and sports. It is widely used as a biofeedback tool to assess muscle fatigue; disorders of motor control and low-back pain is also possible with the EMG sensor. Sensing isometric muscular activity, where no movement is produced, enables a definition of classes of subtle motionless gestures to control interfaces without being noticed and without disrupting the surrounding environment. These signals can be used to control prosthetic devices such as prosthetic hands, arms, and lower limbs or as a control signal for an electronic device such as a mobile phone.

Conduction of action potentials through the heart generates electrical currents that can be picked up by electrodes placed on the skin. A recording of the electrical changes that accompany the heartbeat is called an electrocardiogram (ECG). Variations in the size and duration of the waves of an ECG are useful in diagnosing abnormal cardiac rhythms and conduction patterns. The ECG works mostly by detecting and amplifying the tiny electrical changes on the skin that are caused during the heart muscle cycle during each heartbeat. The

ECG sensor provided by BITalino uses only two electrodes to acquire the signal. The essential ECG sensor applications focus on the patient's wellness and include heart rate and stress monitoring, biometric verification, and live monitoring.

Electrodermal Activity (EDA) is defined as a transient change in the skin's electrical properties associated with the sweat gland activity and elicited by any stimulus that evokes an arousal or orienting response. The EDA sensor can measure skin activity with high sensitivity measurement power in a miniaturized form factor. With low noise signal conditioning and amplification circuitry, the EDA sensor provides accurate sensing capability and detects even the feeblest electrodermal skin response events using two electrodes. Some of this sensor's applications include the detection of changes in the conservative, cognitive, and emotional states. EDA sensors were also used for relaxation biofeedback, sympathetic nervous system reaction detection, among many others.

The triaxial accelerometer is based on MEMS (Micro-Electro-Mechanical Systems) technology and has been developed for biomedical applications where kinematic and motion measurements are required. This sensor can measure accelerations relative to free fall, and the model available can detect the magnitude and direction of this same acceleration as a vector quantity. This resulting vector can then be used to sense position, vibration, shock, and fall. Attaching the accelerometer to a limb, for example, acceleration can be measured within the sensor's dynamic range.

The revolutionary kit comes with a Microcontroller Unit (MCU) in a tiny size that can connect all the sensors. The MCU has six analog input ports 4 (10-bit), 2 (6-bit), and it has eight digital ports, four ports digital input (1-bit), four ports digital output (1-bit). All acquired signals can be transmitted wirelessly using Bluetooth V2.0.

The BITalino kit has some advantages in terms of the number of sensors embedded inside it and the wireless communication with the central processor. Also, the size of the sensors is tiny to be embedded inside any wearable device. This system's shortcoming is that the electrodes are wet since it needs a gel and are connected via wires to the human skin, making uncomfortable feeling to the user. (S. Said, S. Alkork, T. Beyrouthy, and M. Fayek, 2017)

1.2.2 MySignals Kit

MySignals is a development platform for medical devices and eHealth applications. It is used to develop eHealth web or even to build new medical wearable devices. MySignals hardware

(HW) Complete Kit includes seventeen sensors that allow the user to measure 20 different biometric parameters. The parameters are oxygen in the blood, pulse rate, breath rate, oxygen in the blood, electrocardiogram signals, blood pressure, muscle electromyography signals, glucose levels, galvanic skin response, lung capacity, snore waves, patient position, airflow, and body scale parameters (weight, bone mass, body fat, muscle mass, body water, visceral fat, Basal Metabolic Rate, and Body Mass Index). With all the sensors and features allow MySignals Kit to be the complete eHealth platform in the market. All the data acquired by MySignals is encrypted for personal information security and sent to the user's private account at Libelium Cloud through Wi-Fi or Bluetooth. The data can be visualized in any smart devices ranging from smartphones to PCs.

1.2.3 Myo Armband

Myo Armband is the basic concept of Human-Computer Interaction (HCI) in which humans interact with computers and design technologies that let humans interact with computers interactively. Hence Myo is a new way that is used to control the real-life applications by the human. The structure of Myo consists of the EMG (electromyography) sensor and an Inertial Measurement Unit (IMU), which includes a gyroscope, accelerometer, and a magnetometer (S. Rawat, S. Vats and P. Kumar, 2016) (Myo Armband, n.d.).

Thalamic Labs developed Myo Armband. Myo is an armband that can be worn on the forearm below the elbow controlled by human gestures and movements. With Myo's help, many tasks are done easily, like controlling lights, robots, drones, and change slides of the presentation by just waving a hand in lectures. Myo can be used to interface with software and electronics by their gestures and hands movement. Myo plays a vital role in the medical field; doctors can examine the EMG reports and control their electronic devices (S. Rawat, S. Vats and P. Kumar, 2016).

Myo Armband detects the electrical activity in forearm muscles just below the elbow. The human forearm has different types of muscles, each of which has another arrangement, and these muscles control the movement of the wrist, such as moving fingers, making a fist, turning left or right.

Myo armband is designed in a wearable way. It can fit in the human forearm easily. Sizing clips are available, which allow for a more constrained grip, better suited for smaller arms. The sizing clips enable it to expand between 7.5 - 13 inches (19 - 34 cm) forearm circumference.

Unlike other EMG sensors, the Myo armband does not require the wearer to shave the area around which the armband electrodes will be worn. This allows for more comfortable setup procedures in real-world environments. The Myo armband weighs 93 grams, which gave it the ability to be wearable for a long time without uncomfortable feeling to the wearer. The Myo armband design is thin with a thickness of 0.45 inches (1.14 cm), which allows it to be worn under the shirts.

The Myo armband structure shown in Figure 1-1 has eight medical dry grade stainless steel EMG sensors like other surface electrodes (sEMG), the EMG signals returned by the sensors represent the electric potential of the muscles because of muscle activation (Myo Armband, n.d.). These electrodes don't need any gel to be added to human skin to acquire the signal. However, since the electric potential of muscle is small in the range of sub millivolts, signals are sensitive to other electric noise sources such as electric noise induced by wall-electricity. The content of potentials provided by the Myo armband is between -128 and 128 in units of activation. These units of activation are integer values of the amplification of the potentials measured by the sEMG sensors. The Myo armband can pull sEMG data at a sample rate of 200Hz.

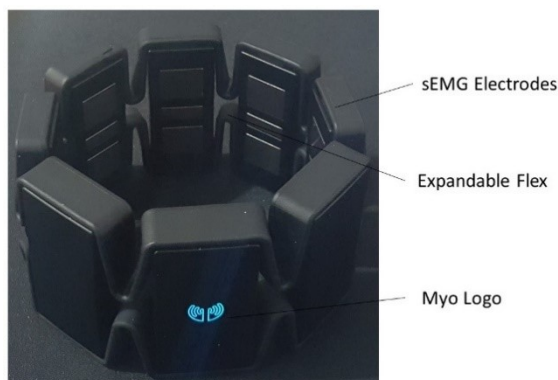


Figure 1-1 Myo armband structure

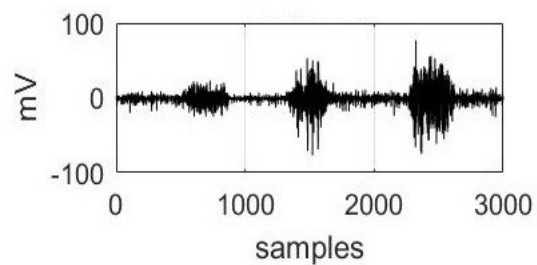


Figure 1-2 sEMG signal generated by Myo Armband

1.3 EMG Signal

EMG signals record the electric potential activities generated by skeletal muscles, which usually have a potential difference when the muscles are electrically or neurologically activated. Therefore, when recording EMG signals, at least one pair of electrodes are needed to capture the signal. Sometimes an array of multiple electrodes is used to record the activities

of more than one muscle simultaneously. (Qingqing Li, Penghui Dong and Jun Zheng, 2020) (Robertson, D. G. E., Caldwell, G. E., Hamill, J., Kamen, G., and Whittlesey, 2014).

There are two types of EMG: surface EMG (sEMG) and intramuscular EMG (imEMG). sEMG signals which are used in this work are obtained by measuring muscle activities on the skin surface. On the other hand, imEMG signals are recorded from the muscle tissue acquired by percutaneous wire needle electrodes inserted into a muscle with a surface electrode on the skin as a reference. Compared with imEMG, sEMG is a way more convenient to acquire and is non-invasive. In this study, sEMG signals are recorded from the forearm muscle as the biometric information for user verification. The sEMG signals are obtained using the 8-channel wearable bracelet. Figure 1-2 shows the raw sEMG signal from one electrode acquired by Myo armband, while the user performs three hand gestures before signal processing.

1.4 Wearable Technologies in Bionic arm

Many people have difficulty in their lives because of disability, which stops them from performing their daily activities. The statistics study stated that 15% of the world's population having some forms of disability. Amputee's number is around 10 million out of the world's population, of which 30% of them are arm amputees (Hawking, 2011). The total number of amputees and limb dysfunction patients are increasing due to many reasons. Arm amputation is classified as either born without an arm or portion of it or wholly lost of the arm due to disease or accident. Both cases are suffering while performing their daily life activities, indeed help from others (S. Hasan, K. Al-Kandari, E. Al-Awadhi, A. Jaafar, B. Al-Farhan, M. Hassan, S. Said, and S. AlKork, 2018).

There are different solutions to help the amputees, but these solutions have some drawbacks like being costly to the point that not everyone can afford it or hard to install or maintain or require surgical operations. Surgical arms rely on the nerves, which, might be damaged, in some cases (Junhua Li, Gong Chen, Pavithra Thangavel, Haoyong Yu, Nitish Thakor, Anastasios Bezerianos, and Yu Sun, 2016). The mind-controlled made of the 3D printed material arm has the requirements to help amputees perform many of their daily activities, provide a better life, and improve the quality of life. Besides, it uses brain-signals and thoughts to allow amputees to control the arm actuators. There are also several existing solutions, such as surgical arm, myoelectric-controlled arm, and cosmetic restoration. Each type has advantages and drawbacks. One of the solutions for amputees is having a prosthetic arm. The

prosthetic arm needs to be customized to the patient's needs. The second solution is the surgical limbs, where the patient will have to undergo a surgical operation to attach the arm to the bones and nerves. The surgical method is very costly. Some problems may happen due to the surgical arm. For example, sometimes the nerves may cause a problem when they are damaged totally, making it hard to perform surgery. Also, the surgical method causes heart disease and back pain in some patients. The amputees face nociceptive and neuropathic pain due to bone and soft tissue injury.

On the other hand, the prosthetic arm has fewer problems when compared to the surgical arm. Prosthetic arm avoids many medical issues that may result from the surgery procedure. There are many techniques to control a robotic arm. One method is to use an electroencephalogram (EEG) device. The EEG is a headset that records the brain waves when the person thinks of action or implements a facial expression. The EEG will read signals and then convert them to commands to send them to the arm. The second technique is to use Muscle Activity Sensors called surface electromyography (sEMG) sensors. The signals can be analyzed to detect medical abnormalities, activation levels, or recruitment orders or analyze humans' biomechanics. sEMG signals are processed for multiple hand gestures and movement recognition. EMG monitors the electrical signals under human skin that are produced by the muscles.

Myo Armband has been used in a very efficient way by researchers at Johns Hopkins University (2016) to control a prosthetic limb using electric impulses transmitted from an amputee's mind to his limb. The armband works by reading the electromyographically (EMG) impulses triggered by a thought from a person's brain, sending a signal to a limb, which causes a movement. A transradial myoelectric prosthesis based on an innovative mechanism called Adam's hand has been developed. It can actuate five three-phalanx fingers (15 degrees of freedom). Adam's Hand fingertips are provided with temperature and pressure sensors, while the myoelectric user signals are acquired wirelessly employing the Myo armband (Gaetani, F., Primiceri, P., Zappatore, G. A., and Visconti, P., 2018).

1.5 Wearable Technologies in Biometrics

The growing popularity of wearable devices leads to new ways to interact with the environment (J. Blasco, T. M. Chen, J. Tapiador and P. Peris-Lopez, 2016), with other smart devices, and with other people. Wearables equipped with an array of sensors can capture the owner's

physiological and behavioral traits, thus are well suited for biometric systems to control other devices or digital access services. However, wearable biometrics have substantial differences from traditional biometrics for computer systems, such as fingerprints, eye features, or voice.

Biometric recognition can be viewed as a pattern recognition problem in which a user who wants to be authenticated provides a set of physiological and behavioral characteristics to match a previously registered signature (or reference). Biometrics takes advantage of the fact that humans have natural diversity and certain traits are unique for everyone. Biometric systems, whether traditional or not, are usually composed of the three main functional components:

- (i) Sensor or set of sensors that capture raw biometric signals (r).
- (ii) A signal-processing unit that pre-processes and extracts feature vectors from the signals.
- (iii) Recognition system, which usually includes a signature (or template) database and implements a pattern recognition function. The physical features include fingerprint, face recognition, and eye (Iris) scan. While the behavioral ones have gait recognition, voice recognition, Electrocardiography (ECG), Electromyography (EMG), and an electroencephalogram (EEG) (Moon, K. Y., 2005) (Bailey, K. O., Okolica, J. S., and Peterson, G. L, 2014).

The matching phase depends on the mode of operation, either verification or identification. Biometric verification systems are configured by a sole user to verify the user's identity later. In biometric identification, the system is presented with a biometric signal and must decide who is the owner of that signal from a pool of registered users

A biometric system should fulfill the following requirements:

- Performance: The system should respond promptly to queries with satisfactory accuracy
- Acceptance: The system must be accepted by its intended users to be practical. If a sensor or device is not comfortable enough, it will not be used.
- Circumvention: The system should not be easy to circumvent. This implies that the system should be protected against unauthorized access to any of its components.

The wearable biometric system in which its primary user controls all the system components, including the signature database. A wearable biometric system requires owners to wear the sensor that captures their biosignals continuously. The signal processing and recognition units can also be embedded in the same wearable device or a different smart device (e.g., a smartphone, pc). The resources unlocked when the wearable successfully recognizes the user right include the rest of the services provided by the wearable or a cryptographic key that can be used to prove the identity of the user to other systems (Rathgeb, C., and Uhl, A, 2011). In any case, the process triggered after verification is out of the scope of this survey.

In this configuration, wearable sensors are capable of reading signals from the subject at any time. This enables the biometric system to authenticate the wearer continuously. Figure 1-3 shows the process of biometrics systems to verify a user.

Wearable biometric systems are generally used for identity verification processes. In this case, the subject's biometric traits never leave the user; they are stored in the wearable or a smart device in the user's possession. This avoids other entities accessing the user's biometric traits provided that the devices are correctly configured and protected against external attackers. An example of a commercial product implementing this philosophy is Nymi (<https://nyimi.com/>, n.d.). Nymi is a biometric verification wristband that includes one electrode in direct contact with the wrist and a second electrode that the user must touch with a finger from the opposite hand. When the user identity is verified, it has access to previously stored security tokens that can be used to verify the user against other devices, such as a car or a lock.

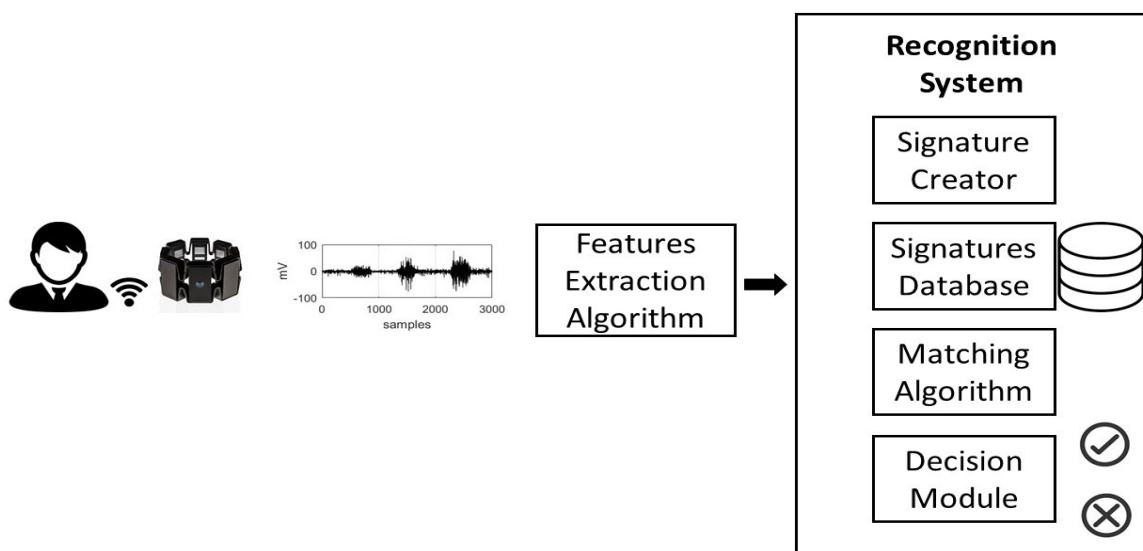


Figure 1-3 Wearable Armband for biometrics verification

With advancements in biometrics technology nowadays, some biometric systems don't meet security levels' requirements to support their operations in different scenarios. Among the existing difficulties are the sensitivity to spoofing persons who act as others to get illegal access to protected information, services, or facilities (Abdenour Hadid, Nicholas Evans, Sébastien Marcel, and Julian Fierrez, 2015) (Evans, 2019). While the study of spoofing, or rather anti-spoofing, has attracted growing interest in recent years, the problem is still requiring more research in the coming years. Table 1-1 shows various crimes or falsifying biometrics identity.

Table 1-1 Examples of crimes using physical features

Country	Details
USA	Hacking using live images of the registered user's face
Brazil	Passing through the entrance using fake silicon fingerprint
Korea	Korea Financial accidents 3- Dimensional (3-D) printed fake fingerprint
Japan	Japan Electronic passports using fake fingerprint
Russia	Russia Hacking using the iris reproduced from the president's photo

1.6 Conclusion

Wearable systems are used in several applications such as biomedical devices control and biometrics systems to control user and clinical applications access. sEMG sensors are used to record the electric potential activities generated by skeletal muscle. Different available methods on the market are presented, focusing on the Myo armband, which will be used in this research. The applications of sEMG signals in the bionic arm are important to control the devices' actuation by the users' muscles. Also, sEMG signals in biometrics applications are discussed in this chapter. The thesis focuses on sEMG signal applications to control a 3D printed Bionic arm and control users' access to the biometrics system.

2 Chapter 2 State of the Art on sEMG Control Systems

Chapter Content

2.1	Introduction	35
2.2	State of the Art on EMG Gesture Recognition System and Bionic Arm.....	35
2.2.1	Review of EMG Gesture Recognition System	35
	• Gesture Acquisition Systems	38
	• Features Extraction Techniques for Gestures Recognition System.....	39
	• Classifiers for sEMG Gestures Recognition System.....	40
2.2.2	Review of 3D printed Bionic Arm.....	41
2.3	State of the Art of EMG biometrics system	44
2.4	Conclusion.....	47

Summary: This chapter shows a detailed state of the art on the applications of the sEMG signal in the control system. The chapter states different types of machine learning algorithms applied in gesture recognition systems in general and specifically in the control of bionic arms.

The EMG signal is used in the biometrics verification system due to its live detection and hidden nature. Several kinds of research conducted in that field with different machine learning and deep learning applications are stated in the chapter to provide the reader with the previous study conducted in the area.

The chapter starts with a general introduction about the EMG signals application in the bionic arm and biometrics system in section 2.1. A detailed literature study about the gesture recognition system in section 2.2. Different 3D printed research work utilizing the technology of 3D printers is in section 2.2.2. The state of the art on the sEMG biometrics system is written in section 2.3.

2.1 Introduction

Wearable technologies, consisting of a smart device that is to be worn by the users and equipped with biosensors embedded inside them, are the focus of the majority of researchers in this modern era. Smart-textile or contactless electrodes and algorithms that are effective for signal processing in embedded systems, along with sensing platforms and machine learning algorithms, are a short glimpse of examples of such technologies. Few types of research results will be stated in the wearable systems field in this chapter.

Moreover, in biosensors or wireless body sensors networks, special efforts have been made for harvesting energy and small-scale integration of analog and digital sensor signal conditioning. Published researches during the last few decades also confirm the massive impact of wearable technologies.

This chapter focused on the state-of-the-art in the fields of applications of the wearable sEMG sensors. sEMG based bionic arm for amputee cases and biometrics identity based on the sEMG signals.

2.2 State of the Art on EMG Gesture Recognition System and Bionic Arm

2.2.1 Review of EMG Gesture Recognition System

The increase in computing power has brought the presence of many computing devices in human beings' daily lives. A broad spectrum of applications and interfaces have been developed so that humans can interact with them. The interaction with these systems is more comfortable when they tend to be performed naturally (i.e., just as humans interact with each other using voice or gestures). Hand Gesture Recognition (HGR) is a significant element of Human-Computer Interaction (HCI), which studies computer technology designed to interpret commands given by humans.

Hand gestures are communication tools considered non-verbal. The communication is through the human hand combinations of actions. This modality is used either independently or with other communication methods such as speech (Kendon, 2004). Hand gestures are extensively used on different applications, varying from human applications' safety, for example, using hand gestures to direct flight operations to applications that are made for

controlling purposes, like using hand actions in controlling electronics devices (Yasen, M., and Jusoh, S., 2019).

The increase in computing power has brought the presence of many computing devices in human beings' daily lives. A broad spectrum of applications and interfaces have been developed so that humans can interact with them. The interaction with these systems is more comfortable when they tend to be performed naturally (i.e., just as humans interact with each other using voice or gestures). Hand Gesture Recognition (HGR) is a significant element of Human-Computer Interaction (HCI), which studies computer technology designed to interpret commands given by humans. Hand gestures, one of the most famous human-computer interaction applications (Aashni, H., Archanasri, S., Nivedhitha, A., Shristi, P., and Jyothi, S. N., 2017). It does have a wide range of applications that grant the speed of communication with the computer, provide a user-friendly environment to attract users, provide private use of the computer from a distance for user safety and comfort, and control complex and virtual environments more efficiently.

Hand gesture applications require the user to undergo training to be an expert at understanding and employing the mapping of different gestures (Yasen, M., and Jusoh, S., 2019). There are countless numbers of combinations of hand gestures; therefore, for each particular application, a diverse group of gestures is used to perform its functions.

The PC can recognize different users. It can also detect the other environmental factors affecting its surrounding. Hand gesture recognition is a considered perceptual computing user interface used in HCI to provide the computers with the capability to interpret and capture hand gestures and execute commands according to the understanding made for a particular gesture. (Panwar, M., and Mehra, P. S., 2011).

Hand gesture recognition requires steps to accomplish it that vary based on the desired application from simple to complex applications. These steps are categorized: first-hand gesture frame acquisition, followed by hand tracking, then feature extraction, and at the end classification to reach the detect the gesture.

Hand gesture frame acquisition is to record the human hand gesture and store it on the computer. Hand tracking is the computer's ability to recognize the hand and separate it from other items' background in image processing. The extracted features differ from one application to another (Sharrma, A., Khandelwal, A., Kaur, K., Joshi, S., Upadhyay, R., and Prabhu, S.,

2017). In artificial intelligence, machine learning aims to allow the computers to learn without being pre-programmed to adapt to new input and make decisions according to the trained model. There are two types of learning; supervised machine learning, in which the algorithms reflect the gestures that have been learned in advance in the training phase to new gestures, and unsupervised machine learning, in which the algorithms draw inferences from the gestures. Classification aims to build a model to classify new hand gestures based on previous training gestures.

Figure 2-1 shows the steps of hand gesture recognition, image frame acquisition, or gesture acquisition to recognize the computer's human hand gesture image.

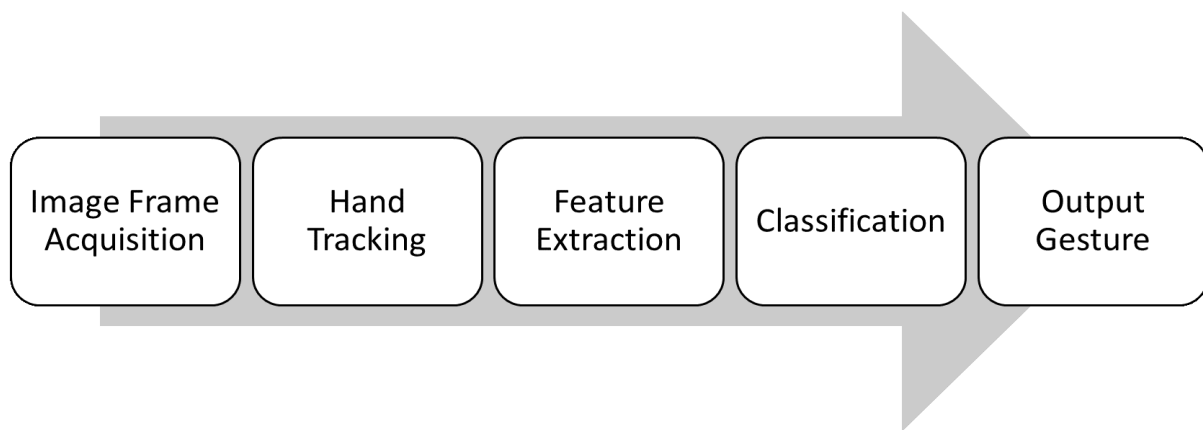


Figure 2-1 Basic Steps of Hand Gesture Recognition (Yasen, M., and Jusoh, S., 2019)

This can be accomplished using simple vision-based recognition, which doesn't require a unique setup, and a web camera or a depth camera is used. Also, special tools can be used like wired or wireless gloves that capture the movements of the wearer's hand and motion sensings input devices such as Leap Motion or Kinect from Microsoft.

The hand tracking process is defined as the computer's capability to detect the hand and exclude it from the background and recognize it. Multi-scale color feature hierarchies give the users hand and the different background shades of colors to identify and remove the background. Also, clustering algorithms can be used to treat each finger as a cluster by itself, removing the empty spaces detected between them.

The features extracted differ based on the required application; some parameters should be taken into consideration are thumb status, finger status, alignments of fingers, skin color, and the palm position. These features, along with other features, are extracted using several techniques available, such as the centroid method, which is used to capture the hand's main

structure, or the Fourier descriptor method, which captures the palm, the fingers, and the fingertips (Matsumoto, Y., and Zelinsky, A., 2000).

The extracted features are input to training and testing the classification algorithm (such as), K-nearest neighbor (KNN), Artificial Neural Networks (ANN), Support Vector Machine (SVM), Naive Bayes (NB)) to detect the output gesture.

- **Gesture Acquisition Systems**

Several hand acquisition systems have been proposed aiming to detect hand gestures. The work in (Gunawardane, P. D. S. H., and Medagedara, N. T., 2017) compared to the Leap Motion Controller's use to track the human hand's motion with a data glove using flex sensors, gyroscopes, and vision data. The results showed that the Leap Motion Controller had high potential and high repeatability for soft finger type applications. Researches showed that the Leap Motion controller is used to detected gestures (Pramunanto, E., Sumpeno, S., and Legowo, R. S., 2017) (Canavan, S., Keyes, W., McCormick, R., Kunnumpurath, J., Hoelzel, T., and Yin, L., 2017).

Siji Rani et al. (Rani, S. S., Dhriya, K. J., and Ahalyadas, M., 2017) used a new Hand Gesture Control in the Augmented Reality System (HGCARS). A secondary camera is used in gesture recognition, and the reality is recorded using an Internet Protocol (IP) camera. The video obtained from the IP camera is fed with a virtual object and controlled using the position and depth of hand, measured using a webcam.

Hafiz et al. (2017) (H. M. Abdul-Rashid, L. Kiran, M. D. Mirrani and M. N. Maraaj, 2017) proposed a CMSWVHG (Control MS Windows via hand Gesture). An internal or external camera is used for taking input instead of a mouse by performing numerous windows actions using hand gestures. This system controls OS on the projected screen for a virtual mouse system without the hardware requirement rather than a camera.

A wearable hand gesture recognition system in real-time, which receives data from surface electromyography (sEMG) has been extensively used in hand gesture recognition system by most of the researchers within the last three years (J. Zhao, J. Mao, G. Wang, H. Yang and B. Zhao, 2017) (Yang, J., Pan, J., and Li, J., 2017) (Redrovan, D. V., and Kim, D., 2018) (Lian, K. Y., Chiu, C. C., Hong, Y. J., and Sung, W. T., 2017) (Tomczyński, J., Mańkowski, T., & Kaczmarek, P., 2017). The commercial wearable sEMG wristband, which is placed in the forearm of a human, has been used extensively for real-time hand gestures recognition systems

(M. E. Benalcázar, A. G. Jaramillo, Jonathan, A. Zea, A. Páez and V. H. Andaluz, 2017) (Krishnan, K. S., Saha, A., Ramachandran, S., and Kumar, S., 2017). It achieved high accuracy in hand gestures recognition-based systems (Sapienza, 2018).

- **Features Extraction Techniques for Gestures Recognition System**

Generally, the feature extraction and pattern recognition stages are crucial for the gesture recognition systems to capture gestures well. In the feature extraction stage (Liu, J.; Zhou, P., 2013), the eigenvalues and the feature vectors for each sEMG sample are selected for classifying the gestures. This procedure can be achieved using several approaches, such as time-domain, frequency-domain, and time–frequency-domain features. Li et al. (Li, X., Fu, J., Xiong, L., Shi, Y., Davoodi, R., and Li, Y., 2015, September) combined force prediction with finger motion recognition, which the time domain and autoregressive methods were both used to extract features along with a principal component analysis (PCA) approach, was used for further dimensionality reduction. Khezri et al. (Khezri, M., and Jahed, M., 2007) proposed a system based on the adaptive neuro-fuzzy inference system to recognize six hand gestures. For the feature extractions, the time and frequency domains, and their combination were used to extract eigenvectors, and the system provided a recognition rate of 92%.

Similarly, Chu et al. (Chu, J. U., Moon, I., and Mun, M. S., 2006) used a wavelet packet transform to extract the feature vectors, and then a dimensional reduction was performed using the PCA algorithm. The results show that the eigenvector extraction procedure has more impact on recognition accuracy than the classifiers' ability. Huang et al. (Huang, Y., Englehart, K. B., Hudgins, B., & Chan, A. D., 2005) proposed a system for multi-limb movements using the Gaussian mixture model (GMM). The obtained results indicated that the GMM algorithm has a reasonable classification recognition rate at a low computational cost. Noce et al. (Noce, E., Bellingegni, A. D., Ciancio, A. L., Sacchetti, R., Davalli, A., Guglielmelli, E., and Zollo, L., (2019)) introduced a new approach for neural control of hand prostheses. This approach is based on pattern recognition applied to the envelope of neural signals. In this approach, sEMG signals were simultaneously recorded from one human amputee, and the envelope of the sEMG signals was computed. The results obtained in this study showed that well-known techniques of sEMG pattern recognition could be used to process the neural signal and pave the way to applying neural gesture decoding in upper limb prosthetics. Shi et al. (Shi, W. T., Lyu, Z. J., Tang, S. T., Chia, T. L., and Yang, C. Y., 2018) proposed a bionic hand controlled by hand gestures, while the gestures were recognized based on surface EMG signals. The proposed

approach was based on extracting multiple features, such as absolute value, zero crossings, slope sign change, and waveform length. The results show that the KNN classifier was able to recognize four different hand postures.

- **Classifiers for sEMG Gestures Recognition System**

The classifier plays an essential role in the pattern recognition block. The features extracted (such as Artificial Neural Networks (ANN), K-nearest neighbor (KNN), Naive Bayes (NB), Support Vector Machine (SVM)) to be able to classify the gestures.

Chun-Jen et al. (C. Tsai, Y. Tsai, S. Hsu, and Y. Wu., 2017) proposed a 3D hand gesture identification using a synthetically-trained neural network. The training phase of a deep-learning neural network required a large amount of training data. Chenyang, Xin et al. (C. Li, X. Zhang and L. Jin, 2017) proposed using the LPSNet, an end-to-end deep neural network for hand gesture recognition with novel log path signature features. Some researchers depend on deep neural networks for hand gestures classification.

Sungho et al. (Shin, S., and Sung, W., 2016) developed two techniques for dynamic hand gesture recognition applying low complexity recurrent neural network (RNN) algorithms utilizing wearable devices, the first approach is based on video signal using convolutional neural network (CNN) with RNN for classification, and the other system utilizing accelerometer data and applied RNN for classification. Also, Xinghao et al. (Chen, X., Guo, H., Wang, G., and Zhang, L., 2017) used a bidirectional recurrent neural network (RNN) with the skeleton sequence to augment the motion features for RNN.

Aditya et al. (Aditya T, Bertram T, Frederic G, and Didier S., 2017) tried to enhance the gesture detection rate by correcting the probability estimate of a Long-Short-Term Memory (LSTM) network by pose prediction performed by CNN. They applied Principal Component Analysis (PCA) as a training procedure to reduce the dimensionality of the labeled data of hand pose classification to improve CNN's initialization of weights.

Support vector machine (SVM) was used for classification in hand gestures recognition system (Zhu, Y., Jiang, S., and Shull, P. B., 2018) (Sugiura, Y., Nakamura, F., Kawai, W., Kikuchi, T., & Sugimoto, M., 2017) (R. A. Bhuiyan, A. K. Tushar, A. Ashiquzzaman, J. Shin and M. R. Islam, 2017) (Tian, Z., Wang, J., Yang, X., and Zhou, M., 2018). Jian et al. (J. Zhao,

J. Mao, G. Wang, H. Yang and B. Zhao, 2017) recognized the pattern of hand gestures using a modified deep forest algorithm.

In the research conducted by Jinxing, Jianhong et al. (Yang, J., Pan, J., and Li, J., 2017), the hand gesture was modeled and decomposed using Gaussian Mixture Model-Hidden Markov Models (GMMHMM); GMMs are used as sub-states of HMMs to decode the sEMG feature of gesture.

Whereas Marco et al. (Benalcázar, M. E., Jaramillo, A. G., Zea, A., Páez, A., and Andaluz, V. H., 2017) used the dynamic time warping algorithm along with the k-nearest neighbor rule together for the classification. Naive Bayes is applied as the training method for classification (Pramunanto, E., Sumpeno, S., and Legowo, R. S., 2017). Multiple linear discriminant analysis (LDA) classifier was adopted to classify different hand gestures (Bulugu, I., Ye, Z., and Banzi, J., 2017).

2.2.2 Review of 3D printed Bionic Arm

3D printing of upper limb prostheses has been significantly developed over the last five years. All over the world, people customize the designs and printing new devices that can easily fit an amputee's arm. Several kinds of research have been published in 3D-printed upper-limb prostheses (Gretsch, K. F., Lather, H. D., Peddada, K. V., Deeken, C. R., Wall, L. B., and Goldfarb, C. A., 2016) (O'Neill C., 2014).

The cost of a commercial body-powered prosthetic hand ranges from \$4000 to \$10,000 (Resnik, L., Meucci, M. R., Lieberman-Klinger, S., Fantini, C., Kelty, D. L., Disla, R., and Sasson, N., 2012) while the cost of an externally powered prosthetic hand can range from \$25,000 to \$75,000 (van der Riet, D., Stopforth, R., Bright, G., and Diegel, O., 2013). The development of a 3D-printed hand prosthesis aimed to offer an affordable low-cost commercial prosthesis for people who cannot afford an expensive prosthesis.

3D-printing is categorized as an additive manufacturing technique. The products are built up layer by layer, which is different from other manufacturing processes based on removing material from a large piece of material, such as in Computer Numerically Controlled (CNC) milling. 3D-printing has several benefits in comparison with other manufacturing techniques (Doubrovski Z, Verlinden JC, and Geraedts JMP., 2011):

- No assembly is required since it is possible to build up products out of one part.

- With the flexibility in the design, therefore, highly complex geometries can be made.
- The designs can be modified and personalized; there is no need to change the machine.
- Parts can be produced quickly and easily from conceptual design to the final product, giving rapid prototyping and design improvements.

Different specifications of the fingers' prostheses and mechanical specifications should be encountered in the design of the upper limb prostheses, weight, function, actuation, comfortability, and cost. Some examples of the 3D-printed upper limb prostheses are shown in Figure 2-2. These can be categorized as three different levels of prostheses: Upper arm, the amputation level is above the elbow, Forearm, the amputation level is below the elbow and Hand, the amputation level is a partial hand. The various types of actuation for the different types of prostheses. Most of the prostheses for people with partial hand amputation are body-powered. There are four actuation techniques for forearm prostheses: two are passive static, one is passively adjustable, are body-powered and externally powered. There are two categories for externally powered prostheses: electrically powered arms and one is powered by pressurized air. All the upper arm prostheses are externally powered, and all are electrically powered.

The prosthetics arm's weight is one of the most critical factors that affect the device's comfort level. The weight is the point that led to the use of the 3d printing technology in the bionic arm. The most massive device is the Roboarm developed by Unlimited Tomorrow (Roboarm, 2015), with a weight of 2000 g. Most of the bionic hand's weight ranging from 240 g to 450 g.

All the active hands are categorized as underactuated, which means that they have more Degree of Freedom (DOF)'s than the number of actuators. This is because of the coupling of the phalanges in the fingers. Most of the body-powered prostheses' fingers are composed of three phalanges that are coupled to each other through cables or cords. The wires from all the separate fingers are attached to one linkage, which guarantees that all the fingers move synchronically. For externally powered prostheses, the phalanges are coupled to each other with cables or mechanical connections and are directly connected to electric motors. The motors control the fingers separately.

An adaptive grip is the fingers' ability to hold the object within the hand and conform to that object's shape. In this case, the force is distributed among the fingers, which guarantees that some fingers can still apply a force when an item halts the other fingers.



Figure 2-2 Models of 3D printed upper limb (Jelle ten Kate, Gerwin Smit & Paul Breedveld, 2017) (a) Andrianesis' Hand: an externally powered forearm prosthesis,(b) Body-powered hand prosthesis, (c) Scand: a passive adjustable forearm prosthesis,(d) IVIANA 2.0: a passive forearm prosthesis, (e) Adams Arm: EMG controlled Bionic Arm

The precision grip and power grip are the two basic grasps a human use (Napier, J. R., 1956). Moreover, these basic grasps, there are four other standard methods of holds used to perform daily living (ADLs). These four types are the hook grip, spherical grip, tripod grip, and lateral grip (Weir, R., and Sensinger, J., 2003).

The prices from only a small number of hands are known. These prices are based on material costs, which range to a maximum of \$100. These costs can't be compared with commercially available non-3D-printed upper limb prostheses since these prices consist of more than only

the material costs. Two well-known companies are selling prosthesis as a commercial product. Youbionic (Youbionic [Internet], [cited 2015 Jun 29]) sells its bionic arm for \$1000 and Open Bionics (Latest Bionic arm [Internet], cited 2015 Jun 24), aiming for a price of \$3000 for their latest developed Bionic Arm. These hands are both myoelectric controlled hands, which are controlled by muscle activities. There is a vast difference in prices with the commercially available myoelectric hands priced at \$25,000 to \$75,000. The development of cheap hand prostheses can especially be a significant benefit for child prostheses. Children with amputation need to change their hand prosthesis faster due to their growth by nature. By 3D-printing a cheap prosthesis every time, there is no need to buy an expensive prosthesis regularly. A prosthesis can be scaled to match the right size and 3D-printed easily.

2.3 State of the Art of EMG biometrics system

The properties of biometric systems mainly depend on the specific traits they use. Fingerprint, iris or retina, and facial features are the three most common biometric traits (Kaur, G., Singh, G., and Kumar, V., 2014). Systems based on these modalities have already been widely used in our daily lives, such as mobile phones, laptops, and smart pads. These traits need to be exposed during recognition, providing the chance to be captured, and then spoofing might happen.

Although biometric technology has seen significant advances, some biometric systems fail to meet security and robustness requirements in specific real-world situations. By way of an example, the susceptibility to spoofing—persons who pretend to be others to obtain illegal access to private information or services (Abdenour Hadid, Nicholas Evans, Sébastien Marcel, and Julian Fierrez, 2015) (Evans, 2019) (Pinto, J. R., Cardoso, J. S., and Lourenço, A., 2018). The study and prevention of spoofing are considered an active area of research and development.

As wearable devices utilizing sEMG can capture the human muscles' detailed characteristics and is thus useful in human gesture recognition applications. The information extracted from sEMG signals obtained via a human arm is sufficient for classifying intended hand gestures (Saponas, T.m Tan, S., Morris, D., and Balakrishnan, R, 2008). This work's primary objective is to demonstrate the utilization of the sEMG multi-channel wearable armband in verifying individuals' identity with the application of Machine learning algorithms.

Recently, there has been a growing interest in using electrical bio-signals as biometric traits, such as electroencephalogram (EEG), electrocardiogram (ECG). The demonstration of electrical activities related to the heart and brain (Gui, Q., Ruiz-Blondet, M. V., Laszlo, S., and Jin, Z., 2019). The hidden nature of electrical bio-signals makes them harder to capture than the three common modalities mentioned, synthesize, and imitate, and the inherent liveness nature ensures their robustness in distinguishing the artifacts from the real biological targets. Moreover, compared to extensive studies done on EEG and ECG, little attention was paid to the application of sEMG in biometrics.

Surface electromyogram signals (sEMG) are used as a bio-signal in hand and wrist gesture recognition (Englehart, K., and Hudgins, B., 2003). However, the high performance of gesture recognition systems is limited to the condition that the training and testing data are acquired from the same user. It is concluded that even with the same settings, the control performance would drop significantly when a classifier was trained by the data from one user and used to predict the gestures from a different individual. This is due to the existence of some differences in sEMG features (Matsubara, T., and Morimoto, J., 2013). This small difference makes it harder to establish calibration-free sEMG-based gesture recognition. Interestingly, such differences also suggest the possibility of sEMG signals as a potential biometric trait.

sEMG signals have a hidden nature, and it is working correctly in live gesture detection. Also, the high performance of sEMG signals reached when applied in gesture recognition gives an advantage of sEMG as a biometrics modality versus EEG and ECG: the user can set their actions based on different wrist and hand combinations gestures to form a password. In this case, the system can provide two levels of protection, physiology-based and knowledge-based, appealing for high-level security targeted applications.

Some researches based on the ECG/EMG sensors fusion to verify the users (Faragó, P., Groza, R., Ivanciu, L., and Hintea, S., 2019). Belgacem et al. (Belgacem, N., Fournier, R., Nait-Ali, A., and Bereksi-Reguig, F., 2015) studied the usefulness of a biometric system utilizing information obtained via ECG and EMG physiological data. A non-intrusive one-lead ECG setup was adapted into the palm of the user to collect ECG biometric data. Subsequently, the authors used Fourier descriptors for feature extraction. Finally, an optimum-path forest classifier was used to distinguish between individuals.

Siho Shin et al. (Shin, S., Jung, J., & Kim, Y. T., 2017) proposed a non-contact secure private verification based on EMG signals. A total of fifty signals were extracted from the arm of

subjects with a two-channel electrode system's assistance. A set of metrics, such as the mean, length, variation, zero crossings, and median frequency, were extracted from the signals to enhance the identification rate and formulate a machine learning algorithm. The artificial Neural Network (ANN) algorithm showed a relatively high accuracy of 81.6%. Holi et al. (Krishnamohan, P. G., and Holi, M. S., 2011) used vector quantization and the Gaussian mixture model to obtain the EMG signals for biometric applications. The identification rate of 97.9% was achieved, with an average of 73.33% obtained from 49 individuals. The experiment demonstrated that EMG signals alone could produce user distinguishable biometric data. Al-Mulla et al. (Al-Mulla, M. R., and Sepulveda, F., 2014) presented a novel Pseudo-Wavelet function for MMG signal extraction during dynamic fatiguing contractions. 8-electrode bio-impedance analysis (BIA) wrist band has been used to measure to identify users. The success rate with BIA was 85%, and by adding circumference with 1mm accuracy, they pulled up the result to 90%. Hisaaki Yamaba et al. (Yamaba, H., Kurogi, A., Kubota, S. I., Katayama, T., Park, M., and Okazaki, N., 2017) presented a method that uses a list of gestures as a password for EMG user's verification system for mobile phone access. Fourier transform has been used to extract the features from the EMG signals. James Cannan et al. (Cannan, J., and Hu, H., 2013) presented a method for enhancing EMG usability based on identifying a user. Experiments were performed to identify small group sizes of 4, 10, and 19. The results show average identification accuracies across all 11 gestures of 55.32%, 75.44%, and 90.32% for groups of 19, 10 and 4 subjects, respectively. Ryohei Shioji et al. (Shioji, R., Ito, S. I., Ito, M., and Fukumi, M., 2017) used eight dry sensors to measure EMG from the wrist and carry out personal verification approach. A convolutional neural network (CNN) is used in the learning phase for verification. Data collected from 8 individuals, 40 data for everyone. The average accuracy of the two-class separation was 94.9 % by CNN.

Development and optimization of the sEMG feature extractions and classification for the control of prostheses and biometrics applications is today an active research topic, even though the analysis is mainly performed from a machine learning perspective (Benatti, S., Milosevic, B., Farella, E., Gruppioni, E., and Benini, L., 2017) (Englehart, K., and Hudgins, B., 2003) (Englehart, K., Hudgins, B., Parker, P. A., and Stevenson, M., 1999). The feature extraction phase transforms the raw signal data into a valuable data structure by removing noise and detecting the crucial data. There are three divisions of features essential in the processing of an EMG based control system. These features might be in the time domain, frequency domain, and the time-frequency domain (Zecca, M., Micera, S., Carrozza, M. C., and Dario, P., 2002).

Steps in analyzing the EMG signals have been presented by Sakshi Sharma et al. (Sharma, S., Farooq, H., and Chahal, N., 2016). Initially, the surface EMG signal is captured from the subject's forearm using a discrete wavelet transform. Then, the singular value decomposition is used for feature extraction.

Moreover, classifiers based on fuzzy-logic are used to recognize various hand gestures in the context of linguistic terms. Zainal Arief et al. (Arief, Z., Sulistijono, I. A., and Ardiansyah, R. A., 2015) used Myo armband with eight channels electromyography (EMG) located on forearm muscles and extracted five different features to obtain significant differences in hand gestures. The time-series features extraction that evaluated are Mean Absolute Value (MAV), Variance (VAR), Willison Amplitude (WAMP), Waveform Length (WL), and Zero Crossing (ZC). MAV and WL are found to be giving a better recognition rate. Chantaf et al. (S. Chantaf, A. Naït-Ali, P. Karasinski, and M. Khalil, 2010) captured EMG signals from the BIOPAC system. Then, seven frequency domain features (e.g., average frequency, kurtosis, median frequency) are extracted and classified using a Radial Basis Function (RBF) network. The system accuracy estimated was 80%. Yamaba et al. presented a method that is based on a list of gestures as a pass-gesture (i.e., password). They manifested that the same gestures obtained from the same person are similar in behavior, but they are different from those of other persons (Yamaba, H., Kurogi, T., Aburada, K., Kubota, S. I., Katayama, T., Park, M., and Okazaki, N., 2018). To identify pass-gestures, four time-domain features were extracted, a maximum and minimum value of raw s-EMG and their associated time t-min and t-max. SVM classifier is used in the classification of each subject, which were trained under these four features, and cross-validation was carried out using the same raw data.

2.4 Conclusion

The research on the applications of wearable technologies in the biomedical field and biometrics field has been increased over the last decades. The research in bionic arms controlled by arm gestures is of great importance. The gesture recognition system can be accomplished in several ways, vision-based systems, wearable gloves, and sEMG signals. The control of the bionic arm using gesture recognition system based on sEMG signal needs specific steps database of sEMG signals represents arm gestures, followed by signal preprocessing, features extraction, then the classification of signals using machine learning approaches. Several researches showed that the different sEMG signals acquisition varies from single-channel to multi-channel. The database is different from one research to another

research. The research showed different machine learning classifiers in sEMG gesture recognition systems such as KNN, SVM, ANN, and DT.

3D printing technology offers significant advantages in manufacturing complex shapes, prototyping is easy with 3-D printing, and the flexibility of change the design and reproduce the parts is a way more efficient when using 3-D printing techniques. The prices of producing parts with 3D printing technology decrease the cost of manufacturing the parts and ease the processes. All these advantages are utilized in the production of bionic arms and hands. The 3D printed hands and arms are equipped with actuators to be able to perform grasping actions. Small-scaled sensors and actuators are essential in the advancement of bionics.

The thesis proposes a detailed design of a 3-D printed bionic arm with an artificial hand. The bionic arm is implemented and tested on an amputee case. According to the state-of-the-art systems, a gesture recognition based on sEMG signals has been implemented. A database of sEMG was created for generic control of a bionic arm. 3-D printing technology offered an affordable price solution. Real-time testing of a bionic arm with a gesture recognition system is presented. Machine learning classifiers are tested, and results are compared to find the optimum algorithm to be used with sEMG data.

The biosignals are introduced as biometrics identities in research. In this work, the sEMG signals are studied as a biometrics identity for user verification. The sEMG signals have a hidden nature, which can be treated as hidden biometrics. In the review on sEMG biometrics system review, different sEMG systems have been applied, such as the single-channel and multi-channel. The researchers tested the system on limited users for verification purposes. Several machine learning have been presented in the researches about sEMG signals as biometrics traits. The research presented in this works proposes a biometrics system for verification and identification of the users. The biometric device used to acquire the sEMG signal is a wearable multi-channel armband consisting of 8 electrodes. Multiple users volunteered to test the biometric system. Different classifiers have been applied to optimize the system's results. The system will grant/deny access to the user from the captured sEMG biometrics identity as a signature-based hand gesture. Performance analysis of the biometrics system has been presented to validate the system's capacity by estimating both the false acceptance rate (FAR) and the false rejection rate (FRR).

3 Chapter 3 Design and Implementation of a 3-D Printed Bionic Arm Controlled by Machine Learning Based Algorithm

Chapter Content

3.1	Introduction	51
3.2	Bionic Arm.....	52
3.2.1	Methodology	52
3.2.2	Acquisition of sEMG signal.....	53
3.2.3	Bionic Arm Mechanical Design.....	54
3.2.4	Electronics and Control.....	59
3.3	Feature Extraction and Classification	61
3.3.1	Data Collection Protocol.....	61
3.3.2	Data Processing.....	62
3.3.3	Features Extraction	63
3.3.4	Classification.....	64
3.4	Results	66
3.5	Real-time Implementation.....	68
3.6	Conclusion.....	70

Summary: *In this chapter, a customizable wearable 3D printed bionic arm is designed, fabricated, and optimized for a right arm amputee. An experimental test has been conducted for the user, where control of the artificial bionic hand is accomplished using surface electromyography (sEMG) signals acquired by the multi-channel wearable armband. The 3D printed bionic arm was designed for low cost and lightweight. sEMG signals are collected from different participants to control the hand by gestures. In this study, several classifiers based on neural networks, support vector machine, and decision trees were constructed, trained, and statistically compared. Real-time testing of the bionic arm with the optimum classifier is demonstrated to show the system's robustness.*

It starts with introducing the system and shows the specific user condition that the arm is customized to his amputation case in section 3.1. The detailed mechanical design of the bionic arm, the EMG database creation, and the electronic and control implemented are explained in section 3.2. section 3.3. describes feature extraction of the EMG signal for gesture recognition and the signals' classification. The classifier's testing results and the results of the tests conducted on the bionic arm are stated in section 3.4.

3.1 Introduction

Research into advanced medical and prosthetic devices has generated significant attention in recent years due to the increasing demand for reliable bionic hands capable of manifesting patients' intentions to perform various tasks. In general, gesture recognition techniques have emerged as a key enabling feature for improving both the accuracy and functionality of bionic hands, allowing the patient control over delicate operations in dangerous situations, or to help patients with movement disorders and disabilities, as well as in the rehabilitation training process.

The use of bionic hands is not only limited to medical use but has also found numerous applications in industrial settings; artificial bionic hands can perform certain tasks in hazardous or restricted environments while maintaining the user's level of dexterity and natural response time. Under such circumstances, vision-based gesture recognition using image detection could be enough to provide the correct hand motion. (Ben-Arie, J., Wang, Z.; Pandit, P., and Rajaram, S., 2002) (Kapoor, A., and Picard, R. W., 2001) (Morency, L. P., Sidner, C., Lee, C., and Darrell, T., 2005) (Matsumoto, Y., and Zelinsky, A., 2000)

Recently, wearable devices based on sEMG have become quite attractive in the human gesture recognition domains, as these devices are used to capture the characteristics of the muscles. In general, the sEMG signals obtained from a human arm contain enough information concerning the intended and performed hand gestures (Saponas, T.m Tan, S., Morris, D., and Balakrishnan, R, 2008). Wheeler et al. (Wheeler, K. R., Chang, M. H., and Knuth, K. H., 2006) introduced a gesture-based control system utilizing sEMG signals taken from a forearm, where the proposed systems were successfully able to act as a joystick movement for virtual devices. Furthermore, Saponas et al. (Saponas, T.m Tan, S., Morris, D., and Balakrishnan, R, 2008) proposed a technique based on ten sEMG sensors worn in a narrow band around the upper forearm to separate finger presses' position and pressure.

In this chapter, a customizable wearable 3D-printed bionic arm is designed, fabricated, and optimized for a right arm amputee. An experimental test has been conducted for the user, where control of the artificial bionic hand is accomplished successfully using sEMG signals acquired by a multi-channel wearable armband. The 3D-printed bionic arm was designed for the low cost and light-weight. To facilitate a generic control of the bionic arm, sEMG data were collected for a set of gestures (fist, spread fingers, wave-in, wave-out) from twenty-three

participants. The collected data were processed, and features related to the gestures were extracted to train a classifier. In this study, several classifiers based on neural networks, support vector machine, and decision trees were constructed, trained, and statistically compared. The support vector machine classifier was found to exhibit an 89.93% success rate. Real-time testing of the bionic arm with the optimum classifier is demonstrated.

3.2 Bionic Arm

Amputees are suffering while doing their necessary daily life activities. The presented bionic arm is a solution for upper limb amputees. Considering all the facts that most of the amputees are suffering from. The proposed arm is a low-cost, comfortable, and easy to use the bionic arm.

3.2.1 Methodology

The bionic arm implemented and tested was customized for a specific user to fit with his amputation conditions. It was made to provide the user with the ability to perform necessary grasping actions and effectively participate in his daily activities. The user was born with a small portion of his right arm, as shown in Figure 3-1. The user is a 24-year-old male with no other significant health issues. He used several previous prosthetic arms, whose components and make are not detailed. He found that all these arms are not sufficiently functional or heavy or are uncomfortable or expensive. The user gave his informed consent for inclusion before he participated in the study.

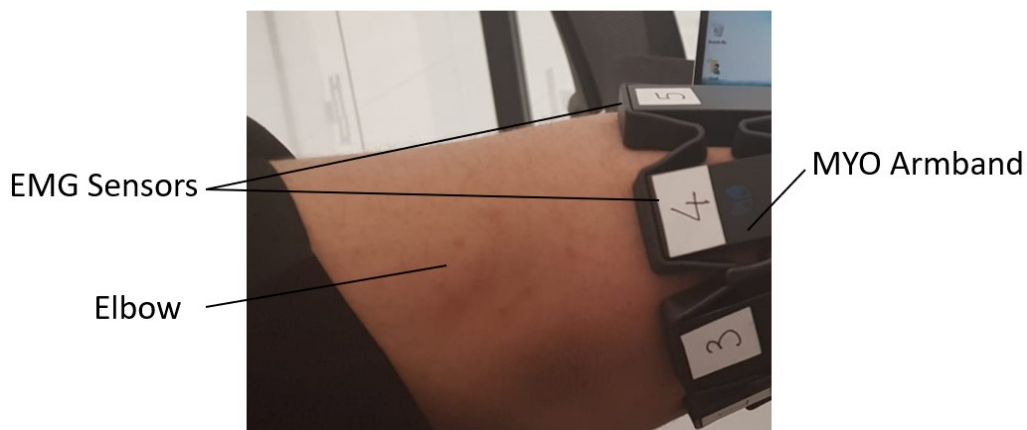


Figure 3-1 Amputation case with the user wearing a Myo armband

The user’s feedback was taken into consideration when working on designing a low-cost customized bionic arm. The user was heavily involved in the mechanical design phase of the bionic arm. The prosthetic arm presented in this work is controlled by a multi-channel sEMG sensor that is used to acquire the muscles’ activities. The muscles’ activities represent different gestures, which are used to perform the required action by the hand attached to the arm. The hand has 9 degrees of freedom (DOF), which enable it to serve different accurate actions as per the user’s demand. The schematic chart illustrating the steps required to control the bionic arm is shown in Figure 3-2. A database of sEMG gestures is created with all the units associated with signal processing, feature recognition, and machine learning to catalog the signals that are required for movements of the finger actuators in the bionic hand to perform specific hand postures.

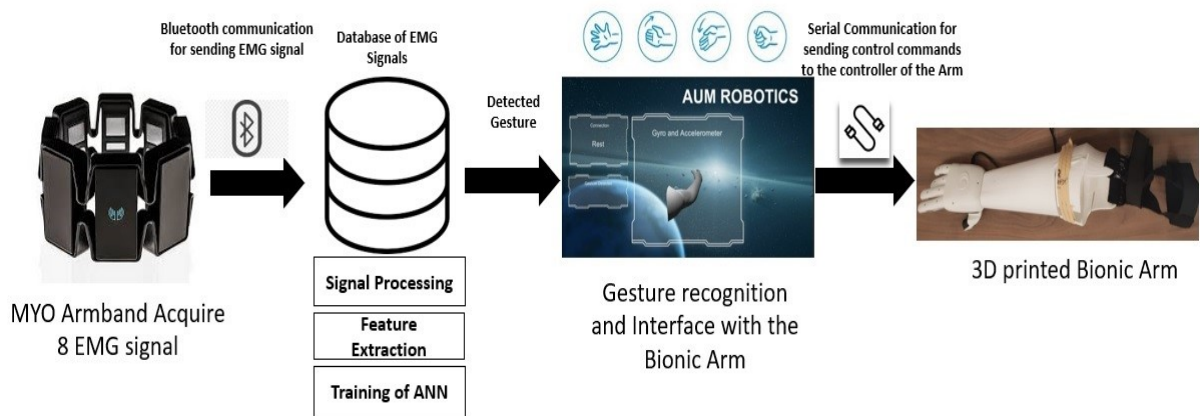


Figure 3-2 Schematic chart of the process for bionic arm control

3.2.2 Acquisition of sEMG signal

The user was trained to perform the following four gestures: Fist (close), spread fingers (open), wave-in, and wave-out. The detected gestures were displayed on the PC screen to provide the user with feedback during the training phase (Said, S., Sheikh, M., Al-Rashidi, F., Lakys, Y., Beyrouthy, T., and Nait-ali, A., 2019). The concept behind creating the sEMG database using Myo is to enable a more generic arm design for any amputee with a similar arm amputation. The bionic arm proposed aims to be used for any amputee suffering from upper-limb amputation, not only limited to a specific user who has been involved in this study. Myo's combination of the eight different sEMG electrodes allowed more sEMG signal data for a better gesture recognition system. Figure 3-3 shows the raw sEMG signals acquired by Myo while the user performs hand gestures prior to signal processing. The sEMG sensors of the armband

are numbered from 1 to 8 to be able to match the signals with the muscles. Sensor 3 is placed in the area least affected by the surrounding muscles.

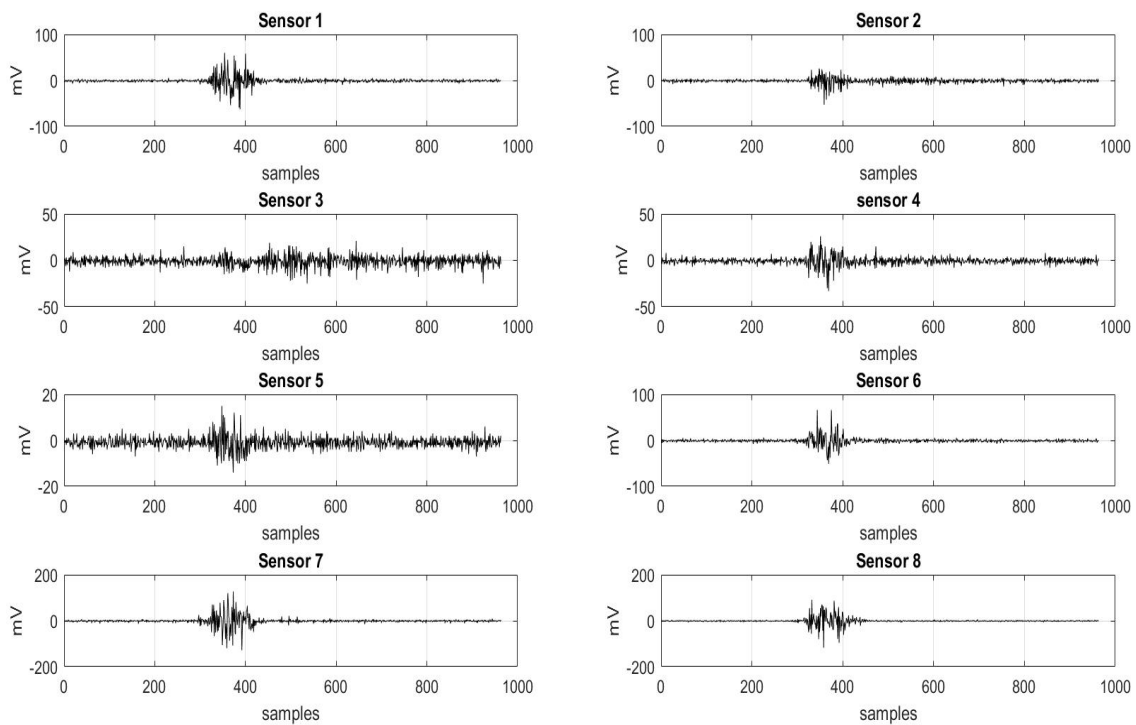


Figure 3-3 Eight (sEMG) sensors raw data for wave-out hand action

3.2.3 Bionic Arm Mechanical Design

Amputees with limb amputation may be disappointed with aspects of available limbs in the market due to their limitations. Customized design for the user through a unique design process has been undertaken here, which has the capacity to target a design that fulfills the need of an individual amputee case, particularly in terms of its low cost and lightweight. The current devices available in the market range from 4000 to 20,000 USD (Zuniga). Some researchers compiled a detailed market analysis of the cost associated with prosthetic limbs. A simple cosmetic arm and hand may cost between 3000 and 5000 USD. The cost of a functional prosthetic arm, on the other hand, may cost between 20,000 to 30,000 USD.

The main target is to optimize manufacturing a bionic arm to have an affordable bionic arm for amputees costing around 295 USD. Nowadays, the advancement of and easy access to 3D-printing technology has reduced the cost of manufacturing bionic arms and provides more straightforward solutions for prosthetic arms customized for users. Simultaneously, the advancement in the materials used in the 3D printing arm products allows a robust design able

to withstand various loading conditions. The user's left arm dimensions were measured to fabricate the right arm with the same dimensions for an asymmetric look and balanced design. The balance in loads between the not affected arm and the bionic arm provides a comfortable feeling and avoids pain in the right shoulder due to the bionic arm's load. Thus, make the bionic arm more comfortable for a long time without feeling pains in the muscles. A mirrored geometry was assumed using computer-aided design (CAD) software. The dimensions of the affected arm were taken into consideration and used in the design to develop a wearable arm with enough room for the Myo armband to fit and be concealed from view. The user was heavily involved in the design process, especially in the socket design. The socket is the contact point between the bionic arm and the user's affected hand. That is why the comfortable feeling will come from the optimized design of a socket that fulfills the arm's ergonomics.

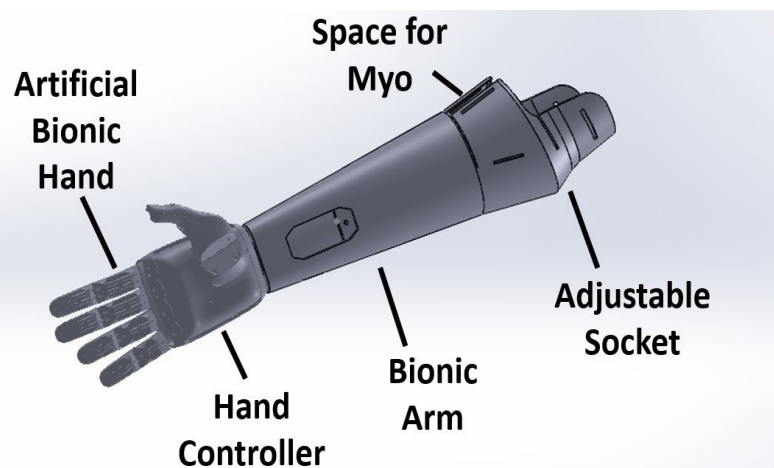


Figure 3-4 Bionic arm 3D model on computer-aided design (CAD) software.

The 3D model design for the bionic arm is shown in Figure 3-4. The design consists of different parts, the artificial hand, the arm, the adjustable socket. The details of each part will be explained in the upcoming sections. The design is based on different criteria, as listed and described below:

- **Adjustable socket**

The adjustable socket is the portion that joins the limb (stump) to the bionic arm. A strap adjusts the socket designed for this arm. The user is wearing the Myo armband at a set location on his arm before adjusting the socket's size to have a tight fit. Designs were iteratively created, tested, and the subject's feedback was considered until an improved design was reached, implemented, and tested. The comfort feeling is one of the most important points considered in the socket's

design, allowing the user to mount the bionic arm for up to four hours with the help of the bicep support.

- **Dimensions**

The symmetry of arm length is critical for the user to avoid serious muscle asymmetry symptoms and muscle pain from disbalance. Consequently, the designed arm was engineered to match the dimensions of the physical left arm.

- **Artificial Hand**

A 3D model assembled of the open-source Brunel hand was made to ensure the fitting between the arm and the hand. The hand consists of 9 degrees of freedom and 4 degrees of actuation. It can perform complex tasks with precision. The four linear motors are attached to threads along with springs to allow smooth linear motion. These linear actuators consist of feedback that allows the control of the location of the fingers precisely. Most parts are printed with Polylactic Acid (PLA) material to provide a strong structure, whereas the outer layer and the joints are printed with Thermoplastic polyurethane (TPU) to provide a soft cushioning and flexible movement. Small printers were used for the small parts and an industrial-size printer for the larger pieces. The complete hand fabrication required less than 2 kg of filament. The total weight of the Brunel's hand adds up to just below 350 grams.

- **Bicep Support**

An arm harness made of straps was added to release the socket joint pressure with bicep support made of a 25 mm width black nylon strap.

- **Myo Integration**

The Myo armband is integrated into the bionic arm to ensure correct surface electromyography signal capturing.

- **Light Weight**

The arm is made to be lightweight by strategically designing the arm to fulfill the design requirements ensuring the strength of the bionic arm at the same time. The material used in the manufacturing of the arm is PLA. PLA is biodegradable and made from renewable resources, for example, corn starch. This implies that PLA minimally affects the earth and doesn't produce

poisonous vapor when dissolved. It likewise means that PLA is commonly non-poisonous when inadvertently devoured, which implies use around a little kid is not an unsafe circumstance. PLA is also a broadly utilized plastic, indicating that it will be genuinely modest to purchase. PLA typically brings about less distorting and doesn't require a heated bed well.

The arm's total weight, including the hand with the actuators and excluding the Myo armband, is 428 grams.

- **Electronics and Battery**

To ensure safe and organized assembly, the electronic wiring and cables were concealed, while the battery was placed in the user's pocket to minimize weight.

- **Stress Analysis of the Arm**

SOLIDWORKS Simulation is an easy-to-use portfolio of structural analysis tools that use Finite Element Analysis (FEA) to predict a product's physical behavior by virtually testing CAD models. The portfolio provides linear, non-linear static, and dynamic analysis capabilities. Using a simulation of the design to estimate the maximum load, the design can withstand after applying forces and check for the maximum yield stress.

Case 1:

Applying a point load of 0.35 kg (hand weight) and adding a 3 kg point load.

Case 2:

Applying a point load of 0.35 kg (hand weight) and adding a distributed load of 2 kg.

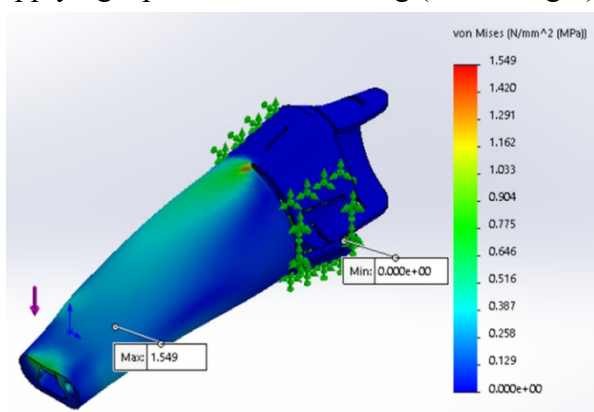


Figure 3-5 Case 1: Stress results at 3.350 Kg load

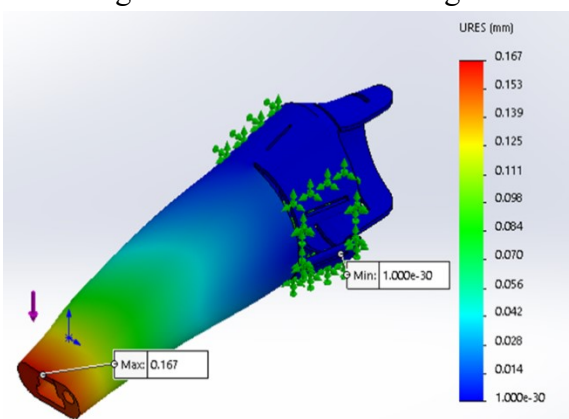


Figure 3-6 Case 1: Displacement results at 3.350 Kg load

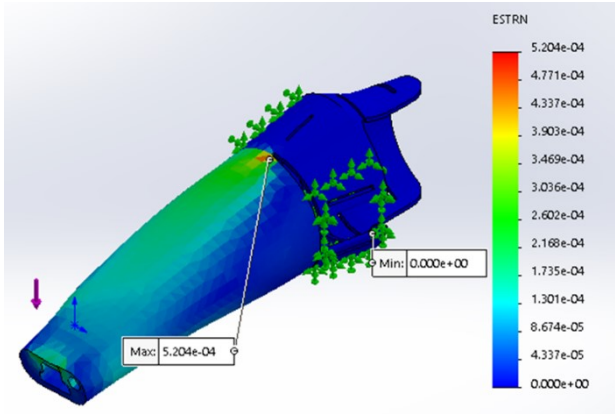


Figure 3-7 Case 1: Strain Result at 3.350 kg load

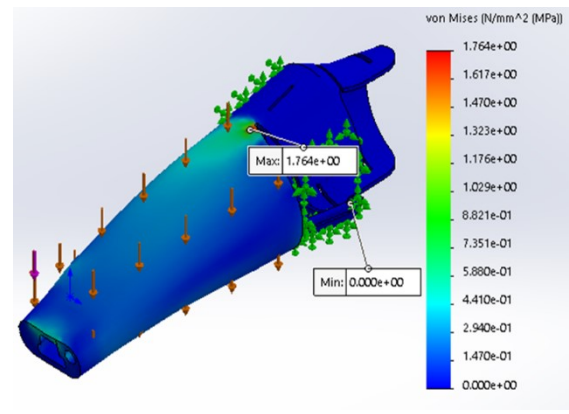


Figure 3-8 Case 2: Stress result at 2.350 combined load

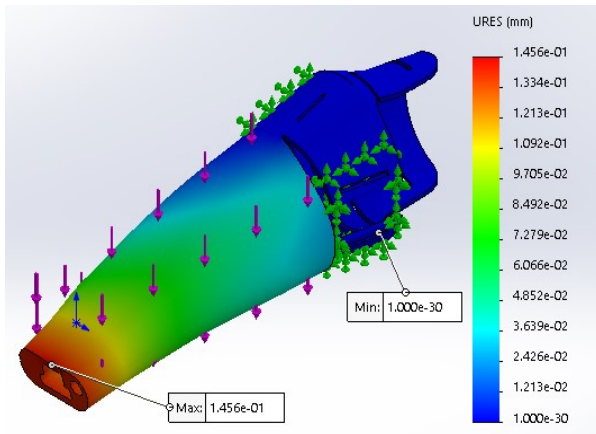


Figure 3-9 Case 2: Displacement results at 2.350 kg combined load

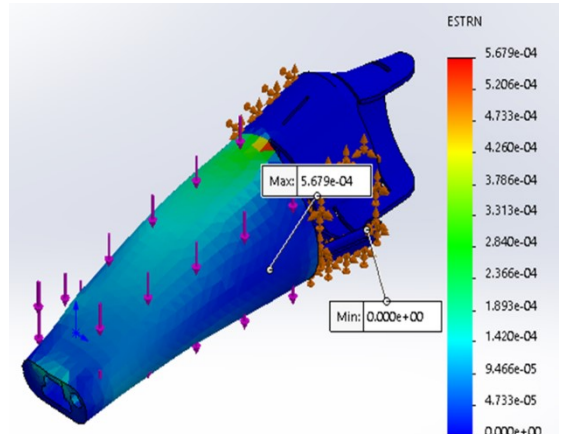


Figure 3-10 Case 2: Strain result at 2.350 kg combined load

Table 3-1 Stress Analysis Results

Force Apply	Stress [MPa]		Displacement [mm]		Strain	
	Max	Min	Max	Min	Max	Min
350 grams on the edge	0.16	0	0.017	0	5.38×10^{-5}	0
350 g + 2 Kg on the edge	1.087	0	0.117	0	3.65×10^{-4}	0
350 g + 3Kg point	1.549	0	0.167	0	5.20×10^{-4}	0
350 g + 2kg distributed	1.76	0	0.1456	0	5.68×10^{-4}	0

Finite element analysis software is used to test the constructed prototype. The software analysis indicates that lifting a 3 kg load is possible with the fixture at the insertion point and the load on the far end while considering the 350-gram artificial hand. Experimental load tests indicated that the user could carry a maximum load of 4 kg for 10 seconds or 3 kg for 30 seconds before feeling stress on his muscles. A test conducted by the user is to carry a load of 1.5 kg for 60 seconds, as shown in Figure 3-11

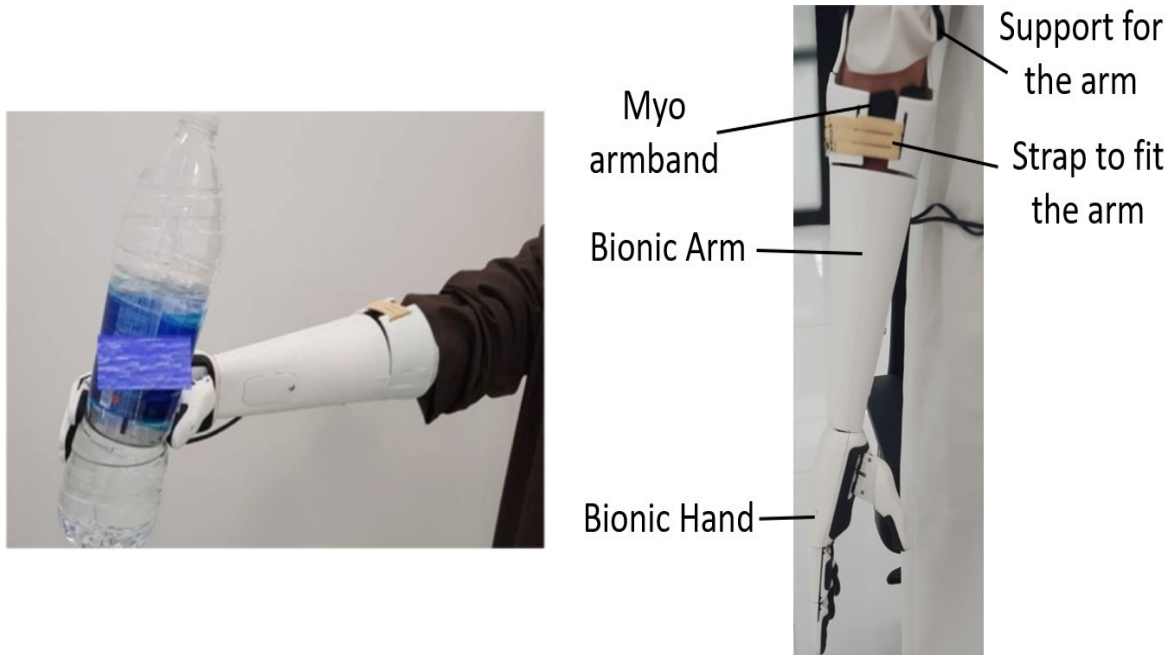


Figure 3-11 Bionic Arm load test

Figure 3-12 Amputee wearing the bionic arm

After completing and evaluating the design, a large-scale industrial 3D printer (Bigrep Studio) was used to 3D print the hand parts to be assembled with actuators and electronics. The arm part until the socket was printed in one print. The arm's cost estimation includes the electronics, actuators, and the 3D-printed material used in hand. The whole arm's total cost with parts and electronics is less than 300USD, as detailed in Table 3-2, which is affordable compared to commercially available systems on the market. As the adoption of the proposed arm design will increase the arm's cost depending on the amputation case, the time for measuring, printing, and assembling is indicated. The final 3D-printed arm while the user wears it is shown in Figure 3-12.

3.2.4 Electronics and Control

The bionic hand actuators are controlled by a Chestnut board placed inside the bionic hand, featuring the ARM Cortex M0+ Processor. The board is designed to be embedded within

robotic hands. It can control up to four motors simultaneously. The board's mass 15 g, and its dimensions are small at 57×45×9 mm shown in Figure 3-13, allowing it to fit inside the bionic hand (Open Bionics lab, 2019).

All the data acquired by Myo armband transferred wirelessly via Bluetooth at a fixed sampling rate of 200 Hz and transmitted serially to a PC. Each transmitted serial datum corresponds to a gesture. These signals are compared with the trained model of gestures. A graphical user interface (GUI) screen for interfacing with the user was developed to indicate the detected gesture. The GUI also shows the orientation of the arm in real-time. The Myo EMG sensors' detected gesture was mapped to perform hand movements; for example, closing the hand, opening the hand, closing one finger, or two fingers. These actions are achieved by precise control of the linear actuators' motion inside the bionic hand. The control signals are transferred through the Chestnut board to actuate the linear actuators of the hand. Although the bionic arm hardware was customized for a single user, the software was meant to be adaptable for any user. The chestnut board is programmed by Arduino based language. Consequently, sets of gesture data were collected from different participants to enable feature extraction and classification, as detailed in the following section. The flowchart explains the procedure of controlling the bionic arm shown in Figure 3-14.

Table 3-2 Detailed cost analysis of the bionic arm

Index	Property	Value
1	Time to print and assemble the hand	28 h
2	Time to print the arm	10 h
3	Total weight without support material	78.78 g
4	Material Cost	\$32.4
5	Hand print	\$20
6	Electronics	\$20
7	Actuators	\$240
	Total Cost	\$295

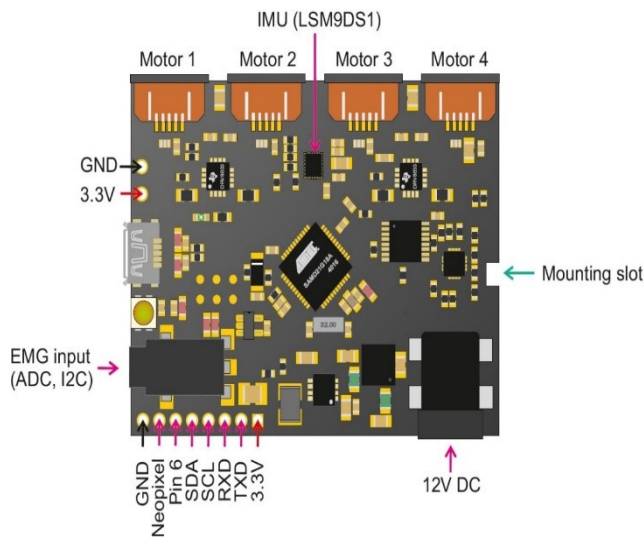


Figure 3-13 Chestnut board controller

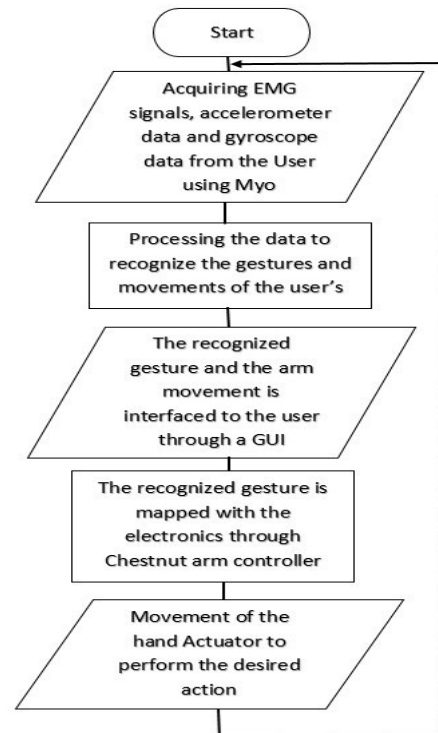


Figure 3-14 Flowchart of controlling the bionic arm

3.3 Feature Extraction and Classification

3.3.1 Data Collection Protocol

In this work, a Myo armband was used to collect the data of the selected four gestures from twenty-three participants (twelve males and eleven females with ages ranging from 18 to 45 years). First, the armband was connected wirelessly to the computer, and several numerical algorithms were used to transform the collected data from the official Myo software, called Myo-Connect, to a matrix data format. This procedure simplified the data collection process and allowed visualization of data while recording. Only data used to train and test the offline classifiers were collected using numerical tools, while the online implementation of this project was being performed using Python code. There are three distinct phases involved: Data collection, data processing, and rectification, and feature extraction.

As part of the data collection procedure, participants were instructed to keep an angle of 90° at the elbow joint during data collection. The dataset was collected in several sessions (within a period of two months), and every time the Myo armband was attached at the same location

around the forearm of all participants. Data were collected from participants in several sessions in the first phase, where data associated with four hand gestures were recorded: Spread fingers, closed hand, wave-in, and wave-out. The participants were instructed to move their hand from the resting position to perform one of the proposed gestures and then move back to the resting position for around four seconds. The participants repeated this procedure more than 10 times for every single gesture. The same method was applied to all four gestures. As a result, a dataset of 7360 files was collected, where each file contains the signals of several gestures. In the second phase, the collected data were processed and rectified to simplify the third phase (the feature extraction phase).

3.3.2 Data Processing

The second phase shows the processing steps of raw sEMG signals. First, the raw sEMG signal which are acquired by a sampling rate of 200 Hz was modified by removing its mean value, resulting in an AC coupled signal. Next, a band-pass filter was used to remove distortions and non-EMG effects from the recorded signal. Generally, raw EMG signals have a frequency between 6–500 Hz. However, specific fast oscillations, which are caused by unwanted electrical noise, may appear within the signal frequency band. Furthermore, slow oscillations, which are caused by movement artifacts or electrical networks, may also contaminate the EMG signals. These unwanted signals can be removed from the original EMG signal using a band-pass filter with cut-off frequencies between 20 and 450 Hz. The resulting data signals may be further rectified by taking the absolute value of all EMG values. This step will ensure that negative and positive values of the EMG signals will not cancel each other upon further analysis, such as calculating the mean values of the absolute EMG signal or obtaining other features. Finally, the second phase was concluded by capturing the envelope of the filtered and rectified EMG signal, as the obtained shape gives a better reflection of the forces generated by the muscles. The signal length is 1000 samples.

Figure 3-15 summarizes phase two steps: figure (a) shows a raw EMG signal obtained in one channel. Figure (b) illustrates the second step, in which the mean value of the signal was deducted from the signal. Figure (c) presented in the bottom left shows the signal after a pass-band filter was applied, and then the absolute values of the filtered signal were taken. Finally, figure (d) shows the envelope of the processed signal. These four steps will be used to process all sEMG signals.

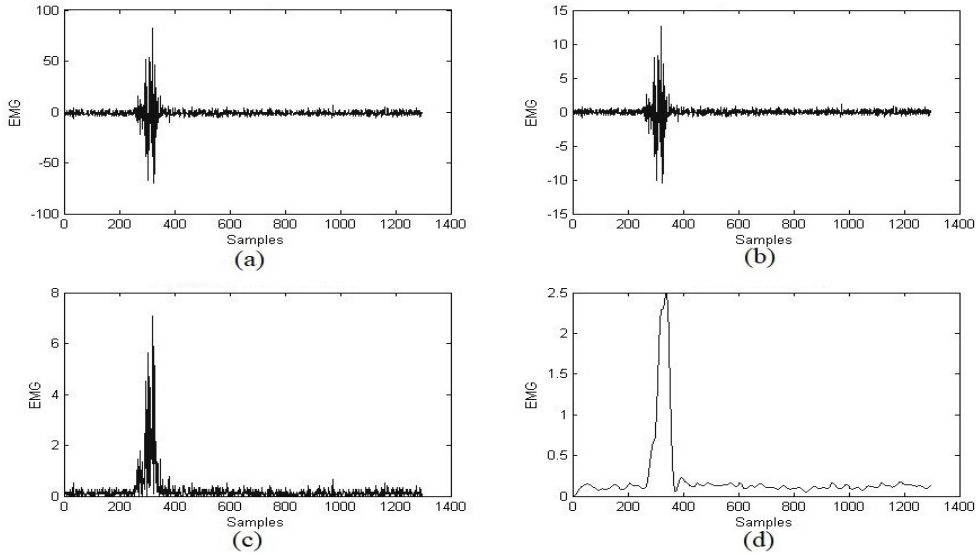


Figure 3-15 Filtered and rectified EMG signal (a) Raw sEMG signal, (b) Mean value removed sEMG signal, (c) Filtered and rectified sEMG signal, (d) sEMG envelope signal

3.3.3 Features Extraction

In the feature extraction procedure, which is the third phase, the dimensionality of the processed data was reduced to simplify the classification step. Generally, sEMG data may contain relevant and irrelevant information, and mapping sEMG data can discard irrelevant information to another reduced space (reduced dimensionality). This step is known as feature extraction, and the main advantage of this step is the reduction of the dimensionality of the problem, which eventually simplifies the classification process. In this work, a combination of two statistical features, mean absolute value (MAV) and standard deviation (SD), along with the auto-regressive coefficients (AR) approach, is used to extract important information from the data, which reflects the targeted gestures (Baillie, D. C., & Mathew, J., 1996) (Vu, V. H., Thomas, M., Lakis, A. A., and Marcouiller, L., 2011) (Akhmadeev, K., Houssein, A., Moussaoui, S., Høgestøl, E. A., Tutturen, I., Harbo, H. F., and Gourraud, P. A., 2018). First, the Mean Absolute Value (MAV) method is used to extract muscle contraction levels from sEMG data. The mathematical expression of MAV is presented as the moving average of a rectified EMG signal:

$$MAV = \frac{1}{N} \sum_{i=1}^N |x_i| \quad (3-1)$$

N represents the length segment of the EMG data, x_i is the value of the signal amplitude, and i is the segment increment. Then, the standard deviation of EMG (SD), which is expressed as

the square root of the EMG signal's power, is used to extract features from the EMG data. The SD is defined as:

$$SD = \sqrt{\frac{1}{N-1} \sum_{i=1}^N (x_i)^2} \quad (3-2)$$

Finally, an auto-regressive coefficients (AR) approach is adopted to extract features from sEMG data. The main idea is to use the sEMG data to fit an auto-regressive model, where the coefficients of the model and MAV and SD values, are then considered as inputs to the classifier for gesture recognition. For each sEMG envelope signal, the AR model is fitted, such as:

$$x(t) - \sum_{k=1}^m a_k x(t-k) = e(t) \quad (3-3)$$

where a_k , $k = 1, \dots, m$, are the AR model parameters, m is the order of the model, and $e(t)$ is the error. Then, the parameters a_k , $k = 1, \dots, m$ are used to represent the EMG signal. In this work, the value of $m = 8$. As a result, a vector of size ten is needed to capture the 8 AR parameters, and both MAV and SD values. Furthermore, eight sEMG signals were involved in the collection procedure, and the classifier inputs are reduced to eighty entries.

3.3.4 Classification

In this section, the extracted features and the corresponding known outputs are used as the input data to train a classifier or recognition algorithms. Based on a pre-selected optimization algorithm, the classifier is prepared to learn and identify patterns in the data and respond to the inputs according to the given outputs. After successful training, the reliability of the classifier is tested with a different dataset.

Training and testing classifiers help to validate the results and obtaining an accurate classification model. In this section, three classifiers are investigated: The artificial neural network (ANN), support vector machine (SVM), and decision trees (DT) algorithms to identify which classifier is better suited for building the bionic hand.

- **Artificial Neural Network**

Artificial neural networks (ANN), also known as multi-layer perceptrons (MLP), are one of the main pattern recognition techniques; they comprise many neurons, and these neurons are connected in a layered manner. The training procedure of a neural network can be easily achieved by optimizing the unknown weights to minimize a pre-selected fitness function.

Generally, the neuron architecture can be summarized as the following: A neuron (or node) receives inputs, and then respective weights are applied to these inputs. Then, a bias term is added to the linear combination of the weighted input signals. The resulting mixture is mapped through an activation function.

Usually, the ANN consists of input and output layers and hidden layers that permit the neural network to learn more complex features. In this work, one of the most recognized ANN algorithms, the feed-forward neural network, is used as a supervised classifier for gesture recognition. The feed-forward classifier is trained with data (called training data); the trained classifier is then tested with a different dataset. Finally, the resulting ANN classifier is used to recognize online input data (Ahsan, M. R., Ibrahimy, M. I., and Khalifa, O. O., 2011) (Zhang, X. H., Wang, J. J., Wang, X., and Ma, X. L., 2016) (Dai, Y., Zhou, Z., Chen, X., & Yang, Y., 2017) (Zhang, Z., Yang, K., Qian, J., and Zhang, L., 2019).

- **Support Vector Machine**

A support vector machine (SVM) is a multi-class classifier that has been successfully applied in many disciplines. The SVM algorithm gained its success from its excellent empirical performance in applications with relatively large numbers of features. In this algorithm, the learning task involves selecting the weights and bias values based on given labeled training data. This can be achieved by finding the weights and biases that maximize a quantity known as the margin. Generally, the SVM algorithm was first designed for two-class classification. However, it has been extended to multi-class classification by creating several one-against-all classifiers (in which the algorithm solves K two-class problems, and, each time, a class is selected and classified against the rest of the classes), or by formulating the SVM problem as a one-against-one classification problem (in this case, $K(K - 1)/2$ binary classification problems are solved by considering all classes in pairs) (Fong, S. , 2012) (Theodoridis, S., 2015). In this work, a multi-class SVM classifier is trained, tested, and used to classify gestures based on online data.

- **Decision Tree**

Recently, decision tree (DT) algorithms have become very attractive in machine learning applications due to their low computational cost (Marsland, S., 2015) . Furthermore, DT approaches are transparent and easy to understand since the classification process could be visualized as following a tree-like path until a classification answer is obtained. The decision

tree algorithm can be summarized as follows: The classification is broken down into a set of choices, where each alternative is about a specific feature. The algorithm then starts at the tree's base (root) and keeps progressing to the leaves to receive the optimized classification result. The trees are usually easy to comprehend and can be transformed into a set of if-then rules suitable for simplifying machine learning applications' training procedures. Generally, decision trees use greedy heuristic approaches to perform search and optimizations, where these algorithms evaluate their possible options at the current learning stage and select the solution that seems optimal at that instant. In this work, a decision tree algorithm is used to train and test a gesture dataset, and the results are compared with the SVM and ANN to select the best model to be used with the bionic arm.

3.4 Results

After selecting three different types of classifiers, the offline procedure was used to train and test these classifiers to select the model that will be used for the online recognition procedure. The ANN classifier has two hidden layers, with the number of neurons used in each layer set to 116 and 48, respectively. The tanh, which is the hyperbolic tangent function, is considered the ANN's activation function. The training procedure is achieved using an optimizer called the limited-memory Broyden–Fletcher–Goldfarb–Shanno (LBFGS) algorithm. In the decision tree classifier, a Gini impurity was used to measure the split's quality. The lowest number of samples required to split an internal node is two, and only two samples are needed for every leaf node. To obtain an accurate SVM classifier, one should select the correct value for the regularization parameter C , which is, in this case, $C = 80$, and the kernel parameter $g = 0.04$.

The parameter values for the three classifiers were selected after performing a cross-validation process for each classifier. Each classifier was used to train and test the same dataset for a different set of parameters. The best model for each version of the three classifiers was selected based on its performance. Next, a statistical study was used to compare the testing results to choose the best classifier among the three classifiers (ANN, SVM, and DT classifiers). First, each classifier was run for thirty trials, and the testing accuracy for the classification was stored in a table. The SVM classifier provided the highest classification result with a mean value of the training data equal to 91.21% and a standard deviation of 1.92%. Furthermore, the SVM classifier provided an average testing accuracy equal to 90.5% and a standard deviation of 1.75%. The decision tree algorithm produced a training accuracy of

73.46% with a standard deviation of 4.87%, while the testing results were equal to 70.5% with a standard deviation of 2.5%.

Finally, the ANN classifiers provided a training accuracy of 84.78%, with a standard deviation of 4.11%. The testing procedure's ANN accuracy was equal to 83.91%, with a standard deviation of 2.3%. The results are presented in Table 3-3.

Table 3-3 Training and testing results for the three classifiers

Method	Training	Testing
SVM	91.21% ± 1.92%	90.5 % ± 1.75%
ANN	84.78% ± 4.11%	83.91% ± 2.3%
DT	73.46% ± 4.87%	70.51% ± 2.51%

The confusion matrices for the SVM classifier's training and testing procedures are presented in Table 3-4 and Table 3-5, respectively. The four gestures presented in the tables are close, open, wave-in, and wave-out and the reported results represent a classification trial based on the SVM classifier. As observed, the accuracy for both training and testing procedures was higher than 82%. The results also indicate that the misclassification between gestures is relatively low and mostly happens between the open and close gestures.

Table 3-4 Confusion Matrix for the Support Vector Machine (SVM Classifier) Training (93.75%)

Gesture	Close	Open	Wave-In	Wave-out
Close	91.23%	5.26%	0%	3.51%
Open	3.34%	95%	0%	1.66%
Wave-In	0%	3.64%	96.36%	0%
Wave-out	4.41%	0%	2.94%	92.65%

Table 3-5 Confusion matrix for the SVM classifier: Testing (accuracy: 92.62%).

Gesture	Close	Open	Wave-In	Wave-out
Close	94.64 %	0%	3.57%	1.79%
Open	6.35%	88.89%	0%	4.76%
Wave-In	3.75%	0%	96.30%	0%
Wave-out	8.45%	0%	20%	91.55%

Furthermore, the t-test is used to identify a significant difference between the results of all three classifiers. The obtained P-values were found to be relatively small (less than 5%), which indicates that there is a significant difference between the classification results. The Holm approach was then used in the statistical investigation to show that there are statically substantial differences among the three classifiers' results, and the SVM classifier provides better accuracy than both the ANN and the DT classifiers. As a result, the SVM classification model is adopted for online classification.

In Table 3-6, various classifiers accuracies are stated to compare the results obtained with other researchers' work.

Table 3-6 Research Work Results using Myo armband

Evaluated ML models used Myo armband	Accuracy
MYO armband method (Motoche, C., and Benalcázar, M. E., 2018)	83.1 %
Model using k-NN with Dynamic Time Wrapping (DTW) (Benalcázar, M. E., Motoche, C., Zea, J. A., Jaramillo, A. G., Anchundia, C. E., Zambrano, P., and Pérez, M., 2017)	89.5 %
Model using SVM (Benalcázar, M. E., Motoche, C., Zea, J. A., Jaramillo, A. G., Anchundia, C. E., Zambrano, P., and Pérez, M., 2017)	92 %
Model using ANN (Motoche, C., and Benalcázar, M. E., 2018)	90.7 %
Model using Naive Bayes (Wahid, M. F., Tafreshi, R., Al-Sowaidi, M., and Langari, R., 2018)	81.76 %
Model using Random Forest (Wahid, M. F., Tafreshi, R., Al-Sowaidi, M., and Langari, R., 2018)	89.92 %

3.5 Real-time Implementation

Different testing protocols were proposed to the user for testing the arm design and the EMG signal control with the optimum classifier enabled. The user practiced for one week on how to perform different gestures and be able to control his muscles. After the training phase, the user wore the Myo armband in his forearm and then performed the trained gestures (fist (closed), spread fingers (open), wave-in (turn the hand inside), wave-out (turn the hand outside)) using his muscles for 20 consecutive times. Subsequently, the user was asked to perform two different gestures consecutively 20 times to test the daily activities that can be performed by

the bionic arm. The detected hand gestures are mapped with bionic hand actions. The fist will close all the artificial hand fingers; spread fingers will open all the artificial hand fingers, wave-in will close one finger only of the artificial hand while wave-out will close two fingers.

The testing scenarios showed the user's ability to control the bionic hand accurately after the training phase. The bionic hand movements were optimized to allow the user to perform different activities (holding objects, grasping, drinking, and writing). In single-action testing, the user was asked to perform one action at a time. The single measures include making a fist, spreading the fingers, closing one finger, and closing two fingers, as shown in Figure 3-16.

The user performed each action repetitively for 20 consecutive times. The results of testing every single action show a detection rate varying from 85% up to 100%. In combining two actions, the user performed opening and closing with a success rate of 95%, opening and closing one finger with 90%, and opening and closing two fingers with 85%, as shown in Figure 3 17.

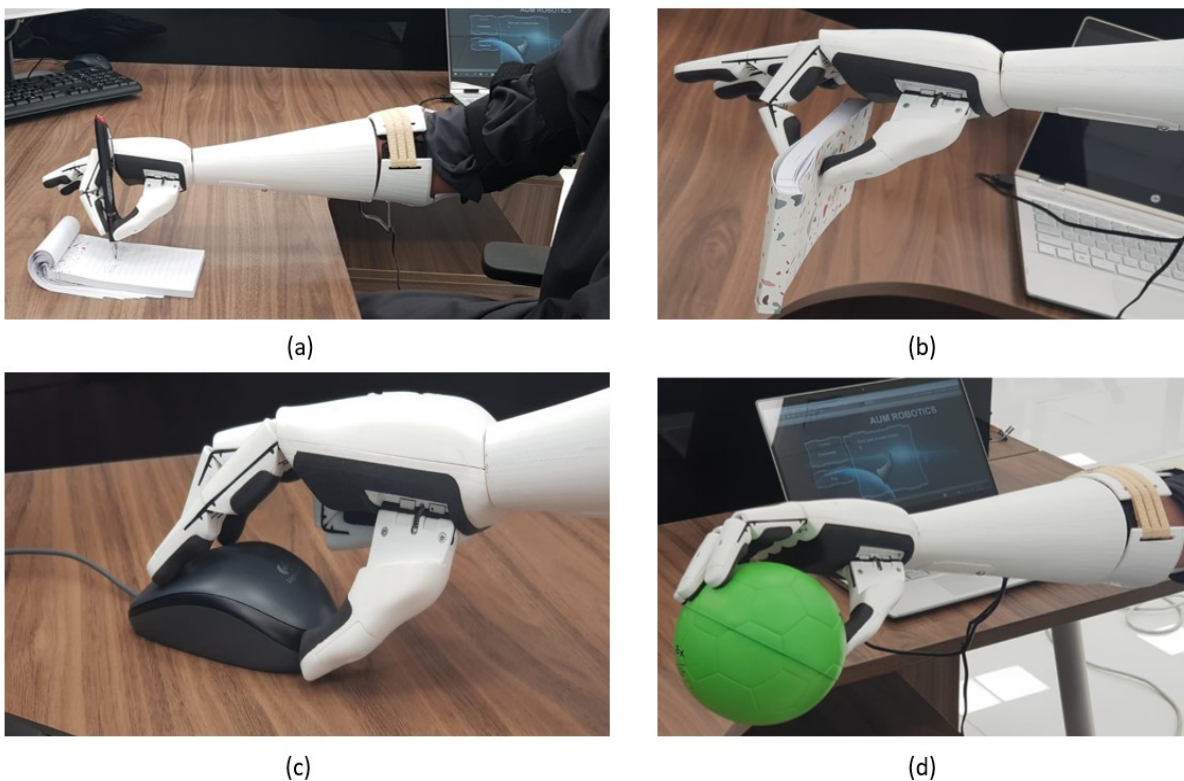


Figure 3-16 (a)Writing with the pen (two fingers closed action); (b) holding of a notebook (one finger closed action); (c) using the PC mouse (one finger closed action); (d) holding a ball (fist action).

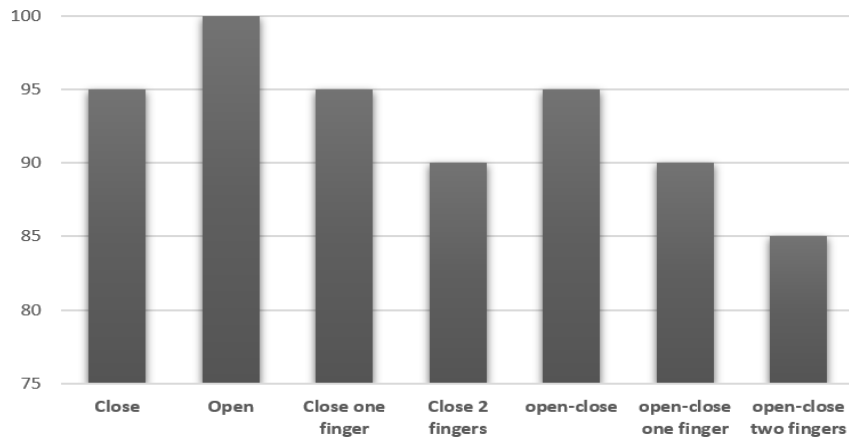


Figure 3-17 Success rate of hand actions.

3.6 Conclusion

A customized 3D-printed bionic arm was designed, fabricated, and tested for a right arm amputee. The 3D-printed bionic arm was designed to have a low cost, comfort, lightweight, durability, and appearance. sEMG data were collected for a set of four gestures (fist, spread fingers, wave-in, wave-out) from a wide range of participants to make the bionic arm control general for amputee cases. The collected data were processed, and feature extraction was performed to train the classifier. The support vector machine classifier was found to outperform the neural network and decision tree classifiers, reaching an average of 89.93% accuracy. Real-time testing of the bionic arm with the associated classifier software enabled the user to perform his daily activities.

Additional features are needed to improve further the bionic arm, such as a multi-degree-of-freedom wrist joint connector. This can be achieved by using two servo motors with brackets or by utilizing a spherical manipulator. Furthermore, air-ducted adjustable sockets can allow the user to mount and dismount the bionic arm with ease. Also, attaching feedback sensors to sense the environment should be considered for further improvements.

4 Chapter 4 EMG based Biometrics Modality for Users Verification

Chapter Content

4.1	Introduction	72
4.2	Database Collection Protocol	73
4.3	Features Extraction for sEMG Users Verification	76
4.4	Machine Learning Models	79
4.5	Results	81

Summary: *In this chapter, the viability of using surface electromyogram (sEMG) as a biometric modality for user verification is investigated. A database of multi-channel sEMG signals is created using a wearable armband from able-bodied users. Several features are extracted in the frequency domain after estimating the power spectral density using Welch's method. Time-domain features are also extracted. Several classifiers based on K-nearest Neighbours (KNN), Linear Discernment Analysis (LDA), and Ensemble of Classifiers are constructed, trained, and statistically compared. False acceptance rate (FAR) and False Rejection Rate (FRR) are estimated for each classifier to determine the biometrics verification system's effectiveness.*

The chapter explains the database creation protocol in detail as this database of sEMG as a password is collected from 56 users and will be used in the next chapters in section 4.2. The features extraction process in the frequency domain and time domain is explained in detail in section 4.3. Three classifiers train the sEMG signals in section 4.4. The results of the testing accuracy, FAR, and FRR are mentioned in section 4.5.

4.1 Introduction

The study's primary purpose is to explore the concept of using sEMG signals in biometrics as a potential modality that can be used to verify individuals using a multi-channel EMG acquisition system. Using a multi-channel sEMG signal will significantly impact the accuracy and noise reduction of the biometrics system. Also, it contains more information that helps to detect the identity of the user. For example, in such systems, the Signal-to-Noise ratio (SNR) can be improved using numerous signal processing approaches such as: averaging, source separation, filtering, and decomposition techniques.

This chapter presents a detailed study using a multi-channel sEMG signal acquired by wearable bracelet Myo armband to be used in a biometric verification system based on the user's hand gestures. This chapter proposes a biometrics verification system for user's verification. The biometric identity studied in this research is sEMG. The biometric device used to acquire the sEMG signal is a wearable multi-channel armband consists of 8 electrodes. Fifty-six users have been enrolled in the biometric system. The users enrolled trained to use the sEMG biometric system before data collection. Eighteen features have been extracted from the signals to distinguish between users, seven frequency domain features, and eleven time-domain features. The power spectral density of each channel is estimated by periodogram using Welch's method first. Then, the signal's power, average frequency, kurtosis, median frequency, deciles, coefficient of dissymmetry, and peak frequency of PSD are calculated as frequency-domain features. The length or duration of data is calculated as a new feature Signal divided into ten equal-length segments, and the root means square (RMS) of each segment is calculated. K-nearest neighbors (kNN), Linear discriminant analysis classifier (LDA), an ensemble of classifiers have been applied to optimize the system's results. The system will grant/deny access to the user from the sEMG biometrics identity of each user. The signature of each user based on hand gestures. Performance analysis of the biometrics system has been presented to validate the system's capacity by calculating the False Acceptance Rate (FAR) and False Rejection Rate (FRR).

In all biometrics systems, users must first register their identity with the system employing recording raw biometric data. This phase is called Enrolment and is consists of three distinct phases: Capture, Process, and Enroll (Dantcheva, A., Velardo, C., D'angelo, A., and Dugelay, J. L., 2011).

In the capture phase, raw EMG signals are acquired by wearable 8-channel EMG armband. In the process phase, features that are unique to users and distinguish individuals from one another are extracted from the raw sEMG signals and transformed into each user's signature. This process is done in two steps, the first one is signal preprocessing, and the second one is feature extraction. The processed template is stored as a database in the hard disk, SD Card, or any other storage device for later comparisons in the Enroll phase.

Once Enrollment is complete, the system can authenticate users by means of using the prerecorded stored template (Soutar, C., Roberge, D., Stoianov, A., Gilroy, R., and Kumar, B. V., 1998). Verification is when a new biometric sample is captured by the individual who is authenticating with the system and compared to the stored biometric template. There are two types of users biometrics systems Verification and Identification.

Verification involves matching the captured biometric sample with the enrolled template saved and requires the user to present a specific identity claim such as a user name / unique key or card (Yamaba, H., Nagatomo, S., Aburada, K., Kubota, S., Katayama, T., Park, M., and Okazaki, N., 2015). Identification performs the process of identifying an individual from their biometric features without declaring their identity.

The biometrics verification system aims to provide enrolled users access to the system based on the individuals' specific features. The schematic chart illustrating the biometrics system steps shown in Figure 4-1. There are two paths of the diagram. The first path is to enroll the users in the system. A database of sEMG gestures that form a password of each user is created with all the units associated with signal processing, feature extraction, and machine learning to catalog the signals required to identify the user. The second path is to authenticate the user's identity by matching the enrolled users' identity with the stored database. The system grant/deny access to the users. In the biometrics verification systems, the user needs to declare his identity first, then declaring his/her biometrics identity, which is the sEMG signal in this system. A database of sEMG signals that forms a password is collected from 56 users able-bodied user.

4.2 Database Collection Protocol

The database of sEMG signal is collected from different volunteers for diverse purposes. All the volunteers are able-bodied with no health issues. Each user recorded the signals at multiple sessions of the same biometric identity to allow for genuine attempts. Myo bracelet was used

to gather the data of user's sEMG signals that form a password. Each user has been asked to select three gestures out of 4 gestures and arrange them to create a password using hand actions. A database of fifty-six participants has been collected (twenty-four males and thirty-two females with ages ranging from 16 to 62 years). The first step is to connect the armband wirelessly to the PC. Software is then developed to connect the Myo armband to the PC and visualize the data during the data acquisition phase. The recorded data is stored in a matrix data format. Features are extracted from the collected database. The extracted features are used to train and test the offline classifiers using numerical tools. There are three phases of data flowchart, data collection, data processing, and feature extraction (Said, S., Boulkaibet, I., Sheikh, M., Karar, A. S., Alkork, S., and Nait-ali, A., 2020) (Barioul, R., Ghribi, S. F., and Kanoun, O., 2016).

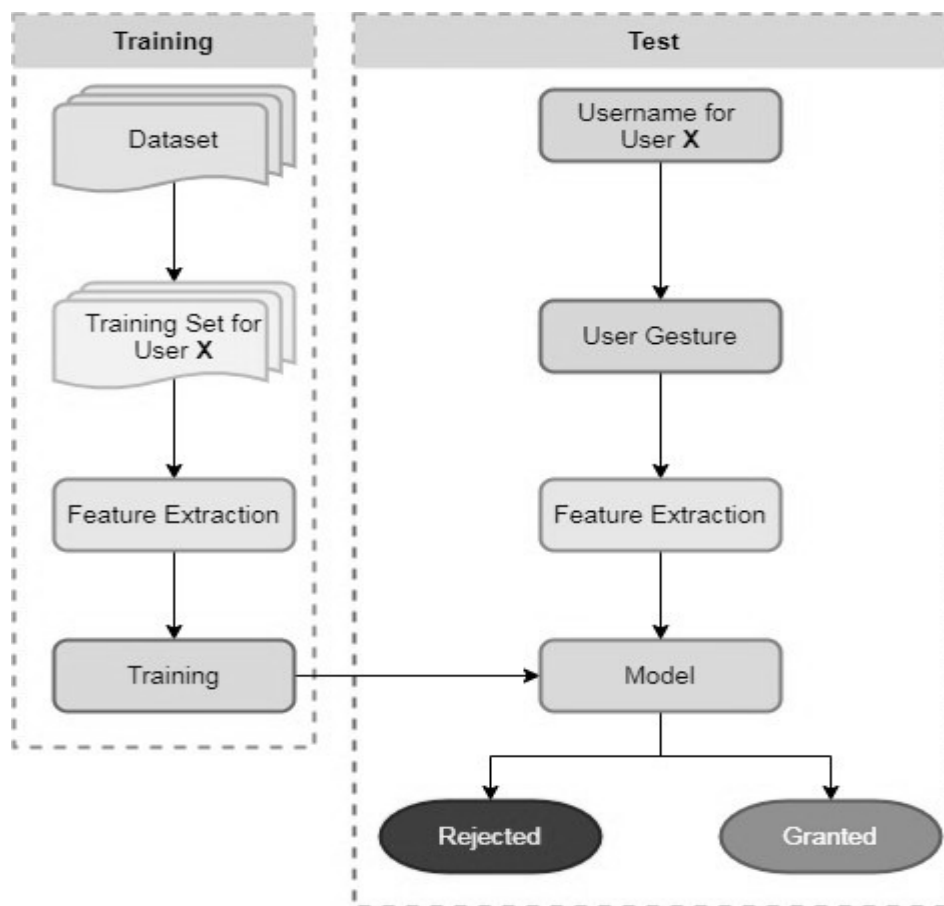


Figure 4-1 EMG Authentication System Schematic Chart

A set of instructions is prepared to apply them for all users as a data collection protocol to ensure the 56 users' data. The users were instructed to adjust their elbow joint at an angle of 90° during the data acquisition. Each volunteer collected the dataset that forms the biometrics password in several sessions to ensure that the user can perform the same pattern, which

consists of a combination of hand gestures. one of the most important instructions is that the Myo bracelet has to be attached at the same position on the forearm of all users with sensor number 4 placed on brachioradialis muscle as shown in Figure 4-2. The users can select three gestures from four hand gestures (Spread fingers, closed hand, wave-in, and wave-out). The participants were instructed to move their hand from the resting position to perform one of the proposed gestures and then move back to the resting position for around four seconds. Each user got a training session, not recorded signals, to get used to the selected hand gestures (signature). Once the user can produce the same pattern each time, for each user enrolled in the system, twenty tests have been recorded. The same procedure was applied to all users.

The characteristics of the database have a significant impact on the outcome of the evaluation. The amount of information available that could be used to characterize the features being compared is what determines the biometrics performance later.



Figure 4-2 Acquisition of sEMG data of a user to create the database (Enrolment)

The system's training phase consists of creating a training set for each user, feature extraction, and classifiers training. There are 56 users with 20 tests for each user. In a total of 1120 tests, each test contains eight signals as a multi-channel wearable armband used to acquire EMG signals. One binary-class classifier is trained for each user. This results in two-class outputs (Access granted or Access rejected) and 56 classifiers. As a random choice, 70% of each user's data selected for the training phase leads to 14 signals for Granted class and 770 signals for Rejected class, making data highly unbalanced. To overcome this problem, the under-sampling process is used. This results 14 signals randomly selected for Granted class and to create a Rejected class, one signal from each user (except valid user) is selected for the Rejected class, making 14 signals for Granted class and 55 signals for Rejected class.

4.3 Features Extraction for sEMG Users Verification

In the feature extraction process, the raw data size was reduced to be able to input these parameters to the Machine Learning (ML) classification model. In general, sEMG data contains essential and irrelevant information. The extrinsic information should be discarded to reduce the features vector's dimensionality by mapping sEMG data to another space. This step is important to extract the main features from the data of each user, which aids in distinguishing between the enrolled users (Akhmadeev, K., Houssein, A., Moussaoui, S., Høgestøl, E. A., Tuttunen, I., Harbo, H. F., and Gourraud, P. A., 2018) (Chantaf, S., Makni, L., and Nait-ali, A., 2020).

The calculation of the Power Spectral Density (PSD) of the sEMG signal is vital since it is calculated by using the relevant parameters used for the authentication of users. The PSD depicts the density of a signal regarding the frequency. The primary purpose of spectral density calculation is to capture the spectral density of the sEMG signal from a series of time samples. There are two different techniques used in the estimation of PSD, parametric and non-parametric. The estimated PSD is calculated directly from the signal in the Nonparametric methods. The most known simple method is called a periodogram. In the periodogram method, the discrete-time Fourier transform of the sampled signal is calculated first, then the magnitude squared of the result is calculated (Kay, 1988). In this research, the PSD is estimated by periodogram applying Welch's method (Proakis, 2001).

The power of the sEMG signal is estimated against frequency to reduce the noise. The signal is converted from the time domain to the frequency domain by using PSD. It is a direct application of using periodograms that convert a signal from the time domain to the frequency domain (Barbé, K., Pintelon, R., and Schoukens, J., 2009). This method is applied by dividing the time signal into successive blocks, forming the periodogram for each block, and calculating all the blocks' average.

Each block is divided as follow (4-1):

$$x_i(n) = x(n + iD) \quad (4-1)$$

such that $n = 0, 1, \dots, M - 1$ and $i = 0, 1, \dots, L-1$

M is the length of the blocks after division. D is the shifting between blocks, and L is the number of blocks.

The periodogram for each block is given by (4-2):

$$\hat{S}^l(f) = \frac{1}{MU} \left| \sum_{n=0}^{M-1} x(n) \cdot w(n) e^{-j2\pi fn} \right|^2 \quad (4-2)$$

U is the normalization factor of the window used to divide the signal into blocks (4-3).

$$U = \frac{1}{M} \sum_{n=0}^{M-1} w(n)^2 \quad (4-3)$$

The Welch PSD estimate is given by (4-4):

$$\widehat{S}_w(f) = \frac{1}{L} \sum_{l=0}^{L-1} \hat{S}^l \quad (4-4)$$

Upon estimating the PSD, the necessary parameters are extracted to be used to classify the users to verify their identity. The extracted features are signal power, kurtosis, median frequency, deciles, dissymmetry coefficient, and frequency peak.

- **Power of signal**

A signal's power represents the distribution of energy M_0 (order 0) on the frequency axis (4-5).

$$M_r = 2 \int_0^{\infty} f^r S_x(f) df \quad (4-5)$$

With S_x the estimation of the PSD by Welch method.

- **Average frequency**

Average frequency represents the statistical average of the signal (4-6)

$$MPF = \frac{M_1}{M_0} \quad (4-6)$$

- **Kurtosis**

Kurtosis measures the degree of peakedness of a distribution, defined as a normalized form of the fourth central moment μ_4 M_4 of a distribution (4-7).

$$CA = \frac{M_4^*}{M_2^{2*}} \quad (4-7)$$

- **Median Frequency**

The median divides the spectral density into two sections: 50% of data are less than the median, and 50% are greater. The median is calculated by (4-8):

$$\int_0^{F_{med}} S_x(f) df = \int_{F_{min}}^{F_{max}} S_x(f) df \quad (4-8)$$

- **Deciles**

The median divides the distribution of the spectral density into two sections. The division of this distribution can be generalized into four, ten, one hundred, or n parts. The obtained values are named quartiles, deciles, percentiles, or quantiles (4-9)

$$\int_{f_{F-1}}^{f_F} S_x(f) df = K \int_0^{F_{max}} S_x(f) df \quad 0 < k \leq 1 \quad (4-9)$$

- **Coefficient of dissymmetry**

This parameter gives information about the shape of the spectral density from a symmetrical point of view. It is given by (4-10) and (4-11):

$$CD = \frac{M_3^*}{\sqrt{M_2^{3*}}} \quad (4-10)$$

$$M_r^* = 2 \int_0^{\infty} (f - MPF) S_x(f) df \quad (4-11)$$

- **Peak Frequency**

The peak frequency is the frequency for which the spectral density function reaches its maximal amplitude. The extracted features are then fed into the classification algorithm in its reduced form rather than the raw data. The classification algorithm presented here will aim to verify or identify the enrolled users in the sEMG based biometrics system. Figure 4-3 shows the PSD of sEMG signal.

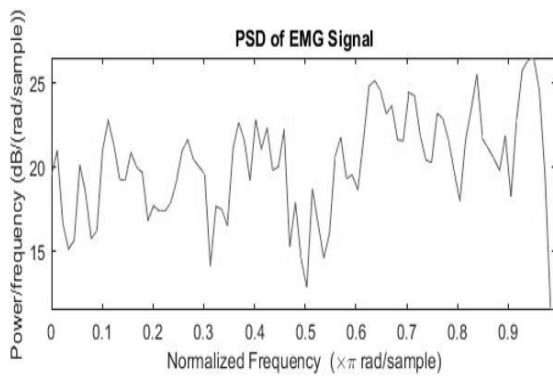


Figure 4-3 PSD of EMG signal

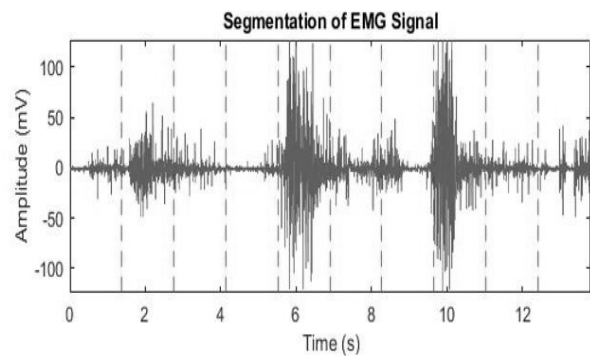


Figure 4-4 Segmentation of EMG signal

These features are called frequency-domain features of the sEMG signal. For better accuracy for the classifier, 3 Time domain features are calculated, Length or duration of data is calculated

as a new feature, Signal divided into ten equal length segments as shown in and the Root mean square (RMS) of each segment is calculated as a new feature.

4.4 Machine Learning Models

Machine-learning models are used widely in the biometrics verification system based on wearable technology systems. The result of machine-learning algorithms executed by the matching unit is a numerical value that estimates the similarity between the input signal and a registered user in the system. After getting this result, a threshold value is usually set to determine the biometrics system's final decision access granted, or access denied (Blasco, J., Chen, T. M., Tapiador, J., and Peris-Lopez, P, 2016). False acceptance rate (FAR) and false rejection rate (FRR) are considered the main biometrics performance analysis parameters used to estimate the system's accuracy. For optimization, three classifiers k-nearest neighbors (kNN), linear discriminant analysis classifier (LDA), and an ensemble of classifier or boosted trees were used to train this dataset and obtain the best model.

- **K-nearest neighbor (KNN) Classifier**

KNN classifier deals on the property that the classification of unknown instances can be accomplished by relating the unknown to the known according to similarity/distance function (Y. Paul, V. Goyal and R. A. Jaswal,, 2017). The unknown instance has a label with the same class label as of the known nearest neighbor. In this research, the Minkowski distance method has been applied in KNN algorithm applications.

The Minkowski distance is a method to find distance based on Euclidean space, defined by

$$d_{st} = \sqrt[p]{\sum_{i=1}^n |x_{sj} - y_{tj}|^p} \quad (4-12)$$

For the particular case of Minkowski distance $p = 1$, the Minkowski metric gives the city block distance, $p = 2$, the Minkowski metric gives the Euclidean distance, and $p = \infty$, the Minkowski metric provides the Chebychev with distance.

- **Linear Discriminant Analysis (LDA) Classifier**

Linear discriminant analysis (LDA) classifier is extensively used in sEMG pattern recognition for bionic arm control (Zhang, H., Zhao, Y., Yao, F., Xu, L., Shang, P., and Li, G., 2013). It depends on the Bayes classification rule, which states that for a given vector x , assign it to the class c_k when the following inequality is satisfied

$$p(c_k|x) > p(c_j|x) \text{ for all } k \neq j \quad (4-13)$$

These posterior probabilities cannot be directly measured but can be obtained from estimates of the prior probabilities and the distribution of the class according to the Bayes formula:

$$p(c_k|x) = \frac{p(c_k)p(x|c_k)}{p(x)} \quad (4-14)$$

Where $p(c_k|x)$ is the probability density function for the vector within k class, $p(c_k)$ is the prior probability for class k and usually assumed to be equal for all classes, $p(x)$ is the probability density function of the input space and is also constant over all the classes. Then the decision rule referred to as equation (4-15) is simplified to:

$$p(x|c_k) > p(x|c_j) \text{ for all } k \neq j \quad (4-15)$$

In the LDA classifier implementation, the probability density functions for all the classes are assumed to follow a multivariate Gaussian distribution.

$$p(x|c_k) = \frac{1}{\sqrt{(2\pi)^f \det(C)}} \exp\left(-\frac{1}{2}(x - \mu_k)^T C^{-1}(x - \mu_k)\right) \quad (4-16)$$

where x is the vector to be classified, f is the dimension of the vector, C is the common covariance matrix of all the classes, k and μ_k is the mean value of class k .

For a given training dataset, the parameters μ_k and C is constant, and the LDA classifier is static. Therefore, the LDA classifier is challenging to maintain the classification accuracy constant when the EMG recordings are changing.

- **Ensemble Classifier (Gentle AdaBoost Algorithm)**

In collective classifiers, more than one singular classifier is brought together to enhance the classification performance. Algorithms such as decision trees, support vector machines, the Naive Bayes method, linear separators, and artificial neural networks are widely used as single classifiers [28].

Boosting is a general technique used in machine learning that aims to extract a robust classifier from a combination of weak classifiers. The Adaboost algorithm proposed by Freund and Schapire which was the first practical boosting algorithm (Freund, Y., and Schapire, R. E., 1995), which serves in many fields of applications (Freund, Y., Schapire, R., and Abe, N., 1999).

The Adaboost algorithm takes input a training set of m examples (x_i, y_i) , $i = 1:m$, where $x_i \in X$ is a vector-valued feature, $y_i \in \{-1, +1\}$ is the class label associated with x_i . The

Adaboost algorithm calls a weak classifier repeatedly in a series of rounds $t = 1, \dots, T$. On each round t , the distribution D_t is provided to the weak learning algorithm over the training set. A given weak classifier is applied to find a weak hypothesis $h_t: X \rightarrow \{-1, +1\}$ that matches with the distribution D_t that indicates the necessity of examples in the data set for the classification. The weights of each incorrectly classified example are increased or alternatively the weights of each correctly classified example (with low weighted error ε_t relative to D_t) are decreased. Once the weak hypothesis h_t has been received, Adaboost chooses a parameter α_t which measures the importance that is assigned to h_t . For this, a coefficient α_t is calculated as:

$$\alpha_t = \frac{1}{2} \ln\left(\frac{1-\varepsilon_t}{\varepsilon_t}\right) \quad (4-17)$$

The final hypothesis H computes the sign of a weighted combination of weak hypotheses:

$$H(x) = \text{sign}\left(\sum_{t=1}^T \alpha_t h_t(x)\right) \quad (4-18)$$

A weak classifier should satisfy two conditions; it should do better than random guessing and should have enough computational power to learn a problem. The simplest weak classifiers are decision stumps, decision trees with only one decision node. A decision stump has the following form: $h(x) = s(x_k > c)$, where $c \in R$, $k \in \{1, \dots, K\}$; K is the dimension of x_k , and $s \in \{-1, 1\}$. In other words, the decision stump gives a prediction based on the value of a single input.

Many variants of the Adaboost algorithm were proposed to enhance the basic algorithm, such as Real Adaboost and Gentle Adaboost. Real Adaboost is more generalized from discrete Adaboost, where the weak learners can output a real value $h_t(x) \in R$. The sign of this output gives the predicted label $\{-1, +1\}$ and its value provides a measure of confidence level in this prediction. Gentle Adaboost (Friedman, J., Hastie, T., & Tibshirani, R., 2000) is a modified version of the Real AdaBoost algorithm. It utilizes a weighting scheme that exploits a function of margins, which decreases slower than the exponential function used by the Adaboost algorithm. Newton steps are used to minimize the exponential loss function of Adaboost (Mekhalfa, F., and Nacereddine, N., 2017). Gentle AdaBoost Algorithm nowadays the most successful boosting procedure because of its robustness and stability to noisy data.

4.5 Results

After selecting three different types of classifiers, the offline procedure was used to train and test these classifiers to select the model that will be best used for the verification system after

calculating the performance analysis parameters. Testing the system has been conducted by the data that kept for testing, representing 30% of the database. As the system is designed to be used for user verification, the user should input the user name first and then enter the biometrics identity.

The parameter values for the three classifiers were selected after performing a cross-validation process for each classifier. Each classifier was used to train and test the same dataset for a different set of parameters. Table 4-1 shows the selected parameter for each classifier used in the training and testing of the data. The best model for each version of the three classifiers was selected based on its performance. Next, a statistical study was used to compare the testing results to select the best classifier among the three classifiers (KNN, LDA, and Ensemble classifier). First, each classifier was run for thirty trials, and the testing accuracy for the classification was stored in a table. The Ensemble classifier algorithm produced the highest testing accuracy of 98.5%. The LDA classifier provided a testing accuracy equal to 98.3%. Furthermore, The KNN classifier provided a mean value of the testing accuracy equal to 97.4%. The results of the average accuracy for the three classifiers are presented in Figure 4-6.

Table 4-1 Selected Parameters for the Classifiers in Users Verification System

k-nearest Neighbors	
Number of neighbors	2
Distance metric	Minkowski
Distance Weight	Inverse
Exponent	0.57
Linear Discriminant Analysis	
Delta	0.01
Gamma	0.7
Discriminant Type	PseudoLinear
Ensemble Classifier	
Weak Learner	Decision Tree
Method	GentleBoost
Number of Learning Cycles	11

Learning Rate	0.95
Minimum Leaf Size	22
Maximum number of Split	1

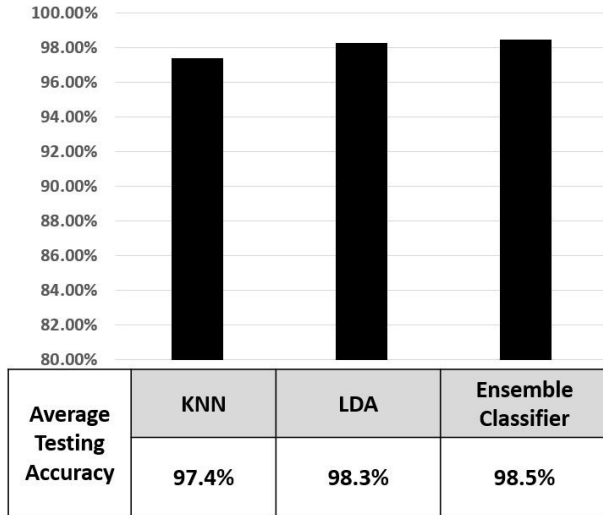


Figure 4-5 Average Testing Accuracy of Verification System

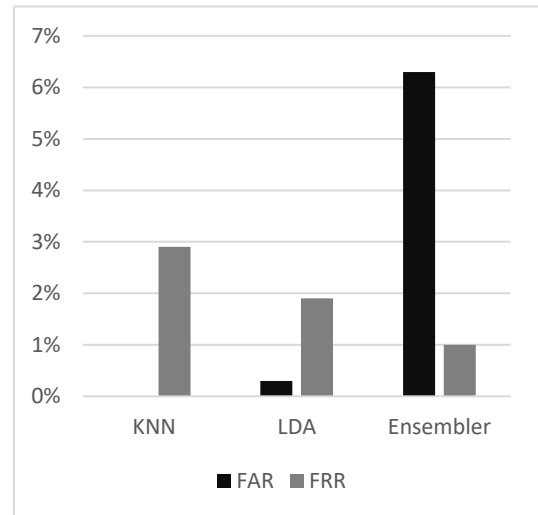


Figure 4-6 FAR and FRR of the Three Classifiers

For performance analysis of the system, accuracy, false acceptance rate (FAR), and false rejection rate (FRR) for each case are calculated.

The FAR is the percentage of incorrect acceptance by unauthorized users requesting attempting to access the system. A system’s FAR typically is stated as the ratio of the number of false acceptances divided by the number of identifications attempts, and it can be calculated as below:

$$FAR = \frac{\text{number false acceptance}}{\text{number of unauthorized attempts}} \quad (4-19)$$

The FRR, on the opposite side, provides the percentage of rejected attempts of authorized users attempted to access the system. A system’s FRR is calculated as the ratio of the number of false recognitions divided by the number of verification attempts. and it can be calculated as below:

$$FRR = \frac{\text{number false recognition}}{\text{number of authorized attempts}} \quad (4-20)$$

For biometrics verification applications, the registered users need to declare their identity, a user name in this particular application, along with the biometric identifier. The authentication system then compares the input identity with the stored template in a database of various claimed identities to confirm or deny the authenticity claims (He, J., and Jiang, N., 2020). As such, the verification mode is a binary classification. FAR and FRR evaluate the performance of the verification system. Table 4-2 detailed the user verification system results using three different classifiers models; for each model, the average accuracy, FAR, and FRR are calculated.

Table 4-2 Results of Biometrics Users verification System

User Name	kNN			Discriminant			Ensemble		
	Acc.	FAR	FRR	Acc.	FAR	FRR	Acc.	FAR	FRR
User 1	98.4	0	1.8	98.4	0	1.8	98.4	0	1.8
User 2	98.4	0	1.8	96.7	0	3.6	98.4	0	1.8
User 3	90.2	0	10.9	93.4	16.7	5.5	100	0	0
User 4	98.4	0	1.8	100	0	0	100	0	0
User 5	96.7	0	3.6	96.7	0	3.6	98.4	0	1.8
User 6	98.4	0	1.8	100	0	0	100	0	0
User 7	93.4	0	7.3	100	0	0	98.4	0	1.8
User 8	95.1	0	5.5	100	0	0	98.4	16.7	0
User 9	98.4	0	1.8	100	0	0	98.4	16.7	0
User 10	96.7	0	3.6	100	0	0	96.7	33.3	0
User 11	100	0	0	100	0	0	98.4	0	1.8
User 12	95.1	0	5.5	100	0	0	100	0	0
User 13	96.7	0	3.6	95.1	0	5.5	100	0	0
User 14	96.7	0	3.6	96.7	0	3.6	98.4	0	1.8
User 15	93.4	0	7.3	98.4	0	1.8	100	0	0
User 16	100	0	0	100	0	0	98.4	0	1.8
User 17	93.4	0	7.3	95.1	0	5.5	93.4	33.3	3.6
User 18	100	0	0	100	0	0	98.4	16.7	0
User 19	100	0	0	98.4	0	1.8	100	0	0
User 20	100	0	0	98.4	0	1.8	100	0	0
User 21	95.1	0	5.5	95.1	0	5.5	95.1	33.3	1.8
User 22	95.1	0	5.5	98.4	0	1.8	98.4	0	1.8

User 23	95.1	0	5.5	98.4	0	1.8	100	0	0
User 24	98.4	0	1.8	100	0	0	100	0	0
User 25	98.4	0	1.8	96.7	0	3.6	98.4	0	1.8
User 26	100	0	0	100	0	0	98.4	16.7	0
User 27	100	0	0	100	0	0	100	0	0
User 28	98.4	0	1.8	100	0	0	100	0	0
User 29	100	0	0	100	0	0	96.7	0	3.6
User 30	98.4	0	1.8	100	0	0	98.4	0	1.8
User 31	95.1	0	5.5	98.4	0	1.8	98.4	0	1.8
User 32	95.1	0	5.5	95.1	0	5.5	95.1	33.3	1.8
User 33	98.4	0	1.8	100	0	0	100	0	0
User 34	100	0	0	100	0	0	100	0	0
User 35	98.4	0	1.8	96.7	0	3.6	98.4	0	1.8
User 36	96.7	0	3.6	95.1	0	5.5	96.7	0	3.6
User 37	96.7	0	3.6	100	0	0	96.7	16.7	1.8
User 38	98.4	0	1.8	96.7	0	3.6	98.4	0	1.8
User 39	96.7	0	3.6	96.7	0	3.6	96.7	16.7	1.8
User 40	100	0	0	100	0	0	100	0	0
User 41	100	0	0	100	0	0	100	0	0
User 42	100	0	0	100	0	0	100	0	0
User 43	96.7	0	3.6	98.4	0	1.8	98.4	16.7	0
User 44	93.4	0	7.3	96.7	0	3.6	100	0	0
User 45	96.7	0	3.6	96.7	0	3.6	98.4	0	1.8
User 46	98.4	0	1.8	98.4	0	1.8	100	0	0
User 47	98.4	0	1.8	100	0	0	96.7	33.3	0
User 48	96.7	0	3.6	96.7	0	3.6	98.4	0	1.8
User 49	98.4	0	1.8	98.4	0	1.8	100	0	0
User 50	95.1	0	5.5	100	0	0	100	0	0
User 51	93.4	0	7.3	95.1	0	5.5	93.4	33.3	3.6
User 52	100	0	0	100	0	0	100	0	0
User 53	100	0	0	98.4	0	1.8	100	0	0
User 54	93.4	0	7.3	96.7	0	3.6	93.4	16.7	5.5
User 55	98.4	0	1.8	98.4	0	1.8	98.4	0	1.8
User 56	100	0	0	96.7	0	3.6	98.4	16.7	0

Mean	97.4	0	2.9	98.3	0.3	1.9	98.5	6.3	1
------	------	---	-----	------	-----	-----	------	-----	---

In all the verification scenarios and for each type of classifiers presented in this research, FAR and FRR are calculated. For the KNN classifier, the average value of FAR is 0% means non of the users is able to access any other user even by mimicking the hand actions, and the FRR is 2.9%, which points out of 100 user, 2.9 users weren't able to access the system due to a deviation in the hand actions which represents the password of their own. For the LDA classifier, the FAR is 0.3%, and FRR is 1.9%. While applying Ensemble Classifier gave FAR 6.3% and FRR 1%. Figure 4-6 Shows the FAR and FRR of the three classifiers.

The ensemble classifier shows the best accuracy in the three classifiers, but the KNN classifier gave FAR of 0% and FRR of 2.9%. This makes the KNN is the best algorithm used in the verification biometrics system presented in this chapter.

A Graphical User Interface (GUI) is developed as a tool for the users to check the system's robustness. The system requires users to declare their identity by entering the user name. The user name entered is case sensitive to provide a more secure biometrics system. If the user entered the wrong user name, the system would deny access. If the user entered the correct user name, the system would ask the user to input the biometrics password, a combination of hand actions. The system extracts the features from the entered sEMG signals and compares the features with the stored database of trained models for this specific user. If the users entered a wrong password or the features didn't match the stored features, the system will deny this user access.

Table 4-3 Comparison between different research work of sEMG biometrics users verification system

Evaluated work on biometrics verification	Accuracy
Seven frequency domain with Radial Basis Function Network using single-channel (S. Chantaf,2011)	80 %
CNN with 8 users using multi-channel (R. Shioji, 2018)	94.9%
Frequency domain features and time domain features classified using SVM and KNN (Kim and Pan, 2017)	85%

4.6 Conclusion

The performance of sEMG signals as a biometric modality for user verification is investigated. The users were able to perform a custom-set gesture code. The resulting sEMG signals were

captured and proceed as a form of hidden biometric identity. The results indicated that the custom-set gesture code improves verification performance. The set of frequency and time-domain features extracted in this study allowed for improved classifier accuracy. The KNN classifier was found to be optimum, with an average accuracy of 97.4%. The FAR and FRR of the KNN classifier results are 0% and 2.9%, respectively.

5 Chapter 5 sEMG Machine-learning based Biometrics Modality for Users Identification

Chapter Content

5.1	Introduction	89
5.2	Features Extraction.....	91
5.3	Machine Learning Model.....	93
5.4	Results	94
5.5	Conclusion.....	97

Summary: *In the user's identification system, a total of 5 features are extracted from the signals to identify between the users from their biometrics identity without declaring their identity. Three classifiers are used to classify the data, KNN, LDA, and Ensemble of Classifiers as well. The average accuracy of the KNN classifier proved the concept of using the sEMG for the user's identification system.*

The chapter starts with an introduction to the identification system based on the sEMG signal in section 5.1. The five extracted features in the time-domain are explained in section 5.2. Section 5.3 describes the three machine learning models. The results of the sEMG biometrics identification system are presented in section 5.4.

5.1 Introduction

the muscle activation process produces an sEMG signal. It is usually measured through the surface differential or double differential electrodes, as explained in the previous chapters. sEMG signal amplitude is always measured in millivolts. sEMG signal has a wide variety of applications. In this chapter, multi-users' biometrics identification systems will be explained in detail, showing the steps of implementing the system.

The physiology of the user is affecting the sEMG signal. Muscle position, orientation, shape, and size are altered during human movement while attaching the sensors to their muscles. While neural activity, blood flow, and skin conductivity can differ depending on the user's mental state. These produce variability into the sEMG signal, which same hand gestures that look identical will always give you different EMG signals.

Everyone is different from others, and every reading is different, but ignoring which factors causes differences in the measurement, the reason that makes sEMG contains physiological dependent variables, provides it with the capability to be used for biometric identification (Krishnamohan, P. G., and Holi, M. S., 2011).

EMG systems can work within four categories:

- 1) A single device used by a single user.
- 2) Multiple devices used by a single user.
- 3) Single device for multiple users.
- 4) Multiple devices for multiple users.

Systems that deal with single users using single devices are relatively advanced and have difficulties with EMG external factors, such as skin-electrode contact, electrodeposition, limb orientation, and temperature. If these parameters are kept unchanged, the user can train the system and use it perfectly until physiological factors change enough to affect classification.

Using multiple devices for one user will face a problem, that single users must train various systems. Each device might behave differently, as the training data will change every time. Multiple users to use single devices will have the problem that each additional user enrolled in the system might affect other users' classification, especially if there are significant

physiological differences between users. Category 4 contains the difficulties mentioned in category 2 and category 3.

All categories need a training session initially, and retraining after a user's physiological features change significantly to the point that affects classification accuracy. Categories 2, 3, and 4 would require additional training and calibration.

In the proposed biometrics identification system, category 3 is based on multiple users using a single device, Myo armband, consisting of eight-channel EMG sensors. sEMG based biometrics verification system has been analyzed and explained in detail. In this chapter, multi-users biometrics identification system performance will be studied. The biometrics users' identification system doesn't require declaring the identity of the users in advance. Only the user's password, which is formed by a combination of hand gestures, will be necessary. Myo armband was used to collect the data of the user's sEMG signals that create a password. Each user has been asked to select three gestures out of 4 gestures and arrange them in a way to form a password using hand actions. A database of fifty-six participants has been collected (twenty-four males and thirty-one females with ages ranging from 16 to 62 years). The database used in the biometrics identification system study is the same database used in the biometrics verification system.

The biometrics identification system aims to recognize the system's enrolled users based on specific features of the individual's passwords. The schematic chart illustrating the biometrics identification system's steps is shown in Figure 5-1. There are two paths of the diagram. The first path is to enroll the users in the system. A database of sEMG gestures that form a password of each user is created with all the units associated with signal processing, features extraction, and machine learning to characterize the signals required to identify the users without declaring their identity. The second path is to the user's identity by matching the enrolled users' identity with the stored database. The system output, in this case, is the user's names in the biometrics identification systems. A database of sEMG signals that form a password is collected from 56 users able-bodied users. The database collection protocol is explained in detail in the section *Database Collection Protocol*. Three machine learning models have been used to train the classifier and obtain the optimum model that produces maximum accuracy.

5.2 Features Extraction

Raw-acquired EMG signals have a complicated wave-form. They are quasi-random. They contain important information, and features related to the users' identity and workings and contamination have always been a challenging task. That is why the sEMG signal needs to be processed initially. One of the most critical steps in sEMG processing is feature extraction. In feature extraction, the operations need to be applied to raw signals to transform the movement into a reduced representation set of features. This process will reduce the dimensionality of the input data and highlight only the needed information. There are three types of features in different domains; Time, Frequency, and Time-Frequency distribution, which each of these categories uses in specific applications. For the biometrics user's identification system, five different time-domain features are extracted from the signals in order to recognize the users enrolled in the database. These features are standard deviation, skewness, zero-crossing rate, mean absolute of the EMG signal, and the maximum value of the logarithm of absolute of EMG.

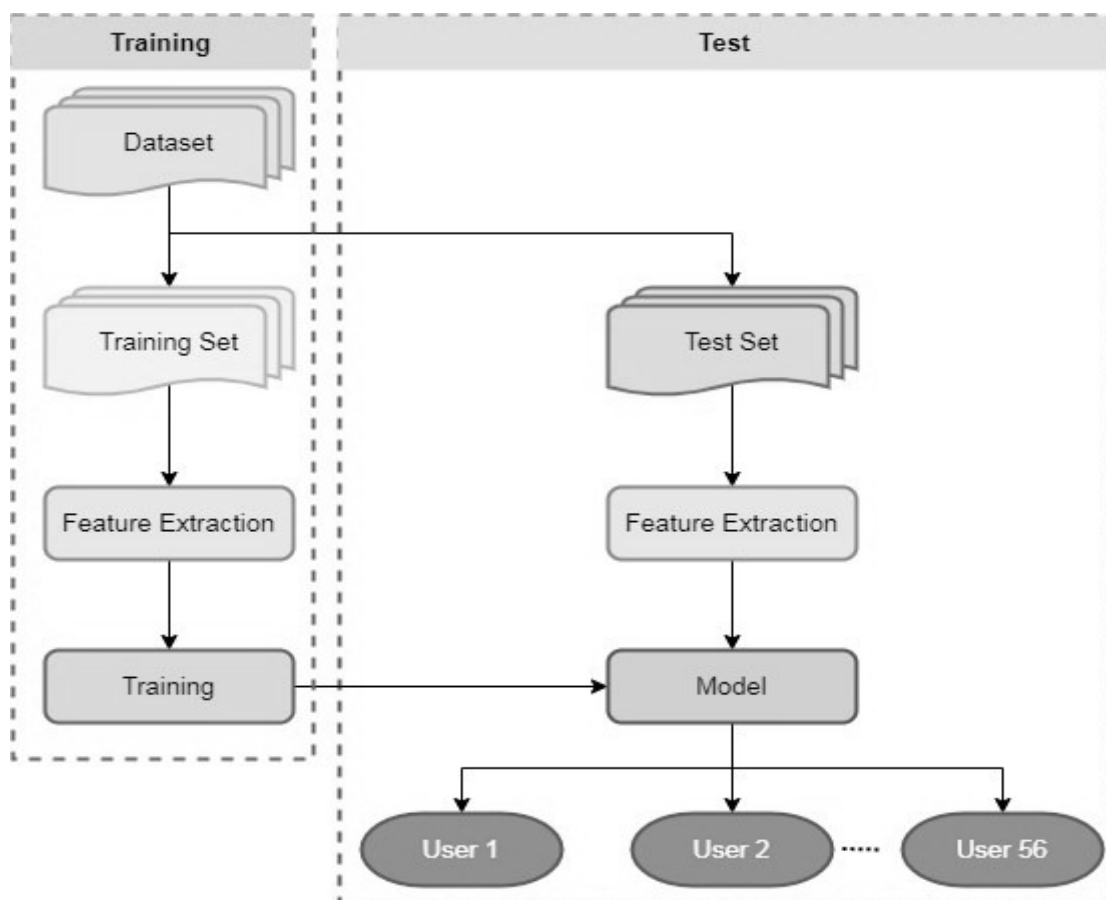


Figure 5-1 Biometrics Identification System Schematic Chart

- **Standard deviation of EMG**

One of the features that are used in the detection of movements of the muscles is the standard deviation of the sEMG signal. SD is expressed as the square root of the EMG signal's power and is used to extract features from the EMG data. The SD is defined as:

$$SD = \sqrt{\frac{1}{N-1} \sum_{n=1}^N (x_n)^2} \quad (5-1)$$

- **Coefficient of dissymmetry of EMG**

Skewness is the inclination distribution of the data. It is one of the sEMG signal features that is used in the time domain function. If the average value's location, the median value, and the data model on a line in the curve, the data is called, they are typically distributed. But if these values are not located in one line in the curve occurs the skewness

$$Skewness = \frac{\frac{1}{N} \sum_{n=1}^N (x_n - \mu)^3}{\sigma^3} \quad (5-2)$$

$$\sigma = \sqrt{\frac{1}{N-1} \sum_{n=1}^N (x_n - \mu)^2} \quad (5-3)$$

$$\mu = \sum_{n=1}^N x_n \quad (5-4)$$

- **Zero crossing rate of EMG**

Zero-Crossing (ZC) is one of the features that characterize the sEMG signal. It represents the number of times the amplitude points of sEMG signal crosses zero in the x-axis. In the sEMG feature, to avoid the background noise, a threshold condition is set. Zero-Crossing gives an estimate of frequency domain properties. The calculation is defined as:

$$ZC = \sum_{n=1}^{N-1} sgn(x_n \times x_{n+1}) \cap |x_n - x_{n+1}| \geq threshold \quad (5-5)$$

$$sgn(x) = \begin{cases} 1, & \text{if } x \geq threshold \\ 0, & \text{otherwise.} \end{cases}$$

- **Mean absolute of EMG**

Mean Absolute Value (MAV) is the same as the Average Rectified Value (ARV). MAV can be found by applying the moving average of full-wave rectified sEMG. This means it is estimated by calculating the average of the absolute value of the sEMG signal. It is a direct way to detect the level of muscle contraction. It is a popular feature used in the myoelectric control application. It is calculated as:

$$MAV = \frac{1}{N} \sum_{n=1}^N |x_n| \quad (5-6)$$

- **Maximum value of the logarithm of the absolute value of EMG**

After calculating the absolute value of the logarithmic value of the sEMG signal, the maximum value is used as one of the features that will input the classifier along with the other calculated features. Figure 5-2 shows the absolute value of the sEMG signal and the Log absolute of the sEMG signal.

$$MLAV = \max(\sum_{n=1}^N \log(|x_n|)) \quad (5-7)$$

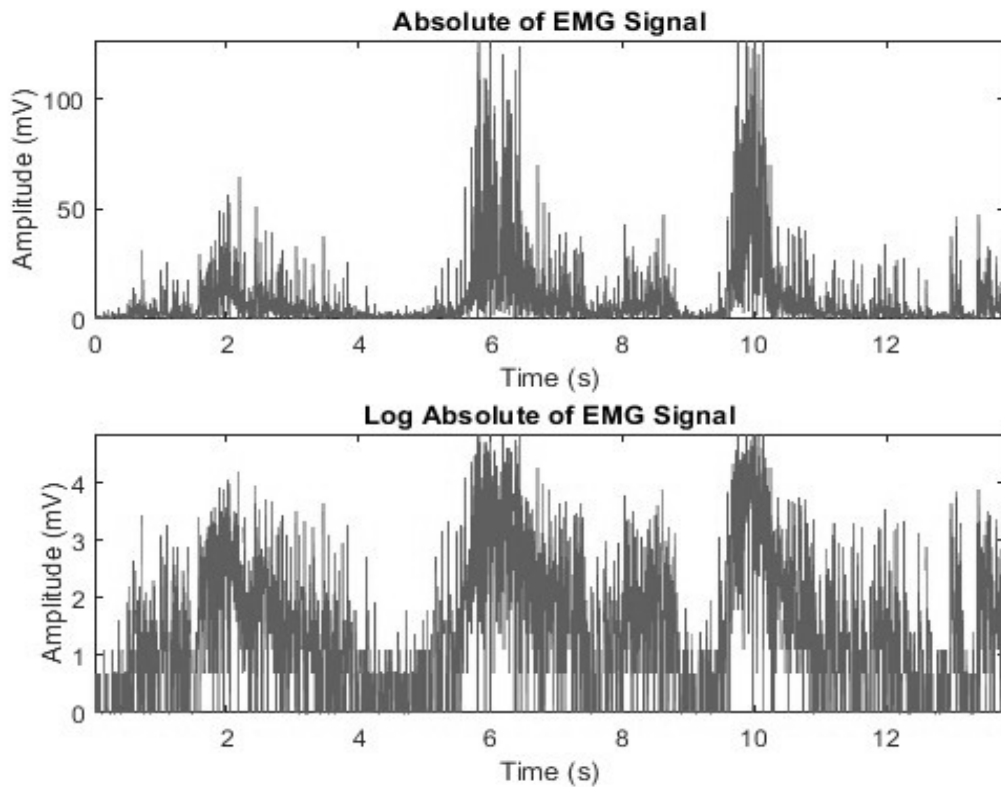


Figure 5-2 Absolute and log absolute value of EMG signal

5.3 Machine Learning Models

The final step for the training phase is the training of classifiers. For comparison, three classifiers k-nearest neighbors (kNN), linear discriminant analysis classifier (LDA), and an ensemble of classifier or boosted trees were used the same as detailed explained in section 4.4 Machine Learning Models. The three classifiers' parameter values were selected after performing a cross-validation process for each classifier. Each classifier was used to train and

test the same dataset for a different set of parameters. Table 5-1 shows the selected parameter for each classifier used in the data's training and testing.

Table 5-1 Selected Parameters of the Classifiers in Identification System

k-nearest Neighbors	
Number of neighbors	2
Distance metric	Minkowski
Distance Weight	Inverse
Exponent	0.57
Linear Discriminant Analysis	
Delta	0.01
Gamma	0.7
Discriminant Type	PseudoLinear
Ensemble Classifier	
Weak Learner	Decision Tree
Method	GentleBoost
Number of Learning Cycles	11
Learning Rate	0.95
Minimum Leaf Size	22
Maximum number of Split	1

5.4 Results

After selecting three different classifiers, the offline procedure was used to train and test these classifiers to select the model that will be best used for the verification system after calculating the performance analysis parameters. The system test phase has been conducted by the data that kept for testing, representing 30% of the database. As the system is designed to be used for user identification, the user should input the biometric identity first, and then the system will then identify the individuals from their password (a combination of hand gestures) and output the user name.

The best model for each version of the three classifiers (KNN, LDA, and Ensemble classifier) was selected based on its performance. Next, a statistical study was used to compare the testing results to choose the best classifier among the three classifiers (KNN, LDA, and Ensemble classifier). First, each classifier was run for thirty trials, and the average testing accuracy for the classification was stored in a table. The KNN algorithm produced the highest testing

accuracy of 86.01%. The LDA classifier provided a testing accuracy equal to 82.74%. Furthermore, the ensemble classifier provided a mean value of the testing accuracy equal to 75.89%. The results of the three classifiers' average accuracy are presented in Table 5-2. The detailed results of the biometrics users identification system analyzed user by user are shown in Table 5-3.

Table 5-2 Classifier Accuracy for users identification system

Classifier	Accuracy (%)	Number of Correctly Classified Signals	Number of Incorrectly Classified Signals
kNN	86.01	289	47
Discriminant Analysis	82.74	278	58
Ensemble Classifier	75.89	255	81

Table 5-3 Results of EMG Identification System

User Name	kNN			LDA			Ensemble		
	Correct	Incor.	Accu.	Correct	Incor.	Accu.	Correct	Incor.	Acc.
User 1	6	0	100	0	6	0	1	5	16.67
User 2	3	3	50	0	6	0	0	6	0
User 3	6	0	100	6	0	100	6	0	100
User 4	6	0	100	6	0	100	6	0	100
User 5	6	0	100	0	6	0	0	6	0
User 6	6	0	100	6	0	100	6	0	100
User 7	6	0	100	6	0	100	6	0	100
User 8	6	0	100	6	0	100	6	0	100
User 9	6	0	100	6	0	100	6	0	100
User 10	6	0	100	6	0	100	6	0	100
User 11	6	0	100	6	0	100	6	0	100
User 12	6	0	100	6	0	100	6	0	100
User 13	6	0	100	6	0	100	6	0	100
User 14	6	0	100	6	0	100	6	0	100
User 15	6	0	100	6	0	100	5	1	83.33
User 16	6	0	100	6	0	100	6	0	100
User 17	5	1	83.33	1	5	16.67	0	6	0

User 18	6	0	100	6	0	100	6	0	100
User 19	6	0	100	6	0	100	6	0	100
User 20	6	0	100	6	0	100	5	1	83.33
User 21	6	0	100	1	5	16.67	1	5	16.67
User 22	6	0	100	3	3	50	1	5	16.67
User 23	6	0	100	6	0	100	6	0	100
User 24	6	0	100	6	0	100	6	0	100
User 25	6	0	100	1	5	16.67	1	5	16.67
User 26	6	0	100	6	0	100	6	0	100
User 27	6	0	100	6	0	100	6	0	100
User 28	6	0	100	6	0	100	6	0	100
User 29	6	0	100	6	0	100	5	1	83.33
User 30	5	1	83.33	5	1	83.33	6	0	100
User 31	0	6	0	0	6	0	1	5	16.67
User 32	0	6	0	3	3	50	1	5	16.67
User 33	6	0	100	6	0	100	6	0	100
User 34	6	0	100	6	0	100	6	0	100
User 35	0	6	0	4	2	66.67	1	5	16.67
User 36	6	0	100	6	0	100	6	0	100
User 37	6	0	100	6	0	100	6	0	100
User 38	0	6	0	4	2	66.67	1	5	16.67
User 39	6	0	100	6	0	100	6	0	100
User 40	6	0	100	6	0	100	6	0	100
User 41	6	0	100	6	0	100	6	0	100
User 42	6	0	100	6	0	100	6	0	100
User 43	6	0	100	6	0	100	5	1	83.33
User 44	6	0	100	6	0	100	6	0	100
User 45	0	6	0	2	4	33.33	1	5	16.67
User 46	6	0	100	6	0	100	6	0	100
User 47	6	0	100	6	0	100	6	0	100
User 48	6	0	100	6	0	100	5	1	83.33
User 49	6	0	100	6	0	100	6	0	100
User 50	6	0	100	6	0	100	5	1	83.33
User 51	0	6	0	2	4	33.33	0	6	0

User 52	6	0	100	6	0	100	6	0	100
User 53	6	0	100	6	0	100	5	1	83.33
User 54	6	0	100	6	0	100	6	0	100
User 55	0	6	0	6	0	100	1	5	16.67
User 56	6	0	100	6	0	100	6	0	100
Mean	5.16	0.84	86.01	4.96	1.03	82.74	4.55	1.45	75.89

5.5 Conclusion

The performance of sEMG as a biometric trait for user identification was investigated. The users were able to perform a custom-set gesture code. The resulting sEMG signals were captured and proceed as a form of hidden biometric identity. The results indicated that the custom-set gesture code could significantly improve identification performance. The set of time-domain features extracted in this study allowed for improved classifier accuracy. The KNN classifier was found to be optimum, with an average accuracy of 86.2%.

The average classifier accuracy can be optimized by collecting 50 tests from each user enrolled in the system instead of 20 tests to have enough data to train the identification system's classifiers. The user's identification system's average accuracy reached 99% during testing the classifier when only 30 users out of 56 users are selected for training the classifier.

6 Chapter 6 Deep Learning for sEMG Biometrics System

Chapter Content

6.1	Introduction	100
6.2	Deep Learning for Biometrics Users Verification System.....	103
6.2.1	Input Generation	103
6.2.2	Continuous Wavelet Transform (CWT)	104
6.2.3	Data Augmentation	106
6.2.4	Convolutional Neural Network Structure and Training.....	106
6.2.5	Testing and Results	109
6.3	Deep Learning for Biometrics Users Identification System	112
6.3.1	Input Generation	113
6.3.2	Wavelet Based Denoising	114
6.3.3	Data Augmentation	115
6.3.4	CNN Architecture and Training.....	115
6.3.5	Testing and Results	116
6.4	Conclusion.....	117

Summary: Recently, deep learning algorithms have become increasingly more prominent for their unparalleled ability to learn from large amounts of data automatically. In the field of electromyography-based biometrics systems, deep learning algorithms are seldom employed as they require an unreasonable amount of effort from a single person to generate tens of thousands of examples. In this chapter, data augmentation is used to create a big database out of a smaller database used in the classical machine learning approach by augmenting multiple users' signals, thus reducing the recording burden while enhancing the recognition rate. Convolutional Neural Network (CNN) is used to train the users in the EMG biometrics system. Squeeze net neural network structure is selected due to its faster training time as it requires fewer parameters while maintaining the accuracy level. Continuous wavelet transforms (CWT) are applied to the database to estimate the EMG signals'

scalograms. The results of the testing accuracy, along with the FAR and FRR values, are calculated. In the Biometrics Identification system, both raw and denoised sEMG signals are used to generate scalograms using CWT. Two CNN structures have been applied squeeze-net structure and Alex-net structure. The classifiers results are mentioned.

The chapter organized as follows, starting with an introduction to the deep learning for sEMG signals as a biometrics modality in section 6.1. The biometrics verification system applying deep learning steps are listed in section 6.2, while the biometrics identification system utilizing the deep learning approach is explained in section 6.3. The chapter ended up with a conclusion for both systems in section 6.4.

6.1 Introduction

Distinguishing sEMG signals acquired from multiple users is the core part of the related applications using sEMG signals as biometrics modality. At present, the literature on biometrics systems based on sEMG signals primarily focuses on the time and frequency domain feature extraction of sEMG signals, which aims to distinguish sEMG signals by feature recognition.

As stated and explained in this thesis, some effective feature combinations have been proposed in both the time domain and frequency domain as described and implemented in the previous thesis chapters, and some fruitful results have been achieved with the dataset of the users collected and explained in detail in section Database Collection Protocol. Selecting the main features to be extracted is extremely important in that different gestures can be distinguished by traditional methods. However, it is difficult to improve the performance of recognition based on sEMG by conventional methods. Nevertheless, designing and selecting features can be complicated, and the combinations of features are diverse, leading to increased workload and dissatisfying results (Wu, Y., Zheng, B., and Zhao, Y., 2018).

Utilizing deep neural networks in the classification of sEMG signals has been proposed by researchers. Wu et al. (Wu, Y., Zheng, B., and Zhao, Y., 2018) proposed LCNN and CNN_LSTM models. The main advantage of these models is that it can be thought of as autoencoders for automatic feature extraction, which does not require traditional feature extraction. The features extraction process requires all efforts and time to optimize the parameters to get the maximum training and testing accuracy in the classical machine learning approaches.

In recent years, deep learning has achieved great success in the field of image recognition. A fantastic idea was presented in (Côté-Allard, U., Fall, C. L., Drouin, A., Campeau-Lecours, A., Gosselin, C., Glette, K., and Gosselin, B, 2019), (Cote-Allard, U., Fall, C. L., Campeau-Lecours, A., Gosselin, C., Laviolette, F., and Gosselin, B., 2017) ta channel's sEMG signals can form a graph after the short-time Fourier transform or wavelet transform of sEMG signals. This is a great concept to convert the sEMG signal into an image. This allowed for a generation of images to represent the signals.

Researchers such as Côté-Allard et al. (Côté-Allard, U., Fall, C. L., Drouin, A., Campeau-Lecours, A., Gosselin, C., Glette, K., and Gosselin, B, 2019), who regarded the original sEMG

signals as an image, constructed the ConvNet model to improve further the classification accuracy of sEMG signals utilizing the deep-learning. However, the LCNN and CNN_LSTM models proposed by Wu et al. (Wu, Y., Zheng, B., and Zhao, Y., 2018), and the ConvNet model used by Côté-Allard et al. (Côté-Allard, U., Fall, C. L., Drouin, A., Campeau-Lecours, A., Gosselin, C., Glette, K., and Gosselin, B., 2019), contain many parameters.

In deep learning algorithms, the final test accuracy is directly proportional to the size of the training data; one participant can't produce tens of thousands of sEMG signals to be enough to train the model with deep learning. Therefore, a large amount of data can be obtained by augmenting the recorded data of multiple participants so that the model can be well pre-trained to reduce the amount of data required to be obtained from hundreds of users. Meanwhile, designing a compact deep neural network structure to reduce the number of parameters can also reduce the need for big data size.

The work presented in this chapter aims to reduce the number of model parameters and increase the training and testing accuracy of model classification utilizing the deep convolutional neural network model for the biometrics authentication system. The target of applying a convolutional neural network (CNN) instead of classical machine learning (ML) is to avoid the features extraction phase needed in classical machine learning. CNN extracts the features from input data by itself. However, the time-frequency representation of input signals is useful when training the CNN model (Madhavan, S., Tripathy, R. K., and Pachori, R. B., 2019).

AlexNet deep neural network proposed by Krizhevsky et al. (Krizhevsky, A., Sutskever, I., and Hinton, G. E., 2012) who won the ImageNet challenge in 2012, deep learning proposed has achieved great success in speech recognition image classification, and other fields. Images can be accurately classified by training the neural network model to learn the characteristics of images. Nowadays, exploring network architecture has become part of deep learning.

Currently, sEMG signal classification deploying deep learning has been successfully used by some researchers and explored several effective network frameworks (Zia ur Rehman, M., Waris, A., Gilani, S. O., Jochumsen, M., Niazi, I. K., Jamil, M., and Kamavuako, E. N., 2018). Utilizing CNN to classify sEMG signals, researchers in (Atzori, M., Cognolato, M., and Müller, H., 2016) used the raw signals as input space. The spectrograms of raw sEMG signals were extracted by applying Short-Time Fourier Transform (STFT) and input into the convolutional network (Conv-Nets) (Allard, U. C., Nougrou, F., Fall, C. L., Giguère, P., Gosselin, C.,

Lavolette, F., and Gosselin, B., 2016). Conv-Nets are used to classify the sEMG signals' features extracted by a short-time Fourier transform-based spectrogram and Continuous Wavelet Transform (CWT). Since sEMG signals are acquired in the time-domain, Wu. et al. (Wu, Y., Zheng, B., and Zhao, Y., 2018) proposed a method to classify the sEMG signal by combining Long Short-Term Memory (LSTM) and CNN. The temporal information in the signal is retained, and CNN's ability to extract features is utilized.

However, the ConvNets model shown in Figure 6-1 (Côté-Allard, U., Fall, C. L., Drouin, A., Campeau-Lecours, A., Gosselin, C., Glette, K., and Gosselin, B, 2019) was complicated, and the LSTM model was introduced in (Wu, Y., Zheng, B., and Zhao, Y., 2018), which led to expensive computation in sEMG signal training and long-time training. Therefore, a simple network model with fewer parameters was needed to be used in the biometrics system.

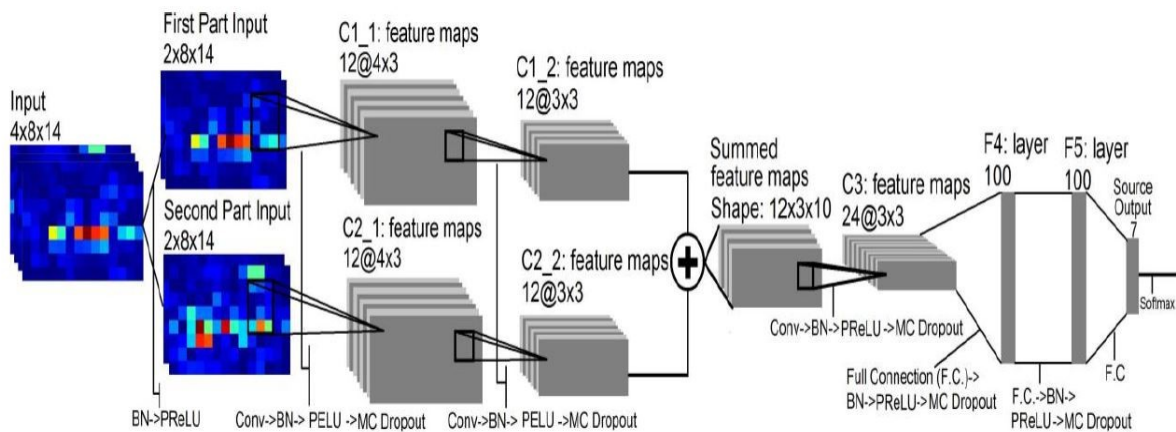


Figure 6-1 Schematic diagram of ConvNet architecture (Chen, L., Fu, J., Wu, Y., Li, H., & Zheng, B., 2020)

The sEMG signals are converted to images generated by a heat map continuous wavelet transform of signals, these images are called scalogram. The CNN model architecture used to train and test the sEMG signals dataset is called squeeze net (Iandola, F. N., Han, S., Moskewicz, M. W., Ashraf, K., Dally, W. J., and Keutzer, K., 2016). For a given accuracy level, multiple CNN structures are typically existing that achieve that accuracy level. For a given equivalent accuracy, a CNN architecture with fewer parameters has several advantages over the other structures.

- More efficient distributed training: the small models train faster because it requires less communication with other servers for data-parallel training (Iandola, F. N., Moskewicz, M. W., Ashraf, K., and Keutzer, K., 2016).

- Less overhead when exporting new models to clients: For the self-driving vehicle applications, the well-known companies copy new models from their servers to the car's life. This process is called over-air updates update (Consumer Reports. Teslas new autopilot: Better but still needs improvements, 2016). Over-air-update using typical CNN models can require large data transfers. The smaller the parameters, requires less and faster communications.

6.2 Deep Learning for Biometrics Users Verification System

The schematics drawing shown in Figure 6-2 represents the phases followed in this work starting with input generation of sEMG signals then the squeeze net structure to the output layer, which will grant/deny access to the users.

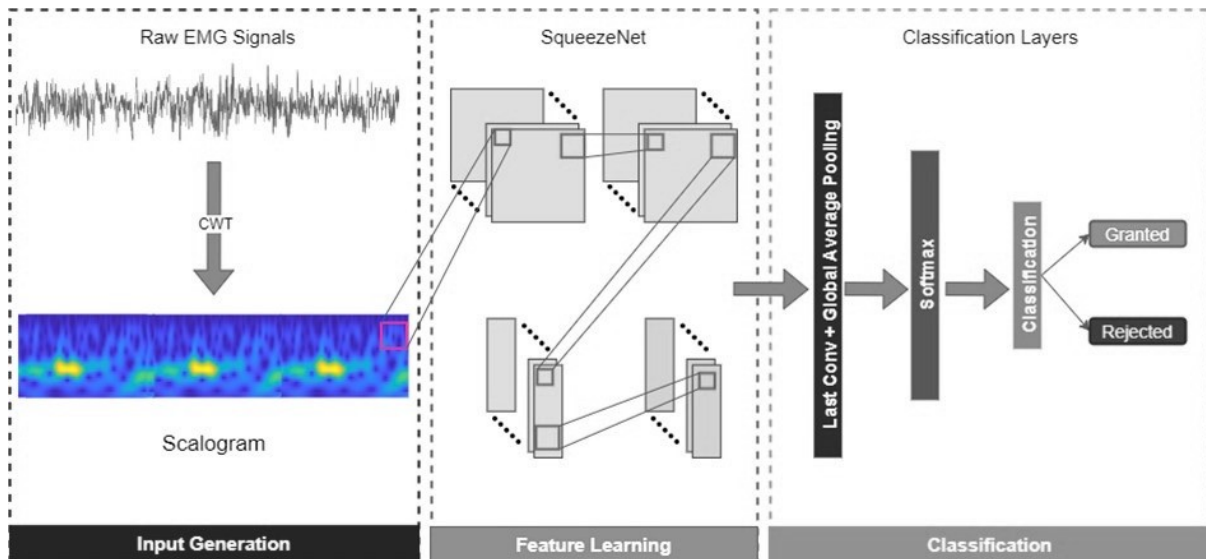


Figure 6-2 Schematic Chart of Users verification System using Deep Learning

6.2.1 Input Generation

sEMG signals database collected by using 8-channel Myo Armband from 56 able-bodied users is used in this work. Each user enrolled in the system customized a password consists of a combination of hand actions and performed the hand actions for 20 tests. These data need to undergo two steps before inputting them to the convolutional neural network. The first step is to convert the signals to scalograms using a heat map of the continuous wavelet transform. While the second step is to augment this data since deep learning needs a large amount of data to classify the signals with high accuracy.

6.2.2 Continuous Wavelet Transform (CWT)

To input data to CNN models, time-frequency representation is used. Scalograms of channel 1 of each EMG signal are used as inputs to CNN. Scalograms are generated using a heat map of continuous wavelet transform (CWT) of the signal.

The Continuous Wavelet Transform (CWT) is used to decompose a signal into wavelets. Wavelets are small oscillations that are highly localized in time. The Fourier Transform decomposes a signal into infinite length cosines and sines; this will cause a loss in all time-localization information. The CWT's basic functions are scaled and shifted versions of the time-localized mother wavelet. The CWT is used to construct a time-frequency representation of a signal that offers a good time and frequency localization. CWT can be calculated as follow:

$$c(s, \tau) = \int_R f(t) \Psi_{s,\tau}(t)^* dt \quad (6-1)$$

$$s \in R^+ - \{0\}, \tau \in R \quad (6-2)$$

$$\Psi_{s,\tau}(t) = \frac{1}{\sqrt{s}} \Psi\left(\frac{t-\tau}{s}\right) \quad (6-3)$$

Here, $\Psi_{s,\tau}(t)^*$ is the complex conjugate of mother wavelet, $c(s, \tau)$, is wavelet coefficients, $f(t)$ is the original signal, s is scale, and τ is translation.

CWT is calculated by the following steps:

1. Choose a mother wavelet and measure similarity.
2. Use equation given to calculate wavelet coefficients using initial scale and translation.
3. Repeat 2nd step by changing translation (shift) until the complete signal is covered.
4. Repeat 2nd and 3rd steps by changing scale until all scale values are used.

A discrete wavelet transform is used to calculate the wavelet transform Since the computer cannot process continuous signals. Scale and translation values, all of them should be discretized. After discretization, the equations above become:

$$c(j, k) = \sum_t f(t) \Psi_{j,k}(t)^* \quad (6-4)$$

$$\Psi_{j,k}(t) = 2^{j/2} \Psi(2^j t - k) \quad (6-5)$$

Here, j is the number of scale values, and k is the number of translation values. The same steps are followed to calculate the Discrete Wavelet Transform.

Parameters used for CWT are listed in Table 6-1. Some generated scalograms are depicted in Figure 6-3.

Table 6-1 Parameters of CWT

Wavelet Family	Analytic Morlet
Voices Per Octave	10
Time Bandwidth	60

Labels, titles, and other information are removed from scalograms because this info doesn't have positive effects on CNN's performance.

After inputs are generated, they are treated in the same way as the previous system. Images are arranged to form a training and test set for each user. In the training set, there are two classes: granted and rejected. Granted class is created by 70% of valid user's data, and the rejected class is formed by one image from the remaining user's images. The test set also is formed similarly. This time 30% of valid user's data is used for the training set. Since there are 56 users, the training set consists of 69 images (14 granted and 55 rejected), and the test set consists of 61 images (6 granted and 55 rejected) for each user.

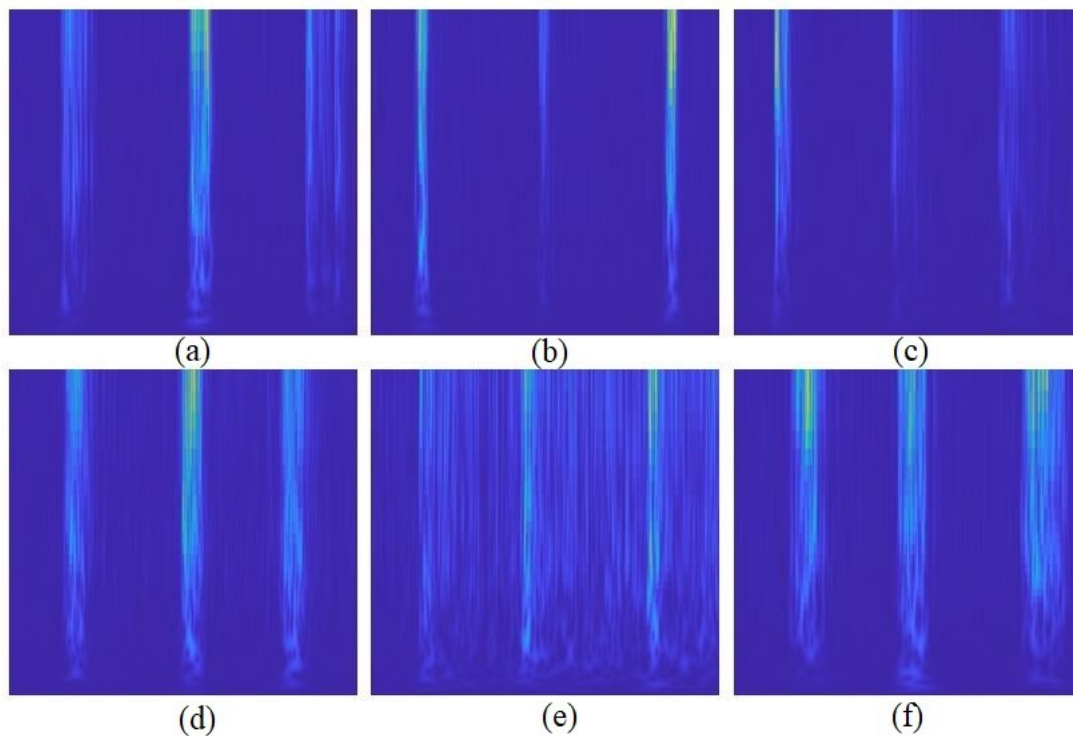


Figure 6-3 Generated Scalograms of 6 different sEMG signals for different users, (a)User 1,(b)User 2, (c)User 3, (d)User 4, (e)User 5, (f)User 6.

6.2.3 Data Augmentation

A limited amount of data is one of the main limitations in applying deep learning models like convolutional neural networks. Often, imbalanced classes can cause another problem; while there may be enough data for some classes, equally important but under-sampled classes will suffer from low class-specific accuracy. This phenomenon is intuitive. If the model learns from a few examples of a given class, it is less likely to predict the class in validation and test applications.

Many ways can address limited data problems in machine learning. Image augmentation is an essential approach in building up convolutional neural networks that can increase the training set's size without acquiring new data from multiple users or the same users. The idea is straightforward; duplicate images with variation so the model can learn from more examples. In this study, training images are randomly translated (shifted) and scaled during training.

6.2.4 Convolutional Neural Network Structure and Training

For around 28 years, the term Convolutions have been used in artificial neural networks. CNN has been used for a digital recognition application by LeCun et al. (LeCun, Y., Boser, B., Denker, J. S., Henderson, D., Howard, R. E., Hubbard, W., and Jackel, L. D., 1989), which popularized CNN's use at that time. The convolution filters mostly are 3D in neural networks with height, width, and channels as the key dimensions. Applying CNN filters to the images typically has three channels in their first layer, such as RGB, and the filters have the same number of channels in each subsequent layer. Simonyan et al. (Simonyan, K., and Zisserman, A., 2014) proposed VGG, which are architectures extensively use 3x3 filters. Models such as Network-in-Network (Lin, M., Chen, Q., and Yan, S., 2013) and the GoogLeNet (Szegedy, C., Ioffe, S., Vanhoucke, V., and Alemi, A., 2016) family of architectures use 1x1 filters in some layers. It is an adjective to manually select the dimensions of the filter for each layer to design deep CNNs. Various higher-level modules consist of multiple convolution layers with a specific fixed organization that have been presented to accomplish this. Szegedy et al. (Szegedy, C., Ioffe, S., Vanhoucke, V., and Alemi, A., 2016) proposed inception modules in GoogLeNet, which contains a set of different dimensionalities of filters, usually including 1x1 and 3x3, plus sometimes 5x5 and sometimes 1x3 and 3x1.

The convolutional neural network is a deep neural network class principally applied to images for classification, object detection, segmentation, and image processing (Mahajan, N. V., Deshpande, A. S., and Satpute, S. S., 2019). A CNN can consist of several types of layers: convolution, rectified linear unit (ReLU), pooling, dropout, fully connected (FC).

- Convolution Layer: This layer is the building block of CNN. In this layer, image or feature maps from the previous layer are convolved with sliding kernels to extract new features.
- ReLu Layer: This layer removes negative values from feature maps by applying activation function $f(x) = \max(0, x)$ to introduce nonlinearity in feature maps.
- Pooling Layers: This layer reduces the dimensionality of feature maps by sliding windows, calculating the mean, max, or sum of values inside the window to make the network invariant to small transformations.
- Dropout Layer: This layer sets input elements to zero with a given probability to reduce overfitting.
- Fully Connected Layer: This layer is a traditional multi-layer perceptron which uses softmax activation function in the output layer. It classifies inputs images using features extracted by previous layers.
- **Squeeze-net structure**

The CNN architecture used in this work has a few parameters (Squeeze-net). It consists of a Fire module, a new building block out of which to build CNN architectures. The squeeze-net was constructed mainly from fire modules. The main objective of implementing squeeze-net to maintain accuracy with CNN structure with fewer parameters. To accomplish this target, three strategies applied in the structure of the squeeze-net:

- Use 1x1 filters instead of 3x3 filters: For an adequate number of convolution filters, most of the filters should be 1x1 since a 1x1 filter has nine times fewer parameters compared to a 3x3 filter.
- The number of input-channels to be reduced to 3x3 filters: A convolution layer composed of 3x3 filters. The total number of parameters in this convolutional layer is equal to (number of input channels) * (number of filters) * (3*3). To keep a low number

of parameters in a CNN, the number of 3x3 filters must be decreased and reduce the number of input channels to the 3x3 filters.

- To increase the size of activation maps in the convolution layers by down sample late in the network: In the network, each convolution layer produces an output activation map with a spatial resolution that is at least 1x1 and often much larger than 1x1. The activation maps height and width are controlled by the input data size and the choice of layers to down-sample in the CNN architecture

The Fire module is composed of a squeeze convolution layer (which has only 1x1 filters), inputting into an expand layer that has a combination of 1x1 and 3x3 convolution filters as illustrated in Figure 6-4. The freedom of use of 1x1 filters in Fire modules is to reduce the number of parameters inputting the network. In a Fire module, s_{1x1} is the filter number in the squeeze layer (all 1x1), e_{1x1} is the number of 1x1 filters in the expand layer, and e_{3x3} is the number of 3x3 filters in the expand layer. The rule here is if the fire modules set to be s_{1x1} , it should be less than $(e_{1x1} + e_{3x3})$, the squeeze layer assists in eliminating the number of input channels to the 3x3 filters.

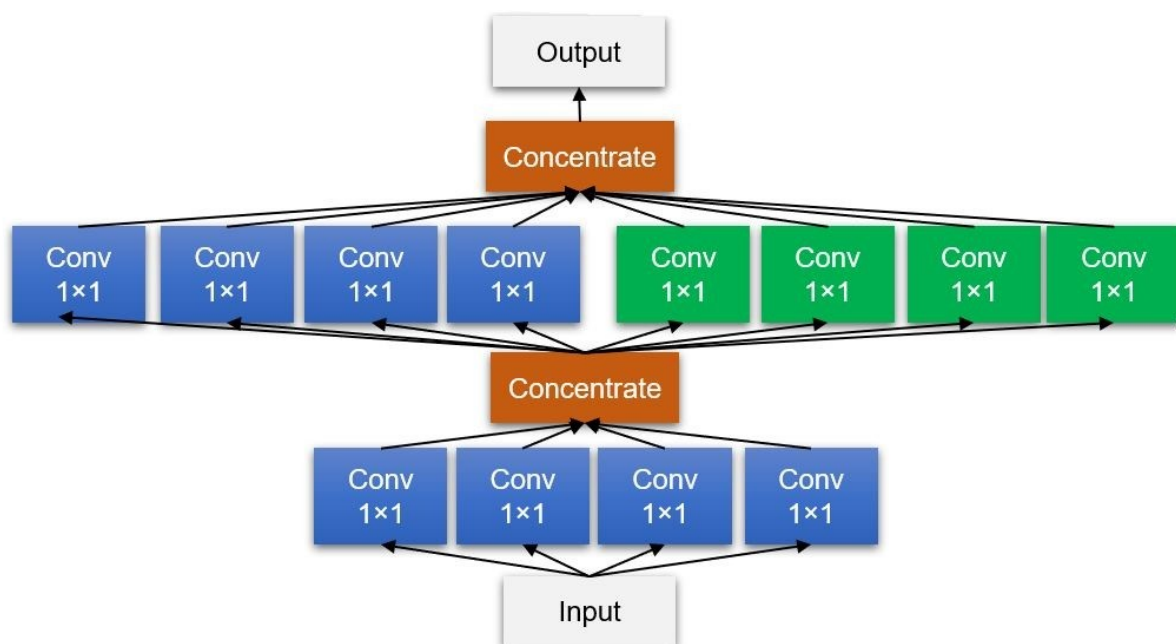


Figure 6-4 Organization of Fire Modules in the Convolutional Layer

The Squeeze-Net starts with a separate convolution layer (conv1), then 8 Fire modules, and finishes with a final conv layer (conv10). The number of filters increases per fire module from

the start until the deep neural network. Max pooling is performed in the Squeeze-Net structure with a stride of 2 after layers conv1, fire4, fire8, and conv10.

Squeeze-Net is a pre-trained CNN model structure. Original Squeeze-Net was trained on millions of images to classify them into 1000 categories. Therefore, the Squeeze-Net should be fine-tuned to be used for a new image classification problem. Convolutional layers of the network extract the features from the image that the last learnable layer and the final classification layer use to classify this input image. These two layers inside Squeeze-Net contain information about combining the network extracts' features into class probabilities, a loss value, and predicted labels. To retrain a pre-trained network to classify new images, these two layers should be replaced with new layers adapted to the new data set. After the original Squeeze-Net is fine-tuned, it is retrained on training data set for each user using parameters listed in Table 6-2. When CNN models are being trained, early stopping is applied to avoid over-fitting of the models. Therefore, each CNN model is trained with a different number of iterations.

Table 6-2 Parameters for training fine-tuned Squeeze-Net

Optimizer	Adam
Mini Batch Size	20
Learning Rate	10^{-4}
L ₂ Regularization	10^{-4}

6.2.5 Testing and Results

After CNN models are trained, the last step is to evaluate their performances. Performance evaluation is performed using a retrained CNN model and a test set of each user. Accuracy, false acceptance rate, and false rejection rate are calculated based on the prediction made by each CNN model. The results are given in Table 6-3.

Table 6-3 CNN Performance results for Users Verification

User Name	Accuracy	FAR	FRR
User 1	0.983607	0.018182	0
User 2	0.967213	0.018182	0.166667
User 3	0.967213	0	0.333333

User 4	1	0	0
User 5	0.983607	0.018182	0
User 6	0.983607	0	0.166667
User 7	0.983607	0.018182	0
User 8	1	0	0
User 9	1	0	0
User 10	1	0	0
User 11	1	0	0
User 12	1	0	0
User 13	1	0	0
User 14	1	0	0
User 15	1	0	0
User 16	1	0	0
User 17	0.95082	0	0.5
User 18	1	0	0
User 19	0.983607	0.018182	0
User 20	0.983607	0	0.166667
User 21	0.95082	0.054545	0
User 22	0.983607	0	0.166667
User 23	0.967213	0.036364	0
User 24	0.983607	0.018182	0
User 25	0.95082	0.054545	0
User 26	1	0	0
User 27	1	0	0
User 28	1	0	0
User 29	1	0	0

User 30	1	0	0
User 31	0.95082	0.018182	0.333333
User 32	0.95082	0.054545	0
User 33	0.95082	0.036364	0.166667
User 34	1	0	0
User 35	0.983607	0.018182	0
User 36	0.983607	0	0.166667
User 37	0.983607	0	0.166667
User 38	0.967213	0.036364	0
User 39	0.967213	0.036364	0
User 40	1	0	0
User 41	1	0	0
User 42	0.983607	0.018182	0
User 43	0.918033	0	0.833333
User 44	0.983607	0.018182	0
User 45	0.983607	0.018182	0
User 46	1	0	0
User 47	1	0	0
User 48	1	0	0
User 49	0.95082	0.036364	0.166667
User 50	1	0	0
User 51	0.934426	0.018182	0.5
User 52	1	0	0
User 53	1	0	0
User 54	1	0	0
User 55	0.983607	0.018182	0

User 56	0.983607	0	0.166667
Mean	0.983607	0.01039	0.071429

The obtained average accuracy of the CNN structure was found to be 98.3%. Next, a statistical study was used to evaluate the performance of the system. The FAR value is 1.03%, and the FRR value is 7.14 %. These results showed that using deep neural networks can be used in the sEMG biometrics verification system without extracting the signals' features.

6.3 Deep Learning for Biometrics Users Identification System

The main problem in user identification that doesn't exist in users' verification systems is that user verification is a binary-class classification problem while user identification is a multi-class classification problem. Therefore, although there is one classifier for each user in user verification, only one classifier predicts the identification system's users. The system flowchart is depicted in Figure 6-5. It consists of three phases. In the first phase, both raw and denoised sEMG signals are used for the generation of scalograms. This is applied to training data to increase the number of samples for training the CNN model and it can be considered as an offline data augmentation to overcome the problem of data limitation as it is required to train a network to identify the users by sEMG signals without extracting the features in advance. After input generation, inputs are used for training and testing the CNN model, which is squeeze-net. Data augmentation is applied to the generated scalograms to increase the classifier's data input for better results.

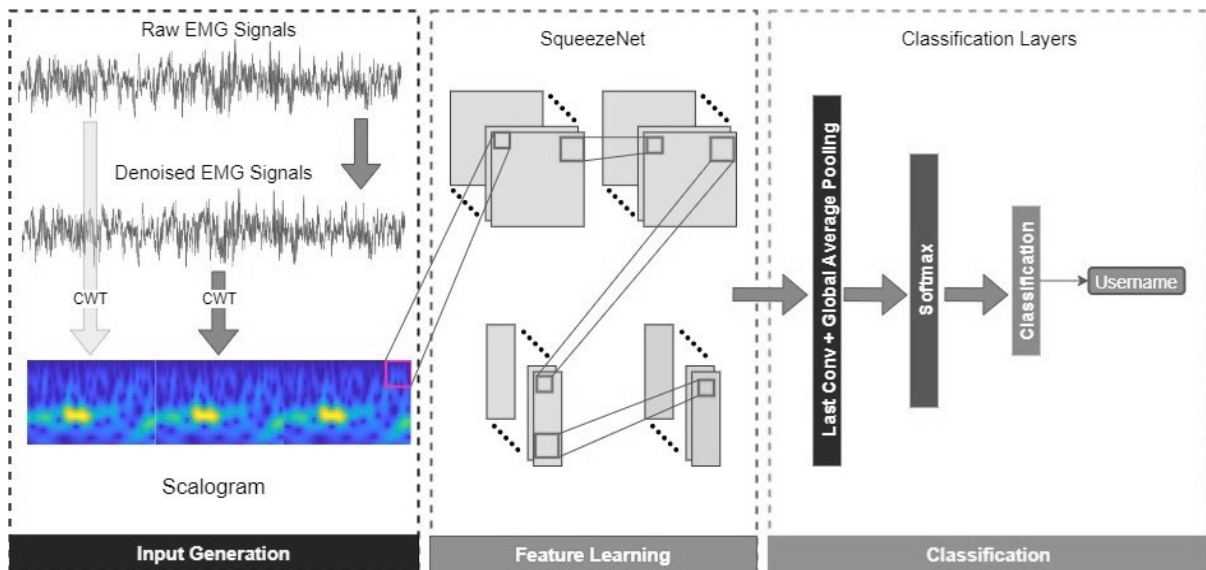


Figure 6-5 Schematic Chart of Users Identification System using Deep Learning

6.3.1 Input Generation

Scalograms of channel 1 of each raw and denoised EMG signal are used as inputs to the CNN. Denoising is used to create slightly different signals and scalograms. Wavelet transform-based denoising (Kania, M., Fereniec, M., and Maniewski, R., 2007) with varying composition levels is applied to each signal. As a result, several slightly altered signals are created from one signal. The parameter used for wavelet transform based denoising is given in Table 6-4.

Table 6-4 Parameters selected for Wavelet Denoising

Mother Wavelet	Sym4
Denoising Method	Bayes
Threshold Rule	Median
Noise Estimation	Level independent
Decomposition Level	1, 2, 3, 4, 5

After several denoised versions of raw EMG signals are created, the denoised sEMG signals and raw signals are represented as images (scalograms) using CWT. Some denoised signals and their scalograms are given in Figure 6-6, and Figure 6-7. Since this procedure is employed to increase the number of training samples, the procedure is only applied to training data, namely 70% of the signals. The remaining 30% of signals, test datasets, are used as raw signals, and scalograms are created from raw signals.

6.3.2 Wavelet-Based Denoising

The noisy signal can be modeled as a superposition of signal and noise as follow:

$$X(k) = S(k) + E(k) \quad (6-6)$$

where, $X(k)$ is a noisy signal, $S(k)$ is the original signal, and $E(k)$ is white Gaussian noise. Since Wavelet transform is a linear transform, wavelet coefficient of $X(k)$ still has two components. One component is from the original signal, and the other is from noise. Wavelet transform can intensify signal energy on large coefficients and distribute noise energy. Therefore, it can be assumed that those large coefficients represent the original signal, and small coefficients represent noise. Based on this, wavelet-based denoising can be applied as follow:

- Choose the mother wavelet and decomposition level and corresponding computing coefficients.
- Choosing a threshold and threshold function, then calculating the estimated value of coefficients.
- Reconstructing the signal using an inverse discrete wavelet transform based on estimated coefficients.

Although there are many methods for determining the threshold, the universal threshold is the most used thanks to its simplicity. The universal threshold is calculated as follow:

$$\lambda = \sigma \sqrt{2 \ln(N)} \quad (6-7)$$

where σ is the average variance of the noise, and N is the length of the signal. σ can be calculated using the median estimate method. The formula is as follow:

$$\sigma = \frac{\text{Median}(|W_{1,K}|)}{0.6745} \quad (6-8)$$

where $W_{1,K}$ is all 1st level wavelet coefficients. There are two well-known thresholding functions: hard and soft thresholding. Both functions remove small coefficients and lessen large coefficients (Khmag, A., Al-Haddad, S. A. R., and Hashim, S. J. B., 2014).

The equation of hard thresholding is mentioned in equation (6-9), and the soft thresholding is mentioned in equation (6-10).

$$\delta_{\lambda}(W) = \begin{cases} w & |w| \geq \lambda \\ 0 & |w| < \lambda \end{cases} \quad (6-9)$$

$$\delta_{\lambda}(W) = \begin{cases} \text{sign}(w) & |w| \geq \lambda \\ 0 & |w| < \lambda \end{cases} \quad (6-10)$$

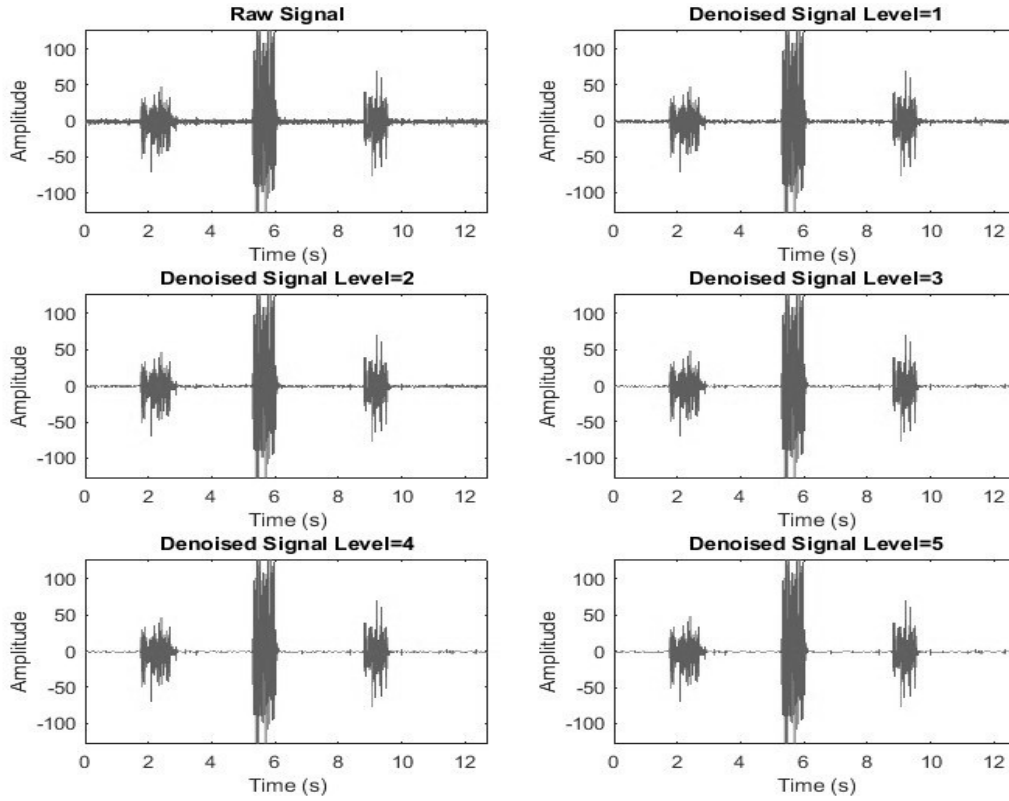


Figure 6-6 Denoised Signal using Different Threshold Values

6.3.3 Data Augmentation

To increase the number of training data further, image augmentation is applied to the scalograms during training, meaning training images are randomly translated (shifted) and scaled during training.

6.3.4 CNN Architecture and Training

Again, pre-trained SqueezeNet is used for the classification of EEG signals. The only difference is the number of classes. Since there are 56 users, SqueezeNet is fine-tuned for the classification of 56 classes. After the original SqueezeNet is fine-tuned, it is retrained on training data set users using parameters listed in Table 6-5. For comparison, AlexNet (Krizhevsky, A., Sutskever, I., and Hinton, G. E., 2012) is trained using the same parameters as well.

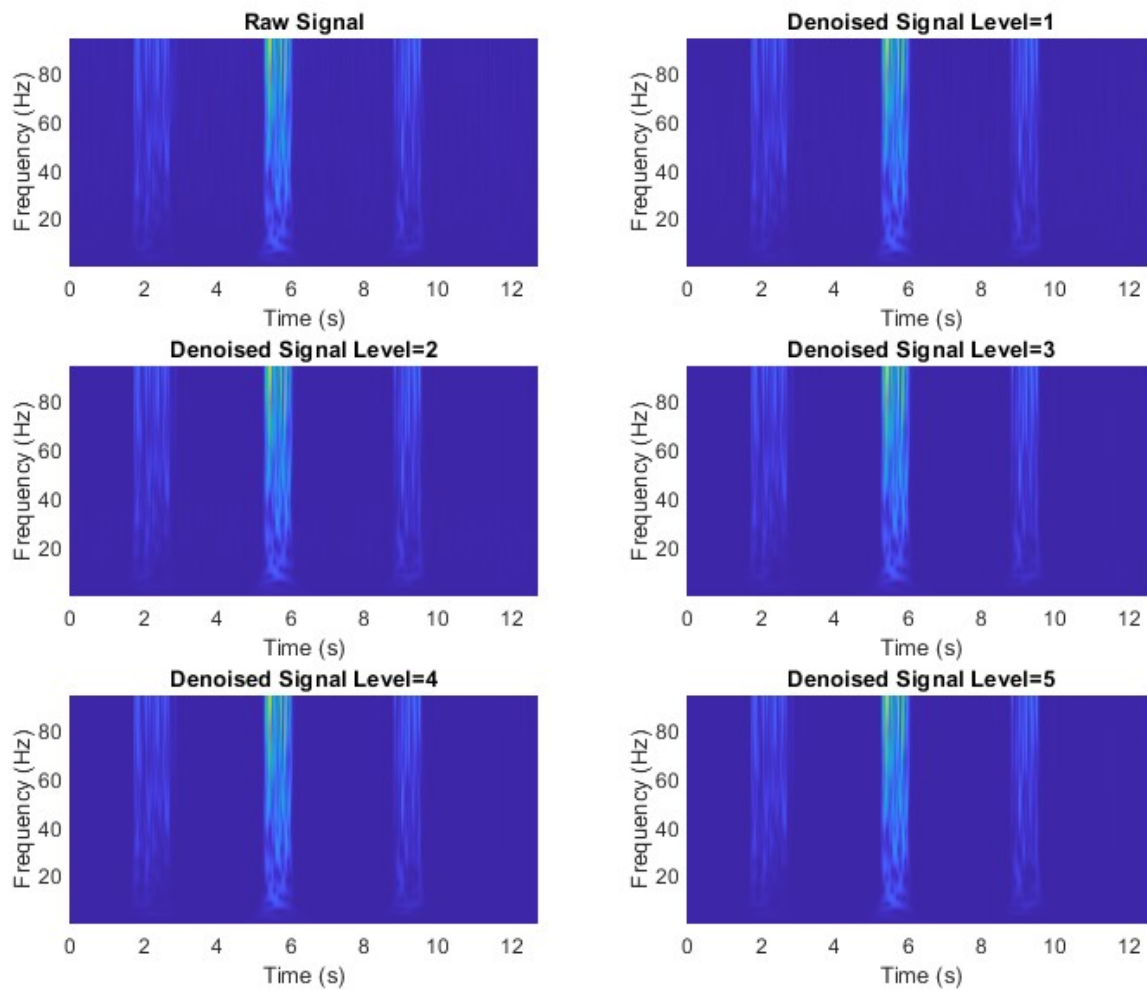


Figure 6-7 Scalograms of Denoised Signal using Different Threshold Values

6.3.5 Testing and Results

After the CNN model is trained, the last step is to evaluate its performances. Performance evaluation is done using a pre-trained CNN model and test set. While the accuracy is calculated based on the prediction made by each CNN model. Results are given in Table 6-6 and **Error!**

Reference source not found..

Table 6-5 Parameters for Training Fine-Tuned SqueezeNet

Optimizer	Adam
Mini Batch Size	32
Learning Rate	10^{-4}
L2 Regularization	10^{-3}

Table 6-6 Performance Result for User Identification System

Model	Accuracy	Correctly Classified Signals	Incorrectly Classified Signals
SqueezeNet	81.84%	275	60

Number of Epoch	37
-----------------	----

AlexNet	78.87%	265	70
---------	--------	-----	----

6.4 Conclusion

In recent years, deep learning has achieved great success in the field of image recognition. A deep neural network is used in the classification of bio-signal data. The sEMG signals of a channel can form a graph, by applying a wavelet transform of sEMG signals. This is a great concept to convert the sEMG signal into an image. This allowed for a generation of images to represent the signals. These images are called scalograms of sEMG signals. In deep learning algorithms, the final test accuracy is directly proportional to the size of the training data; one participant can't produce tens of thousands of sEMG signals to be enough to train the model with deep learning. Therefore, a large amount of data can be obtained by augmenting the recorded data of multiple participants so that the model can be well pre-trained to reduce the amount of data required to be obtained from hundreds of users. Meanwhile, designing a compact deep neural network structure to reduce the number of parameters can also reduce the need for big data size. The squeeze-net structure is used in the training of augmented scaograms generated by sEMG signals. The obtained average accuracy of the CNN structure was found to be 98.3%. The FAR value is 1.03%, and FRR value is 7.14 %. These results showed that using deep neural networks can be used in the sEMG biometrics verification system without extracting the signals' features. In the biometrics user's identification system, both scalograms of the raw data and denoised sEMG signal are used as inputs to CNN. Denoising is used to create slightly different signals and scalograms. Wavelet transform-based denoising with different decomposition is applied to each signal. As a result, several slightly altered signals are created from one signal. Two CNN structures have been applied to the data to compare between them. The CNN structures are squeezeNet and Alex-Net, which exhibits a testing accuracy of 81.84% and 78.87%, respectively.

7 Chapter 7 Conclusion & Perspectives

The thesis presented the advances in wearable technology systems raised during the last decades. The wearable system that is available in the market is briefing its advantages and disadvantages. The work presented in this thesis is based on Multi-channel sEMG signals acquired by using Myo armband, which is a wearable bracelet contain eight dry sEMG electrodes.

The thesis proposed a detailed design of a customized 3-D printed bionic arm with an artificial hand. The bionic arm is implemented and tested on an amputee case with right arm amputation from his born. According to the state-of-the-art systems, a gesture recognition based on sEMG signals has been implemented. A database of sEMG created for generic control of a bionic arm consists of four hand gestures (fist, spread fingers, wave-in, wave-out) from a wide range of participants to control four hand movements. The 3-D printing technology offered an affordable price solution for 295\$. The collected data were processed, and feature extraction was performed to training a classifier. Real-time testing of a bionic arm with a gesture recognition system is presented. Machine learning classifiers are tested, and results are compared to find the optimum algorithm to be used with sEMG data. The support vector machine classifier was found to out-perform the neural network and decision tree classifiers, reaching an average of 90.5%% accuracy. Real-time testing of the bionic arm with the associated classifier software enabled the user to perform his daily activities

The research on biometrics systems, especially in the anti-spoofing system, showed great use of sEMG as a biometrics modality due to its hidden biometrics natures and liveness detection. The research work proposed a biometrics authentication system for user's verification. The biometric identity studied in this research is based on the EMG signal. The biometric device used to acquire the sEMG signal is a wearable multi-channel armband consisting of 8 electrodes. A total of 56 users were enrolled in the biometric system to create a database of sEMG signals. The users enrolled trained to use the sEMG biometric system prior to data collection. Each user has been asked to select three gestures out of 4 gestures and arrange them in a way to form a password using hand actions. A database of fifty-six participants has been collected (twenty-four males and thirty-two females with ages ranging from 16 to 62 years). A total of 18 features were extracted from the signals to distinguish between users. Seven frequency domain features and eleven-time domain features were analyzed. Initially, each

channel's power spectral density (PSD) was estimated using the periodogram function, implementing Welch's method. Subsequently, average frequency, kurtosis, the signal's power, median frequency, coefficient of dissymmetry, deciles, and peak frequency of PSD were calculated as frequency-domain features.

Furthermore, data's length or duration is calculated as a new feature by dividing the signal into ten equal length segments and calculating each segment's root mean square (RMS). The K-nearest neighbors (kNN), linear discriminant analysis classifier (LDA), and classifier ensemble have been applied to optimize the system's results.

The system will grant/deny access to the user from the captured sEMG biometrics identity as a signature-based on hand gestures. Performance analysis of the biometrics system has been presented to validate the system's capacity by estimating both the false acceptance rate (FAR) and the false rejection rate (FRR). The performance of sEMG signals as a biometric modality for user verification is investigated. The users were able to perform a custom-set gesture code. The resulting sEMG signals were captured and proceed as a form of hidden biometric identity. The results indicated that the custom-set gesture code improves verification performance. The set of frequency and time-domain features extracted in this study allowed for improved classifier accuracy. The KNN classifier was found to be optimum, with an average accuracy of 97.4%. The FAR and FRR of the KNN classifier results are 0% and 2.9%, respectively.

The performance of sEMG as a biometric trait for user identification was investigated as well in the research. The users were able to perform a custom-set gesture code. The resulting sEMG signals were captured and proceed as a form of hidden biometric identity. The results indicated that the custom-set gesture code could significantly improve identification performance. The set of time-domain features extracted in this study allowed for improved classifier accuracy. The KNN classifier was found to be optimum, with an average detection accuracy of 86.2%.

The average classifier accuracy can be optimized by expanding the database by collecting 50 samples from each user enrolled in the system instead of 20 samples to have more data to train the classifiers for an improved identification system. The user's identification system's average accuracy reached 99% during testing the classifier when only 30 users out of 56 users are selected for training the classifier.

In recent years, deep learning has achieved great success in the field of image recognition. A deep neural network is used in the classification of bio-signal data. The sEMG signals of a

channel can form a graph by applying a wavelet transform of sEMG signals. This is a great concept to convert the sEMG signal into an image. This allowed for a generation of images to represent the signals. These images are called scalograms of sEMG signals. In deep learning algorithms, the final test accuracy is directly proportional to the size of the training data. One participant can't produce tens of thousands of sEMG signals to be enough to train the model with deep learning. Therefore, a large amount of data can be obtained by augmenting the recorded data of multiple participants so that the model can be well pre-trained to reduce the amount of data required to be obtained from hundreds of users.

Meanwhile, designing a compact deep neural network structure to reduce the number of parameters can also reduce the need for big data size. The squeeze-net structure is used in the training of augmented scalograms generated by sEMG signals. The obtained average accuracy of the CNN structure was found to be 98.3%. The FAR value is 1.03%, and the FRR value is 7.14 %. These results showed that using the deep neural network can be used in the sEMG biometrics verification system without extracting the signals' features. In the Biometrics Identification system, both raw and denoised sEMG signals are used to generate scalograms using CWT. Two CNN structures have been applied, squeeze-net structure and Alex-net structure, which exhibit a testing accuracy of 81.84% and 78.87%, respectively.

Perspectives

In this thesis, we have encountered many challenges, and plenty of questions have been raised that lead us to further improvement and future works. These future perspectives are presented below:

- **Increasing the degree of freedom of bionic arm:** The bionic arm design shown in the thesis is directly attached to an artificial hand. The artificial hand has a 9 DOF that makes it able to perform the required grasping features. Adding a wrist joint mechanism will enhance the arm's functionality and make it able to do roll and yaw actions that will help perform more of the daily life activities.
- **Adding feedback sensors to the bionic hand:** Adding feedback sensors to the bionic hand to make it able to feel the environment. These embedded sensors to be attached to the fingertips and palm, such as pressure, heat to provide further feedback of the user surrounding objects.
- **Autonomous adjustable socket:** The adjustable socket presented in the thesis is adjusted by the user manually to fit his/her arm. A pressure pump with valve control can be used to adjust the fit of the socket autonomously. This section of the bionic arm is critical, as this is the contact point between the arm and the user's skin.
- **Expand the database of sEMG signals for a password:** The database collected from 56 users to propose a biometric system based on sEMG signals. Each user in the database performed the password for 20 times. Increasing the number of enrolled users to 100 users and each user to perform the password 50 times will increase the biometrics system identification accuracy.
- **Add more sensors with EMG sensors:** The database created was based on sEMG signals acquired by Myo armband without recording signals related to the arm's position. The Myo armband is equipped with IMU and gyroscope. Their signals can be acquired and recorded to get feedback about the arm's position during the acquisition time. Adding more inputs to the training algorithm will improve the classifiers' results, especially in the user's identification system.
- **Data augmentation of the signals:** In the deep learning algorithm presented in this thesis, data augmentation is done on the scalograms as an image by shifting and scaling

the pictures to augment them. Augmenting the sEMG signals by using gaussian noise has not been tested on this database.

8 Bibliography

- (2016, January 01). (Johns Hopkins University) Retrieved from "https://www.cantechletter.com/2016/01/thalamic-labs-myoe-armband-allows-amputee-to-control-prosthetic-limb/,"
- Aashni, H., Archanasri, S., Nivedhitha, A., Shristi, P., and Jyothi, S. N. (2017). S. N. . *International conference on advances in computing & communications*. 115, pp. 367-374. Science Direct.
- Abdenour Hadid, Nicholas Evans, Sébastien Marcel, and Julian Fierrez. (2015). Biometrics Systems Under Spoofing Attack. *IEEE SIGNAL PROCESSING MAGAZINE* , 32(5), 20-30.
- Aditya T, Bertram T, Frederic G, and Didier S. (2017). A probabilistic combination of CNN and RNN estimates for hand gesture based interaction in car. *International symposium on mixed and augmented reality ISMAR-adjunct*, 1-6.
- Ahsan, M. R., Ibrahimy, M. I., and Khalifa, O. O. (2011). Electromyography (EMG) signal based hand gesture recognition using artificial neural network (ANN). *4th International Conference on Mechatronics (ICOM)* (pp. 1-6). Kuala Lumpur, Malaysia: IEEE.
- Akhmadeev, K., Houssein, A., Moussaoui, S., Høgestøl, E. A., Tuttoren, I., Harbo, H. F., and Gourraud, P. A. (2018). Svm-based tool to detect patients with multiple sclerosis using a commercial emg sensor. *2018 IEEE 10th Sensor Array and Multichannel Signal Processing Workshop (SAM)* (pp. 376-379). Sheffield, UK: IEEE.
- Allard, U. C., Nougrou, F., Fall, C. L., Giguère, P., Gosselin, C., Laviolette, F., and Gosselin, B. (2016). A convolutional neural network for robotic arm guidance using sEMG based frequency-features. *IEEE/RSJ International Conference on Intelligent Robots and Systems (IROS)*.
- Al-Mulla, M. R., and Sepulveda, F. (2014). Novel Pseudo-Wavelet function for MMG signal extraction during dynamic fatiguing contractions. *Sensors*, 14(6), 9489-9504.

- Arief, Z., Sulistijono, I. A., and Ardiansyah, R. A. (2015). Comparison of five time series EMG features extractions using Myo Armband. *International Electronics Symposium (IES)*, 11-14.
- Atzori, M., Cognolato, M., and Müller, H. (2016). Deep learning with convolutional neural networks applied to electromyography data: A resource for the classification of movements for prosthetic hands. *Frontiers in neurorobotics*, 10, 9.
- Bailey, K. O., Okolica, J. S., and Peterson, G. L. (2014). User identification and authentication using multi-modal behavioral biometrics. *Computers & Security*, 43, 77-89.
- Baillie, D. C., & Mathew, J. (1996). A comparison of autoregressive modeling techniques for fault diagnosis of rolling element bearings. *Mechanical Systems and Signal Processing*, 10(1), 1-17.
- Barbé, K., Pintelon, R., and Schoukens, J. (2009). Welch method revisited: nonparametric power spectrum estimation via circular overlap. *IEEE Transactions on signal processing*, 58(2), 553-565.
- Barioul, R., Ghribi, S. F., and Kanoun, O. (2016). A low cost signal acquisition board design for myopathy's EMG database construction. *13th International Multi-Conference on Systems, Signals & Devices (SSD)*. 274-279: IEEE.
- Belgacem, N., Fournier, R., Nait-Ali, A., and Bereksi-Reguig, F. (2015). A novel biometric authentication approach using ECG and EMG signals. *Journal of medical engineering & technology*, 39(4), 226-238.
- Benalcázar, M. E., Jaramillo, A. G., Zea, A., Páez, A., and Andaluz, V. H. (2017). Hand gesture recognition using machine learning and the Myo armband. *25th European Signal Processing Conference (EUSIPCO)* (pp. 1040-1044). Kos, Greece: IEEE.
- Benalcázar, M. E., Motoche, C., Zea, J. A., Jaramillo, A. G., Anchundia, C. E., Zambrano, P., and Pérez, M. (2017). Real-time hand gesture recognition using the Myo armband and muscle activity detection. *IEEE Second Ecuador Technical Chapters Meeting (ETCM)* (pp. 1-6). Salinas, Ecuador: IEEE.

- Ben-Arie, J., Wang, Z.; Pandit, P., and Rajaram, S. (2002). Human Activity Recognition Using Multidimensional Indexing. *IEEE Trans. Pattern Anal. Mach. Intell.*, 24, 1091–1104.
- Benatti, S., Milosevic, B., Farella, E., Gruppioni, E., and Benini, L. (2017). A prosthetic hand body area controller based on efficient pattern recognition control strategies. *Sensors*, 17(4).
- Blasco, J., Chen, T. M., Tapiador, J., and Peris-Lopez, P. (2016). A survey of wearable biometric recognition systems. *ACM Computing Surveys*, 49(3), 1-35.
- Bulugu, I., Ye, Z., and Banzi, J. (2017). Higher-order local autocorrelation feature extraction methodology for hand gestures recognition. *2nd International Conference on Multimedia and Image Processing (ICMIP)* (pp. 83-87). Wuhan, China: IEEE.
- C. Li, X. Zhang and L. Jin. (2017). LPSNet: A Novel Log Path Signature Feature Based Hand Gesture Recognition Framework. *IEEE International Conference on Computer Vision Workshops (ICCVW)* (pp. 631-639). Venice: IEEE.
- C. Tsai, Y. Tsai, S. Hsu, and Y. Wu., (2017). Synthetic Training of Deep CNN for 3D Hand Gesture Identification. *International Conference on Control, Artificial Intelligence, Robotics & Optimization (ICCAIRO)* (pp. 165-170). Prague: IEEE.
- Canavan, S., Keyes, W., McCormick, R., Kunnumpurath, J., Hoelzel, T., and Yin, L. (2017). Hand gesture recognition using a skeleton-based feature representation with a random regression forest. *IEEE International Conference on Image Processing (ICIP)* (pp. 2364-2368). Beijing, China: IEEE.
- Cannan, J., and Hu, H. (2013). Automatic user identification by using forearm biometrics. *IEEE/ASME International Conference on Advanced Intelligent Mechatronics* (pp. 710-715). Wollongong, NSW, Australia: IEEE.
- Chantaf, S., Makni, L., and Nait-ali, A. (2020). Single Channel Surface EMG Based Biometrics. In *Hidden Biometrics* (pp. 71-90). Singapore: Springer.
- Chen, L., Fu, J., Wu, Y., Li, H., & Zheng, B. (2020). Hand gesture recognition using compact CNN via surface electromyography signals. *Sensors*, 20(3), 672.

- Chen, X., Guo, H., Wang, G., and Zhang, L. (2017). Motion feature augmented recurrent neural network for skeleton-based dynamic hand gesture recognition. *IEEE International Conference on Image Processing (ICIP)* (pp. 2881-2885). Beijing, China: IEEE.
- Chu, J. U., Moon, I., and Mun, M. S. (2006). A real-time EMG pattern recognition system based on linear-nonlinear feature projection for a multifunction myoelectric hand. *IEEE Transactions on biomedical engineering*, *53*(11), 2232-2239.
- (2016). *Consumer Reports. Teslas new autopilot: Better but still needs improvements.* <http://www.consumerreports.org/tesla/tesla-new-autopilot-better-but-needs-improvement>.
- Cote-Allard, U., Fall, C. L., Campeau-Lecours, A., Gosselin, C., Laviolette, F., and Gosselin, B. (2017). Transfer learning for sEMG hand gestures recognition using convolutional neural networks. *IEEE International Conference on Systems, Man, and Cybernetics (SMC)* (pp. 1663-1668). Banff, AB, Canada: IEEE.
- Côté-Allard, U., Fall, C. L., Drouin, A., Campeau-Lecours, A., Gosselin, C., Glette, K., and Gosselin, B. (2019). Deep learning for electromyographic hand gesture signal classification using transfer learning. *IEEE Transactions on Neural Systems and Rehabilitation Engineering*, *27*(4), 760-771.
- Dai, Y., Zhou, Z., Chen, X., & Yang, Y. (2017). A novel method for simultaneous gesture segmentation and recognition based on HMM. *International Symposium on Intelligent Signal Processing and Communication Systems (ISPACS)* (pp. 684-688). Xiamen, China: IEEE.
- Dantcheva, A., Velardo, C., D'angelo, A., and Dugelay, J. L. (2011). Bag of soft biometrics for person identification. *Multimedia Tools and Applications*, *51*(2), 739-777.
- Dobrovski Z, Verlinden JC, and Geraedts JMP. (2011). Optimal design for additive manufacturing: opportunities and challenges. *ASME 2011 International Design Engineering Technical Conferences and Computers and Information in Engineering Conference. American Society of Mechanical Engineers.* Washington, DC, USA: ASME.

- Englehart, K., and Hudgins, B. (2003). A robust, real-time control scheme for multifunction myoelectric control. *IEEE transactions on biomedical engineering*, 50(7), 848-854.
- Englehart, K., Hudgins, B., Parker, P. A., and Stevenson, M. (1999). Classification of the myoelectric signal using time-frequency based representations. *Medical engineering & physics*, 21(6-7), 431-438.
- Evans, N. (2019). *Handbook of Biometric Anti-spoofing: Presentation Attack Detection*. Springer.
- Faragó, P., Groza, R., Ivanciu, L., and Hintea, S. (2019). A Correlation-based Biometric Identification Technique for ECG, PPG and EMG. *42nd International Conference on Telecommunications and Signal Processing (TSP)* (pp. 716-719). Budapest, Hungary: IEEE.
- Fong, S. . (2012). Using hierarchical time series clustering algorithm and wavelet classifier for biometric voice classification. *Journal of Biomedicine and Biotechnology*, 1-12.
- Freund, Y., and Schapire, R. E. (1995). *A decision-theoretic generalization of on-line learning and an application to boosting*. Berlin, Heidelberg.: Springer.
- Freund, Y., Schapire, R., and Abe, N. (1999). A short introduction to boosting. *Journal-Japanese Society For Artificial Intelligence*, 14(1612), 771-780.
- Friedman, J., Hastie, T., & Tibshirani, R. (2000). additive logistic regression: A statistical view of boosting. *Annals of statistics*, 337-374.
- Gaetani, F., Primiceri, P., Zappatore, G. A., and Visconti, P. (2018). Hardware design and software development of a motion control and driving system for transradial prosthesis based on a wireless myoelectric armband. *IET Science, Measurement & Technology*.
- Gretsch, K. F., Lather, H. D., Peddada, K. V., Deeken, C. R., Wall, L. B., and Goldfarb, C. A. (2016). Development of novel 3D-printed robotic prosthetic for transradial amputees. *Prosthetics and orthotics international*, 40(3), 400-403.
- Gui, Q., Ruiz-Blondet, M. V., Laszlo, S., and Jin, Z. (2019). A survey on brain biometrics. *ACM Computing Surveys (CSUR)*, 51(6), 1-38.

- Gunawardane, P. D. S. H., and Medagedara, N. T. (2017). Comparison of hand gesture inputs of leap motion controller & data glove in to a soft finger. *IEEE International Symposium on Robotics and Intelligent Sensors (IRIS)* (pp. 62-68). Ottawa, ON, Canada: IEEE.
- H. M. Abdul-Rashid, L. Kiran, M. D. Mirrani and M. N. Maraaj. (2017). CMSWVHG-control MS Windows via hand gesture. *International Multi-topic Conference (INMIC)* (pp. 1-7). Lahore: IEEE.
- Hawking, S. W. (2011). *World Report on disability Geneva: World Health Organization*. Geneva: World Health Organization. Retrieved from Hawking, S. W., "World Report on disability," Geneva: World Health Organization, 2011..
- He, J., and Jiang, N. (2020). Biometric From Surface Electromyogram (sEMG): Feasibility of User Verification and Identification Based on Gesture Recognition. *Frontiers in Bioengineering and Biotechnology*, 8, 58.
- <https://nyimi.com/>. (n.d.). (NYMI) Retrieved June 25, 2020
- Huang, Y., Englehart, K. B., Hudgins, B., & Chan, A. D. (2005). A Gaussian mixture model based classification scheme for myoelectric control of powered upper limb prostheses. *IEEE Transactions on Biomedical Engineering*, 52(11), 1801-1811.
- Iandola, F. N., Han, S., Moskewicz, M. W., Ashraf, K., Dally, W. J., and Keutzer, K. (2016). SqueezeNet: AlexNet-level accuracy with 50x fewer parameters and < 0.5 MB model size. *arXiv preprint arXiv:1602.07360*.
- Iandola, F. N., Moskewicz, M. W., Ashraf, K., and Keutzer, K. (2016). Firecaffe: near-linear acceleration of deep neural network training on compute clusters. *Proceedings of the IEEE Conference on Computer Vision and Pattern Recognition* (pp. 2592-2600). Las Vegas, NV, USA: IEEE.
- J. Blasco, T. M. Chen, J. Tapiador and P. Peris-Lopez. (2016). A Survey of Wearable Biometric Recognition Systems. *ACM Computing Surveys*, 49(3), 1-35.
- J. Zhao, J. Mao, G. Wang, H. Yang and B. Zhao. (2017). A miniaturized wearable wireless hand gesture recognition system employing deep-forest classifier. *IEEE Biomedical Circuits and Systems Conference (BioCAS)* (pp. 1-4). Turin, Italy: IEEE.

- Jelle ten Kate, Gerwin Smit & Paul Breedveld. (2017). 3D-printed upper limb prostheses: a review. *Disability and Rehabilitation: Assistive Technology*, 12:3, 300-314.
- Junhua Li, Gong Chen, Pavithra Thangavel, Haoyong Yu, Nitish Thakor, Anastasios Bezerianos, and Yu Sun. (2016). A Robotic Knee Exoskeleton for Walking Assistance and Connectivity Topology Exploration in EEG Signal. *IEEE RAS/EMBS*.
- Kania, M., Fereniec, M., and Maniewski, R. (2007). Wavelet denoising for multi-lead high resolution ECG signals. *Measurement science review*, 7(4), 30-33.
- Kapoor, A., and Picard, R. W. (2001). A real-time head nod and shake detector. In *Proceedings of the 2001 workshop on Perceptive user interfaces* (pp. 1-5). ACM.
- Kaur, G., Singh, G., and Kumar, V. (2014). A review on biometric recognition. *International Journal of Bio-Science and Bio-Technology*, 6(4), 69-76.
- Kay, S. M. (1988). *Modern spectral estimation: theory and application*. Pearson Education India.
- Kendon, A. (2004). *Gesture: Visible action as utterance*. UK: Cambridge University Press.
- Khezri, M., and Jahed, M. (2007). Real-time intelligent pattern recognition algorithm for surface EMG signals. *Biomedical engineering online*, 6(1), 1-12.
- Khmag, A., Al-Haddad, S. A. R., and Hashim, S. J. B. (2014). Additive and multiplicative noise removal based on adaptive wavelet transformation using cycle spinning. *American Journal of Applied Sciences*, 11(2).
- Krishnamohan, P. G., and Holi, M. S. (2011). GMM modeling of person information from EMG signals. *IEEE Recent Advances in Intelligent Computational Systems* (pp. 712-717). Trivandrum, Kerala, India: IEEE.
- Krishnan, K. S., Saha, A., Ramachandran, S., and Kumar, S. (2017). Recognition of human arm gestures using Myo armband for the game of hand cricket. *IEEE International Symposium on Robotics and Intelligent Sensors (IRIS)* (pp. 389-394). Ottawa, ON, Canada: IEEE.
- Krizhevsky, A., Sutskever, I., and Hinton, G. E. (2012). Imagenet classification with deep convolutional neural networks. *Advances in neural information processing systems*, 1097-1105.

- Latest Bionic arm [Internet]*. (cited 2015 Jun 24). Retrieved from <http://www.openbionics.com/>
- LeCun, Y., Boser, B., Denker, J. S., Henderson, D., Howard, R. E., Hubbard, W., and Jackel, L. D. (1989). Backpropagation applied to handwritten zip code recognition. *Neural computation*, *1*(4), 541-551.
- Li, X., Fu, J., Xiong, L., Shi, Y., Davoodi, R., and Li, Y. (2015, September). Identification of finger force and motion from forearm surface electromyography. *IEEE International Conference on Multisensor Fusion and Integration for Intelligent System (MFI)*, 316–321.
- Lian, K. Y., Chiu, C. C., Hong, Y. J., and Sung, W. T. (2017). Wearable armband for real time hand gesture recognition. *IEEE International Conference on Systems, Man, and Cybernetics (SMC)* (pp. 2992-2995). Banff, AB, Canada: IEEE.
- Lin, M., Chen, Q., and Yan, S. (2013). Network in network. *arXiv preprint arXiv:1312.4400*.
- Liu, J.; Zhou, P. (n.d.). A novel myoelectric pattern recognition strategy for hand function restoration after incomplete cervical spinal cord injury. *Transactions on neural systems and rehabilitation engineering*, *21*(1), 96-103.
- M. E. Benalcázar, A. G. Jaramillo, Jonathan, A. Zea, A. Páez and V. H. Andaluz. (2017). Hand gesture recognition using machine learning and the Myo armband. *25th European Signal Processing Conference (EUSIPCO)* (pp. 1040-1044). Kos, Greece: IEEE.
- Madhavan, S., Tripathy, R. K., and Pachori, R. B. (2019). Time-frequency domain deep convolutional neural network for the classification of focal and non-focal EEG signals. *IEEE Sensors Journal*, *20*(6), 3078-3086.
- Mahajan, N. V., Deshpande, A. S., and Satpute, S. S. (2019). Prediction of Fault in Gas Chromatograph using Convolutional Neural Network. *3rd International Conference on Trends in Electronics and Informatics (ICOEI)* (pp. 930-933). Tirunelveli, India, India: IEEE.
- Marsland, S. (2015). *Machine learning: an algorithmic perspective*. CRC press.

- Matsubara, T., and Morimoto, J. (2013). Bilinear modeling of EMG signals to extract user-independent features for multiuser myoelectric interface. *IEEE Transactions on Biomedical Engineering*, 60(8), 2205-2213.
- Matsumoto, Y., and Zelinsky, A. (2000). An algorithm for real-time stereo vision implementation of head pose and gaze direction measurement. *Proceedings Fourth IEEE International Conference on Automatic Face and Gesture Recognition*. Grenoble, France: IEEE.
- McGimpsey, G., & Bradford, T. C. (2008). *Limb prosthetics services and devices*. Bioengineering Institute Center for Neuroprosthetics Worcester Polytechnic Institution.
- Mekhalfa, F., and Nacereddine, N. (2017). Gentle Adaboost algorithm for weld defect classification. *Signal Processing: Algorithms, Architectures, Arrangements, and Applications (SPA)*, 301-306.
- Moon, K. Y. (2005). Biometrics technology status and prospects. *TTA journal*, 1,(98), 38-47.
- Morency, L. P., Sidner, C., Lee, C., and Darrell, T. (2005). Contextual recognition of head gestures. *In Proceedings of the 7th international conference on Multimodal interfaces* (pp. 18-24). Toronto Italy : ACM.
- Motoche, C., and Benalcázar, M. E. (2018). Real-time hand gesture recognition based on electromyographic signals and artificial neural networks. *International Conference on Artificial Neural Networks* (pp. 352-361). Rhodes, Greece: Springer.
- Myo Armband*. (n.d.). (Thlamic Lab) Retrieved June 25, 2020, from <https://support.getmyo.com/hc/en-us/articles/203398347-Getting-started-with-your-Myo-armband>
- Napier, J. R. (1956). The prehensile movements of the human hand. *The Journal of bone and joint surgery, British volume*, 38(4), 902-913.
- Noce, E., Bellingegni, A. D., Ciancio, A. L., Sacchetti, R., Davalli, A., Guglielmelli, E., and Zollo, L. ((2019)). EMG and ENG-envelope pattern recognition for prosthetic hand control. *Journal of Neuroscience Methods*, 311, 38-46.
- O'Neill C. (2014). An advanced, low cost prosthetic arm. *IEEE SENSORS*.

Open Bionics lab. (2019, 04 15). Retrieved from Available online:

<https://openbionicslabs.com/shop/chestnut-board>

P. Bonato. (2003). "Wearable Sensors/Systems and Their Impact on Biomedical Applications". *vol. IEEE ENGINEERING IN MEDICINE AND BIOLOGY MAGAZINE.*

Panwar, M., and Mehra, P. S. (2011). Hand gesture recognition for human computer interaction. *International Conference on Image Information Processing* (pp. 1-7). Shimla, India: IEEE.

Pinto, J. R., Cardoso, J. S., and Lourenço, A. (2018). Evolution, current challenges, and future possibilities in ECG biometrics. *IEEE Access*, 6.

Pramunanto, E., Sumpeno, S., and Legowo, R. S. (2017). Classification of hand gesture in Indonesian sign language system using Naive Bayes. *International Seminar on Sensors, Instrumentation, Measurement and Metrology (ISSIMM)* (pp. 187-191). Surabaya, Indonesia: IEEE.

Proakis, J. G. (2001). *Digital signal processing: principles algorithms and applications.* Pearson Education India.

Qingqing Li, Penghui Dong and Jun Zheng. (2020). Enhancing the Security of Pattern Unlock with Surface EMG-Based Biometrics. *Applied sciences*, 541. Retrieved 2020

R. A. Bhuiyan, A. K. Tushar, A. Ashiquzzaman, J. Shin and M. R. Islam. (2017). Reduction of gesture feature dimension for improving the hand gesture recognition performance of numerical sign language. *20th International Conference of Computer and Information Technology (ICCIT)*. Dhaka, Bangladesh: IEEE.

Rani, S. S., Dhriya, K. J., and Ahalyadas, M. (2017). Hand gesture control of virtual object in augmented reality. *International Conference on Advances in Computing, Communications and Informatics (ICACCI)* (pp. 1500-1505). Udupi, India: IEEE.

Rathgeb, C., and Uhl, A. (2011). A survey on biometric cryptosystems and cancelable biometrics. *EURASIP Journal on Information Security*, (1), 3.

- Redrovan, D. V., and Kim, D. (2018). Hand gestures recognition using machine learning for control of multiple quadrotors. *IEEE Sensors Applications Symposium (SAS)* (pp. 1-6). Seoul, South Korea: IEEE.
- Resnik, L., Meucci, M. R., Lieberman-Klinger, S., Fantini, C., Kelty, D. L., Disla, R., and Sasson, N. (2012). Advanced upper limb prosthetic devices: implications for upper limb prosthetic rehabilitation. *Archives of physical medicine and rehabilitation*, 93, 710–717.
- Robertson, D. G. E., Caldwell, G. E., Hamill, J., Kamen, G., and Whittlesey. (2014). *Research methods in biomechanics*. Human Kinetics.
- Roboarm. (2015). *Roboarm (Unlimited tomorrow)*.
- S. Chantaf, A. Naït-Ali, P. Karasinski, and M. Khalil. (2010). ECG modelling using wavelet networks: application to biometrics. *Int. J. Biometrics*, 2(3), 236-249.
- S. Hasan, K. Al-Kandari, E. Al-Awadhi, A. Jaafar, B. Al-Farhan, M. Hassan, S. Said, and S. AlKork. (2018). Wearable Mind Thoughts Controlled Open Source 3D Printed Arm with Embedded Sensor Feedback System. *CHIRA*. Seville, Spain.
- S. Rawat, S. Vats and P. Kumar. (2016). Evaluating and Exploring the MYO Armband. *2016 International Conference System Modeling & Advancement in Research Trends (SMART)*, 115-120.
- S. Said, S. Alkork, T. Beyrouthy, and M. Fayek. (2017). Wearable Bio-Sensors Bracelet for Driver's Health Emergency Detection. *Biosmart*. Paris, France.
- Said, S., Boulkaibet, I., Sheikh, M., Karar, A. S., Alkork, S., and Nait-ali, A. (2020). Machine-Learning-Based Muscle Control of a 3D-Printed Bionic Arm. *Sensors*, 20(11), 3144.
- Said, S., Sheikh, M., Al-Rashidi, F., Lakys, Y., Beyrouthy, T., and Nait-ali, A. (2019). A Customizable Wearable Robust 3D Printed Bionic Arm: Muscle Controlled. *In 2019 3rd International Conference on Bio-engineering for Smart Technologies (BioSMART)* (pp. 1-6). Paris, France: IEEE.

- Sapienza, S. (2018). On-Line Event-Driven Hand Gesture Recognition Based on Surface Electromyographic Signals. *IEEE International Symposium on Circuits and Systems (ISCAS)* (pp. 1-5). Florence: IEEE.
- Saponas, T.m Tan, S., Morris, D., and Balakrishnan, R. (2008). Demonstrating the feasibility of using forearm electromyography for muscle–computer interfaces. *In Proceedings of the 26th SIGCHI Conference on Human Factors in Computing Systems* (pp. 515-524). Florence, Italy: ACM.
- Sharma, S., Farooq, H., and Chahal, N. (2016). Feature extraction and classification of surface EMG signals for robotic hand simulation. *Communications on Applied Electronics (CAE)*, 4(2), 27-31.
- Sharma, A., Khandelwal, A., Kaur, K., Joshi, S., Upadhyay, R., and Prabhu, S. (2017). Vision based static hand gesture recognition techniques. *International Conference on Communication and Signal Processing (ICCSP)* (pp. 0705-0709). Chennai, India: IEEE.
- Shi, W. T., Lyu, Z. J., Tang, S. T., Chia, T. L., and Yang, C. Y. (2018). A bionic hand controlled by hand gesture recognition based on surface EMG signals: A preliminary study. *Biocybernetics and Biomedical Engineering*, 38(1), 126-135.
- Shin, S., and Sung, W. (2016). Dynamic hand gesture recognition for wearable devices with low complexity recurrent neural networks. *IEEE International Symposium on Circuits and Systems (ISCAS)* (pp. 2274-2277). Montreal, QC, Canada: IEEE.
- Shin, S., Jung, J., & Kim, Y. T. (2017). A study of an EMG-based authentication algorithm using an artificial neural network. *IEEE SENSORS*. Glasgow, UK: IEEE.
- Shioji, R., Ito, S. I., Ito, M., and Fukumi, M. (2017). Personal authentication based on wrist EMG analysis by a convolutional neural network. *5th IIAE International Conference on Intelligent Systems and Image Processing*. Japan: The Institute of Industrial Applications Engineers.
- Simonyan, K., and Zisserman, A. (2014). Very deep convolutional networks for large-scale image recognition. *arXiv preprint arXiv:1409.1556*.

- Soutar, C., Roberge, D., Stoianov, A., Gilroy, R., and Kumar, B. V. (1998). Biometric Encryption: enrollment and verification procedures. *International Society for Optics and Photonics.*, 3386, 24-35.
- Sugiura, Y., Nakamura, F., Kawai, W., Kikuchi, T., & Sugimoto, M. (2017). Behind the palm: Hand gesture recognition through measuring skin deformation on back of hand by using optical sensors. *56th Annual Conference of the Society of Instrument and Control Engineers of Japan (SICE)* (pp. 1082-1087). Kanazawa, Japan: IEEE.
- Szegedy, C., Ioffe, S., Vanhoucke, V., and Alemi, A. (2016). Inception-v4, inception-resnet and the impact of residual connections on learning. *arXiv preprint arXiv:1602.07261*.
- Theodoridis, S. (2015). *Machine learning: a Bayesian and optimization perspective*. Academic press.
- Tian, Z., Wang, J., Yang, X., and Zhou, M. (2018). WiCatch: A Wi-Fi based hand gesture recognition system. *IEEE Access*, 6, 16911-16923.
- Tomczyński, J., Mańkowski, T., & Kaczmarek, P. (2017). Influence of sEMG electrode matrix configuration on hand gesture recognition performance. In 2017 (pp. 42-47). *Signal Processing: Algorithms, Architectures, Arrangements, and Applications (SPA)* (pp. 42-47). Poznan: IEEE.
- V. Enzo, P. Scilingo and Gaetano. (2017). "Recent Advances on Wearable Electronics and embedded computing systems for biomedical applications". *electronics MDPI*.
- van der Riet, D., Stopforth, R., Bright, G., and Diegel, O. (2013). An overview and comparison of upper limb prosthetics. *Africon* (pp. 1-8). Pointe-Aux-Piments, Mauritius: IEEE.
- Vu, V. H., Thomas, M., Lakis, A. A., and Marcouiller, L. (2011). Operational modal analysis by updating autoregressive model. *Mechanical Systems and Signal Processing*, 25(3), 1028-1044.
- Wahid, M. F., Tafreshi, R., Al-Sowaidi, M., and Langari, R. (2018). Subject-independent hand gesture recognition using normalization and machine learning algorithms. *Journal of computational science*, 27, 69-76.

- Weir, R., and Sensinger, J. (2003). *The Design of artificial arms and hands for prosthetic application . Handbook of Biomedical Design*. McGraw-Hill.
- Wheeler, K. R., Chang, M. H., and Knuth, K. H. (2006). Gesture-based control and EMG decomposition. *IEEE Transactions on Systems, Man, and Cybernetics, Part C (Applications and Reviews)*, 36(4), 503-514.
- Wu, Y., Zheng, B., and Zhao, Y. (2018). Dynamic gesture recognition based on LSTM-CNN. *2018 Chinese Automation Congress (CAC)* (pp. 2446-2450). Xi'an, China, China: IEEE.
- Y. Paul, V. Goyal and R. A. Jaswal,. (2017). Comparative analysis between SVM & KNN classifier for EMG signal classification on elementary time domain features. *4th International Conference on Signal Processing, Computing and Control (ISPCC)*. Solan, India.
- Yamaba, H., Kurogi, A., Kubota, S. I., Katayama, T., Park, M., and Okazaki, N. (2017). Evaluation of feature values of surface electromyograms for user authentication on mobile devices. *Artificial Life and Robotics*, 22(1), 108-112.
- Yamaba, H., Kurogi, T., Aburada, K., Kubota, S. I., Katayama, T., Park, M., and Okazaki, N. (2018). On applying support vector machines to a user authentication method using surface electromyogram signals. *Artificial Life and Robotics*,, 23(1), 87-93.
- Yamaba, H., Nagatomo, S., Aburada, K., Kubota, S., Katayama, T., Park, M., and Okazaki, N. (2015). An Authentication Method Independent of Tap Operation on the Touchscreen of a Mobile Device. *Journal of Robotics, Networking and Artificial Life*, 2(1)(60-63).
- Yang, J., Pan, J., and Li, J. (2017). sEMG-based continuous hand gesture recognition using GMM-HMM and threshold model. *IEEE International Conference on Robotics and Biomimetics (ROBIO)* (pp. 1509-1514). Macau, China: IEEE.
- Yasen, M., and Jusoh, S. (2019). A systematic review on hand gesture recognition techniques, challenges and applications. *PeerJ Computer Science*, 5.
- Youbionic [Internet]*. ([cited 2015 Jun 29]). Retrieved from www.youbionic.com/

- Zecca, M., Micera, S., Carrozza, M. C., and Dario, P. (2002). Control of multifunctional prosthetic hands by processing the electromyographic signal. *Critical Reviews™ in Biomedical Engineering*, 30, 4-6.
- Zhang, H., Zhao, Y., Yao, F., Xu, L., Shang, P., and Li, G. (2013). An adaptation strategy of using LDA classifier for EMG pattern recognition. *35th annual international conference of the IEEE engineering in medicine and biology society (EMBC)*. Osaka, Japan: IEEE.
- Zhang, X. H., Wang, J. J., Wang, X., and Ma, X. L. (2016). Improvement of dynamic hand gesture recognition based on HMM algorithm. *International Conference on Information System and Artificial Intelligence (ISAI)* (pp. 401-406). Hong Kong, China: IEEE.
- Zhang, Z., Yang, K., Qian, J., and Zhang, L. (2019). Real-time surface emg pattern recognition for hand gestures based on an artificial neural network. *Sensors*, , 3170., 19(14).
- Zhu, Y., Jiang, S., and Shull, P. B. (2018). Wrist-worn hand gesture recognition based on barometric pressure sensing. *15th International Conference on Wearable and Implantable Body Sensor Networks (BSN)* (pp. 181-184). IEEE.
- Zia ur Rehman, M., Waris, A., Gilani, S. O., Jochumsen, M., Niazi, I. K., Jamil, M., and Kamavuako, E. N. (2018). Multiday EMG-based classification of hand motions with deep learning techniques. *Sensors*, 18(8), 2497.
- Zuniga, J. K. (n.d.). A low-cost 3d-printed prosthetic hand for children with upper-limb differences. *BMC research notes*, 8(1), 1-9.